UNIVERSITY OF COPENHAGEN
FACULTY OF SCIENCE

Master Thesis

Kevin Alberto Urquía Calderón

Lepton collider sensitivity to Heavy Neutral Lepton from Left-Right Symmetric Models

Handed in: August 10, 2023

Advisor: Prof. Oleg Ruchayskiy

Abstract

Left-right symmetric models (LRSM) were initially proposed to reconcile violation of parity in weak interactions with our intrinsic notion of a fundamental parity symmetry. Very soon after their proposal, it was realized that LRSM can also fit small neutrino masses, in part due to the incorporation of right-handed neutrinos (or Heavy Neutral Leptons, HNLs), N.

In this thesis we review on fundamental concepts in LRSM, including relatively recent developments. Then we study for the first time the potential that different proposals for lepton colliders (FCC-ee, CEPC, ILC, CLIC and a Muon Collider) have for the production and discovery of a pair of HNLs. Of particular interest are the background free signals that the model can give: doubly-displaced vertices and lepton number violating signals.

We find that some of our results reach regions of the parameter space that are impossible to reach with current experiments.

Contents

1 Introduction

The Standard Model (SM) [1, 2] was initially developed in the '60s to attempt to unify weak and electromagnetic interactions. The construction of the SM stemmed from years of developments in both experimental and theoretical physics, from the discovery of beta decay [3] and parity violation [4, 5] to the development of non-abelian gauge theories [6–8] and spontaneous symmetry breaking [9–13].

Even 60 years after the publication of Weinberg's iconic paper, the SM remains the most precise theory that models interactions between elementary particles [14]. We know the SM is not completely correct it has some theoretical issues and cannot account for all observed phenomena. The observation of neutrino oscillations [15–17], the asymmetry between particles and antiparticles in the universe [18, 19], the lack of a realistic dark matter candidate [20, 21], the lack of charge-parity (CP) violation in strong interactions [22], the fact that it cannot account for gravitational interactions [23–25], and many different anomalies [26] are some of the issues that the SM has.

The most natural way to fix these discrepancies is to introduce extensions to the SM. For example, the so-called Type-I Seesaw in its most minimal form can account for neutrino masses, baryon asymmetry and offers a realistic dark matter candidate [27]; or Grand Unified Theories like SU(5) [28] or SO(10) [29], which can also explain neutrino masses, baryon asymmetry, dark matter, the hierarchy problem, and the strong CP problem.

For the rest of this thesis, we will focus on the Left-Right Symmetric Model (LRSM). Left-right symmetric models were conceived to explain why weak interactions violate parity [30–32]. The explanation is that there is no parity violation at higher energy scales: the parity violation we see in experiments is merely due to a discrepancy between different energy scales. It was soon realized that LRSM could also account for neutrino oscillations [33, 34], baryon asymmetry [35, 36], strong CP violation [37, 38] and potentially provide a dark matter candidate [39, 40].

Some of the first constraints on the energy scale of LRSM came from $K - \bar{K}$ oscillations in meson experiments. It turned out that some of the additional particles that the LRSM introduced gave significant contributions to these experiments unless the new particles were in the $\mathcal{O}$(TeV) range [41–43]. We've only begun to surpass these constraints not that long ago thanks to the Large Hadron Collider (LHC).

The LHC will eventually stop functioning, this has placed the particle physics community at its crossroads: which direction should we take now? The community has given multiple suggestions on what to do next, and it seems the most likely outcome will be a lepton collider. There are different proposals: the Future Circular Collider (FCC) [44–47], the Circular Electron-Positron Collider (CEPC) [48, 49], the International Linear Collider (ILC) [50–53], the Compact Linear Collider (CLIC) [54–56] and a proposal which has been recently gaining plenty of attention: Muon Colliders [57–61].

Ample research has already been done on the sensitivity that different lepton colliders will have on the extended scalar sector of the model [62–66], but almost no studies can be found in the literature on the potential that lepton colliders have on finding Heavy Neutral Leptons (HNLs, or right-handed neutrinos), N, which the model naturally incorporates and which helps explain small neutrino masses. To the best of the authors' knowledge, there is only one study

on the subject [67].

The objective of this thesis is to examine the sensitivity that these proposed experiments have on the discovery of Heavy Neutral Leptons. We will focus on the background-free signals: doubly displaced vertices and lepton number violating processes.

The thesis is organized as follows: in Section 2 we review fundamental concepts within the Standard Model and their problems, Section 3 reviews essential concepts within the LRSM, Section 4 reviews the different proposals for future lepton colliders, Section 5 summarizes the relevant phenomenology of LRSM in lepton colliders, Section 6 obtains an approximate sensitivity that the model will have on these proposals and Section 7 elaborates conclusions and briefly discusses potential avenues of research where the project could be expanded upon.

2 The Standard Model

As we mentioned in the Introduction, the Standard Model (SM) stems from different experimental and theoretical results. The formulation of a quantum theory of relativistic particles (which we now know as Quantum Field Theory, QFT) was perhaps the first stepping stone. Eventually, Yang and Mills developed non-Abelian gauge theories, theories that predict a photon that interacts with other photons, essentially a photon with a charge[1]. Later on, in a series of almost simultaneous papers by Englert, Brout, Guralnik, Hagen, Kibble, and Higgs developed a way to give these charged photons mass, nowadays this mechanism is called the Higgs mechanism[2].

But little did any of the physicists at the time know how these new developments would eventually be used to develop the SM. The hypothesization and eventual discovery of quarks and gluons cemented the SU(3) theory of strong interactions. As for in the realm of electroweak interaction, if we didn't discover that weak interactions violate parity, we would've never been capable of guessing which gauge group to use to model electroweak interactions.

2.1 Non-abelian gauge theories

Yang-Mills, or non-abelian gauge theories, generalize abelian gauge theories, which we use to model quantum electrodynamics (QED). Before properly going into non-abelian gauge theories, let us very briefly review abelian gauge theories. The Lagrangian of an abelian gauge theory remains invariant under the following transformations:

$$\begin{aligned} A_\mu &\to A_\mu + \frac{1}{e}\partial_\mu \alpha(x) = U A_\mu U^{-1} - \frac{i}{e}\left(\partial_\mu U\right) U^{-1}\,, \\ F_{\mu\nu} &\to F_{\mu\nu}\,, \\ \psi &\to e^{i\alpha(x)Q}\psi = U\psi\,, \end{aligned} \tag{1}$$

where A_μ is the photon field, $F_{\mu\nu} = \partial_\mu A_\nu - \partial_\nu A_\mu$ is the usual anti-symmetric strength tensor, ψ is a fermion field, $\alpha(x)$ is a local parameter, Q is the charge operator (the generator of the algebra of U(1)) and $U = e^{i\alpha(x)Q}$ is an element of U(1). The gauge invariant Lagrangian that describes the interactions between these particles is:

$$\mathcal{L}_{\text{abe.}} = -\frac{1}{4}F_{\mu\nu}F^{\mu\nu} + \bar{\psi}\left(i\not{D} - m\right)\psi\,, \tag{2}$$

where $D_\mu = \partial_\mu - ieA_\mu Q$, is the covariant derivative of abelian interactions. We can also define the F tensor as a commutation between the covariant derivatives:

$$\left[D_\mu, D_\nu\right]\phi = -ieF_{\mu\nu}\,Q\phi\,. \tag{3}$$

In the case of a non-abelian theory, considering a semi-simple Lie group, we will have multiple generators of the Lie algebra that we will denote as T^a. The shape that these generators have will depend on the representation that we choose and also on the group itself, for example, in the fundamental representation of SU(2) the generators of the Lie algebra will be proportional

[1] (In)famously, Pauli told Yang after a seminar he gave that his theory is *not even wrong*.

[2] Sometimes also called the ABEGHHK'tH mechanism (Anderson, Brout, Englert, Guralnik, Hagen, Higgs, Kibble, t'Hooft).

to the Pauli matrices. The generators will follow the commutation relations:

$$\left[T^a, T^b\right] = i f^{abc} T^c \,, \tag{4}$$

where f^{abc} are usually known as the structure constants. This equation is in direct contrast with the abelian case, where the algebra of the $U(1)$ group only has one generator that we denoted as Q, which is proportional to the identity. The transformations in Eq. (1) are generalized by substituting the U for an element of a non-abelian semi-simple Lie group, let us say to be SU(n), for example:

$$\begin{aligned} \mathbf{A}_\mu &\to \mathbf{U}\mathbf{A}_\mu\mathbf{U}^{-1} - \frac{i}{g}\left(\partial_\mu \mathbf{U}\right)\mathbf{U}^{-1} \,, \\ \psi &\to \mathbf{U}\psi \,, \end{aligned} \tag{5}$$

where $\mathbf{A}_\mu = A^a_\mu T^a$ and $\mathbf{U} = e^{i\,\alpha^a(x) T^a}$. Due to $\mathbf{U}$ having *the shape of matrix*, we would expect ψ to *have the shape of a vector*. The dimensions of the vector and its shape will depend on the representation under which they transform. In the case of SU(2), if they transform under the fundamental representation (where the generators are a set of 2×2 matrices), then we would call them a doublet and have the shape of a 2-dimensional vector, but if they transformed under the adjoint representation (where the generators are a set of 3×3 matrices), then they would be called a triplet and have the shape of a 3-dimensional vector (or a 2×2 matrix, but then the transformation would be different).

Now our gauge invariant Lagrangian will be:

$$\mathcal{L}_{\text{non-abe}} = -\frac{1}{2}\,\mathrm{Tr}[\mathbf{F}_{\mu\nu}\mathbf{F}^{\mu\nu}] + \bar{\psi}\left(i\not{\mathbf{D}} - m\right)\psi \,, \tag{6}$$

where the covariant derivative is $\mathbf{D}_\mu = \partial_\mu - igA^a_\mu T^a$. Moreover, we can also obtain the shape of $\mathbf{F}_{\mu\nu} = F^a_{\mu\nu} T^a$ from the commutator of the covariant derivatives:

$$\left[\mathbf{D}_\mu, \mathbf{D}_\nu\right]\phi = -ig\,\mathbf{F}_{\mu\nu}\phi \,, \tag{7}$$

which gives us:

$$\mathbf{F}_{\mu\nu} = \partial_\mu \mathbf{A}_\nu - \partial_\nu \mathbf{A}_\mu - ig\left[\mathbf{A}_\mu, \mathbf{A}_\nu\right] \,, \tag{8}$$

or in component form:

$$F^a_{\mu\nu} = \partial_\mu A^a_\nu - \partial_\nu A^a_\mu + g f^{abc}\, A^b_\mu A^c_\nu \,. \tag{9}$$

The details on the quantization of the theory will not be expounded in this thesis but can be found in most QFT books (see e.g., [68]). This procedure is called the Faddeev-Popov procedure, which forces the inclusion of unphysical fields called *ghosts*, which appear to keep the theory Lorentz and gauge invariant.

The salient feature of non-abelian gauge theories, compared to the abelian case, is that gauge bosons can interact with one another. We can see these interactions from first term in Eq. (6) and from the definition of $\mathbf{F}_{\mu\nu}$ in Eq. (9), the kinetic term induces vertices between three and four A^a_μ. Such interactions are unfound in QED: the photon should only couple with particles that have a charge, and photons are chargeless.

The incorporation of a non-abelian SU(3) into strong interactions came through the *eighfold*

way [69–71], it was found out that the different mesons already discovered transform under the octet representation of a group and baryons under a decuplet. Gell-Mann figured that the simplest group that accounts for the transformation was SU(3). This way of organizing hadrons under an SU(3) proved to be an incredibly successful model: it famously predicted the existence of a yet-to-be-discovered particle called the Ω baryon. Eventually we found the Ω baryon.

Then, Gell-Mann and Zweig [72, 73] independently proposed a more fundamental way of organizing hadrons. The idea was that mesons, which transform under the octet representation of SU(3), could be composed of more elementary particles that transform under the fundamental and complex representation of SU(3) ($3 \otimes \bar{3} = 8 \oplus 1$) and baryons composed by three of these elementary particles ($3 \otimes 3 \otimes 3 = 10 \oplus 8 \oplus 8 \oplus 1$). These elementary particles were dubbed *quarks*[3].

The next natural step was to incorporate the SU(3) symmetry into the theory originally done by Yang and Mills [74]. The gauge particle was called gluons. We eventually discovered all of the proposed particles.

Another non-abelian group picked up center stage in the modeling of weak interactions, but before we can properly talk about it, we should discuss the Higgs mechanism.

2.2 Spontaneous symmetry breaking and the Higgs mechanism

Let us consider, as an example, the simplest model that has the breaking of a spontaneous continuous symmetry: a massive complex scalar field:

$$\mathcal{L}_{\mathrm{U}(1)} = \partial_\mu \phi \, \partial^\mu \phi^* - m^2 |\phi|^2 - \frac{\lambda}{4} |\phi|^4 \,, \tag{10}$$

where we have a U(1) symmetry: $\phi \to e^{i\alpha}\phi$. To have a more clear picture of what is going to happen, let us decompose $\phi = \frac{1}{\sqrt{2}}(\sigma + i\chi)$, now the Lagrangian looks like:

$$\mathcal{L}_{\mathrm{SO}(2)} = \frac{1}{2}\partial_\mu \sigma \, \partial^\mu \sigma + \frac{1}{2}\partial_\mu \chi \, \partial^\mu \chi - \frac{m^2}{2}\left(\sigma^2 + \chi^2\right) - \frac{\lambda}{8}\left(\sigma^2 + \chi^2\right)^2 \,, \tag{11}$$

the Lagrangian, of course, still has the same U(1) symmetry, $\binom{\sigma}{\chi}$ transforms under the doublet representation of U(1) (which are elements of SO(2), the group that does bi-dimensional rotations).

If $m^2 > 0$, then we are describing an ordinary scalar field theory with two fields, on the other hand, if $\mu^2 = -m^2 > 0$, then the potential in the Lagrangian $V = m^2|\phi|^2 + \frac{\lambda}{4}|\phi|^4$ will have a local maximum at $\sigma^2 + \chi^2 = 0$, but a local minimum when $\sigma^2 + \chi^2 = \frac{2\mu^2}{\lambda}$. This minimum also has a U(1) symmetry. We can choose any of the points inside the circle. We will select the minima residing at $\sigma^2 = \frac{2\mu^2}{\lambda}, \chi = 0$.

What does this mean? It means that the vacuum expectation value (vev), $v = \sqrt{\frac{2\mu^2}{\lambda}} = \langle 0|\sigma|0\rangle$, of the σ field is non-zero. This is in conflict with the decomposition of creation and annihilation operators we do for scalar fields, the same creation and annihilation operators which create and annihilate particles. It is hard to reconcile the usual particle interpretation we give fields when we do not have a field with a vanishing vev. Therefore, we have to introduce the physical field $h = \sigma - v$, which does have a vanishing vev. The introduction of this field breaks

[3]The term *quark* comes from the unreadable book by James Joyce *Finnegans Wake*. Curiously enough, Zweig called them *aims* in his original paper. Thankfully the particle physics community chose quark.

the original U(1) symmetry:

$$\mathcal{L}_{\text{SSB}} = \frac{1}{2}\partial_\mu h\,\partial^\mu h + \frac{1}{2}\partial_\mu \chi\,\partial^\mu \chi - \mu^2 h^2 - \mu\sqrt{\frac{\lambda}{2}} h\left(h^2+\chi^2\right) - \frac{\lambda}{8}\left(h^2+\chi^2\right)^2 + \frac{m^4}{2\lambda}\,, \tag{12}$$

what is most remarkable here is that h has acquired mass, whereas χ remains completely massless. h is usually called a *Higgs field*, and χ a *Goldstone field*. What we've just witnessed is a special case of the *Goldstone theorem*, which says that for every broken generator of a global symmetry, a massless field will appear. Had we chosen a different symmetry, say an SU(2) symmetry, and broken two generators, two different massless fields would've appeared.

If we upgrade our $U(1)$ global symmetry to a local one, we will then have scalar QED:

$$\mathcal{L}_{\text{sQED}} = -\frac{1}{4}F_{\mu\nu}F^{\mu\nu} + D_\mu\phi\, D^\mu\phi^* + \mu^2|\phi|^2 + \frac{\lambda}{4}|\phi|^4\,, \tag{13}$$

with $D_\mu\phi = (\partial_\mu - igA_\mu)\,\phi$ is the U(1) covariant derivative, where we have given ϕ a charge of $+1$. The theory follows the same transformations we described in Eq. (1). Now, ϕ will acquire a non-zero vev, and we must redefine the σ field. To simplify things for now, we can choose a gauge where the would-be Goldstone boson, χ is zero, this is the *Unitary gauge*. Then our Lagrangian becomes:

$$\begin{aligned}\mathcal{L} =& -\frac{1}{4}F_{\mu\nu}F^{\mu\nu} + \frac{1}{2}\partial_\mu h\,\partial^\mu h - \mu^2 h^2 + \frac{1}{2}g^2v^2A_\mu A^\mu + g^2v^2hA_\mu A^\mu \\ &+ \frac{1}{2}e^2h^2A_\mu A^\mu - \frac{\lambda v}{2}h^3 - \frac{\lambda}{8}h^4\,,\end{aligned} \tag{14}$$

here, due to our choice of gauge, the Goldstone boson has disappeared. The gauge field A has now acquired mass $m_A = gv$ proportional to the vev of the Higgs field, the gauge coupling, and the value of the charge of the Higgs.

We could've chosen other gauges where the Goldstone boson doesn't disappear. For example, in the *Feynman-'t Hooft gauge*, the Goldstone boson remains and acquires the same mass as the gauge boson, in other gauges, like the *Landau gauge* the Goldstone boson remains massless. There are other gauge choices that would have a non-trivial Faddeev-Popov procedure and where ghosts could arise even in the U(1) case. The choice of which gauge to work with depends on the problem at hand, it is sometimes easier to work with the Goldstone bosons, and sometimes it isn't. For example, it was shown that the unitary gauge for non-abelian gauge theories not to be renormalizable [75], but they are in other gauges [8].

Of course, the choice of the gauge should not affect in any way whatsoever the physics, nature should not be gauge dependent. This gives us an indication that the Goldstone bosons, much like the ghost fields, are not actual physical fields. We usually say that the Goldstone fields were *eaten* by the gauge boson, acquiring a mass and a longitudinal degree of polarization.

We have managed to give gauge particles a mass. Can we do the same for fermions? Let us add a Yukawa coupling to the theory:

$$\mathcal{L}_\psi = i\bar\psi_R \not{D}\psi_R + i\bar\psi_L \not{\partial}\psi_L - y\bar\psi_L\psi_R\,\phi + \text{h.c.}\,, \tag{15}$$

here, the sub-indices L and R denote the chirality of the spinor field. Here we will define only

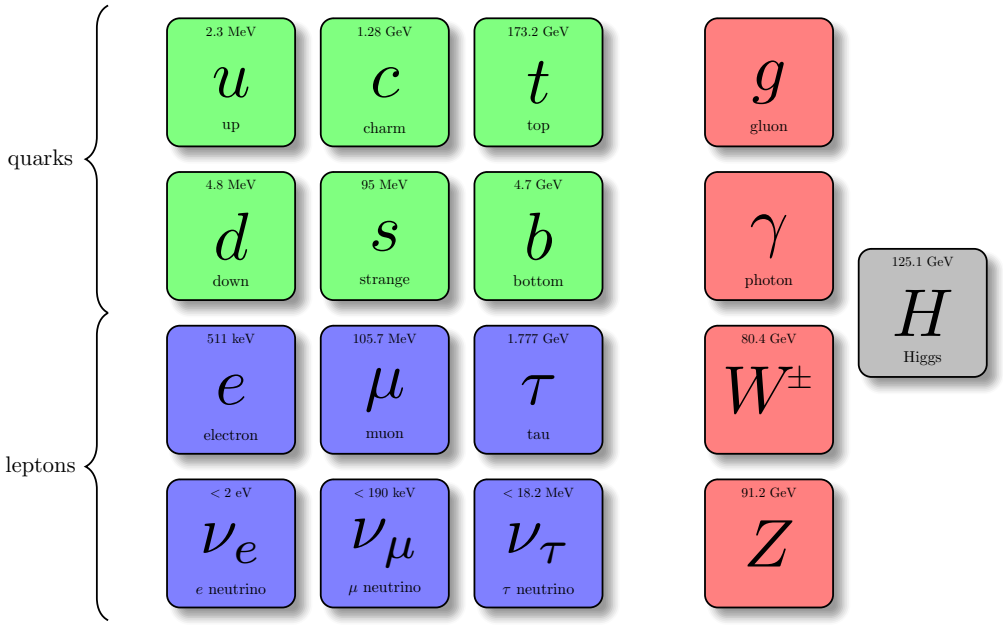

Figure 1: Particle content of the Standard Model

ψ_R to have a U(1) charge, ψ_L will remain a singlet. The eventual symmetry breaking and appearance of the terms proportional to v will give the fermion field a mass proportional to the Yukawa coupling y: $m_\psi = yv$.

Now we have a way to give masses to both gauge and fermion fields. This is known as the *Higgs mechanism*. The theoretical advantage we have when dealing with theories that undergo spontaneous symmetry breaking is that the theory somehow still remembers the underlining symmetries of the theory. Takashi-Ward and Slavnov-Taylor identities remain after the breaking of a symmetry, this was a crucial part in showing that these theories are renormalizable.

The Higgs mechanism applied to non-abelian gauge theories is what led to the development of the unification of electromagnetic and weak interactions. The underlining structure of weak interactions has been mapped out thanks to the discovery of different particles and their decays, from β-decay and its violation of parity, the discovery of the μ and its only(?) decay, and various other hadrons. The question remained in everyone's mind whether weak interactions could also be fitted into a symmetry, and if so, which? Glashow, Weinberg, Salam, and Ward came up with what is the simplest model which can unify that was based on the $\mathrm{SU}(2) \times \mathrm{U}(1)$ group.

2.3 Electroweak theory

The electroweak part of the SM is based on the following gauge group:

$$\mathcal{G}_{\mathrm{EW}} = \mathrm{SU}(2)_L \times \mathrm{U}(1)_Y \,, \tag{16}$$

where the L here denotes the left-weak isospin, and the Y denotes the hypercharge. The gauge group is meant to be spontaneously broken to $\mathrm{U}(1)_Q$ by the Higgs mechanism, where Q is the electric charge from electromagnetic interactions.

$\mathcal{G}_{\rm EW}$ has four different generators. The Higgs mechanism breaks three of the four generators leaving only one unbroken, which is the following linear combination:

$$Q = T_L^3 + \frac{Y}{2}\,, \tag{17}$$

where T_L^3 is the third generator of the SU(2) algebra. The particle content of the SM is shown in Fig. 1: three generations of quarks and three of leptons. W^-, W^+, Z and γ are related to the gauge bosons of the SM gauge group, and H is the Higgs particle responsible for providing the mass to the particle of the SM model. We will not touch on g, the gluon, which is the particle that mediates strong interactions. The left-handed part of each generation of lepton and quarks form an $\mathrm{SU}(2)_L$ doublet:

$$\begin{aligned} \text{Lepton doublets}: &\quad \begin{pmatrix}\nu_{eL}\\ e_L\end{pmatrix}\,, \quad \begin{pmatrix}\nu_{\mu L}\\ \mu_L\end{pmatrix}\,, \quad \begin{pmatrix}\nu_{\tau L}\\ \tau_L\end{pmatrix}\,, \\ \text{Quark doublets}: &\quad \begin{pmatrix}u_L\\ d_L\end{pmatrix}\,, \quad \begin{pmatrix}c_L\\ s_L\end{pmatrix}\,, \quad \begin{pmatrix}t_L\\ b_L\end{pmatrix}\,, \end{aligned} \tag{18}$$

and both elements of the doublet have the same hypercharge Y. The lepton doublets have a hypercharge $Y = -1$, and the quark doublets have $Y = \frac{1}{3}$. The right-handed part of all the particles are $\mathrm{SU}(2)_L$ singlets, but they all have a hypercharge equal to twice their charge. In its original conception, the right-handed component of neutrinos was not included, there are probably two reasons for this: neutrinos were believed to be massless (including a right-handed component would make them massive), and a right-handed component is a singlet of the $\mathcal{G}_{\rm EW}$, making them (almost) sterile, which means they would almost not interact with any other particles.

Moreover, we also have the scalar doublet, where the would-be Goldstone and Higgs bosons reside. They have a hypercharge $Y = 1$:

$$\text{Scalar doublet}: \quad \varphi = \begin{pmatrix}\phi^+\\ \frac{1}{\sqrt{2}}\left(h + v + i\phi^0\right)\end{pmatrix}\,, \tag{19}$$

here ϕ^+ and ϕ^0 are the would-be Goldstone bosons, h is the Higgs boson and v is the vev of the SM. We have not mentioned yet the color charge (the charge of $\mathrm{SU}(3)_C$, the group for strong interactions) but all of the particles, except for the quarks and gluons, are color-singlets. Weak interactions (as far as we know) do not care about color charge, they treat quarks of different colors charges in the same way, how this usually translates itself when computing the cross section or decay rates involving quarks is that an extra factor of three needs to be added, one for each different color charge.

The full Lagrangian of electroweak interactions looks like this:

$$\begin{aligned}\mathcal{L}_{\rm EW} = &-\frac{1}{2}\,\mathrm{tr}[\mathbf{W}_{\mu\nu}\,\mathbf{W}^{\mu\nu}] - \frac{1}{4}B_{\mu\nu}\,B^{\mu\nu} + \sum_{\Psi_L}\bar{\Psi}_L \not{D}\Psi_L + \sum_{\psi_R}\bar{\psi}_R \not{D}\psi_R + |D_\mu\varphi|^2 \\ &- \left(\sum \bar{L}_L\cdot\varphi\, Y_\ell\, \ell_R + \sum \bar{Q}_L\cdot\varphi\, Y_D\, D_R + \sum \bar{Q}_L\cdot\tilde{\varphi}\, Y_U\, U_R + \text{h.c.}\right) \\ &+ \mu^2|\varphi|^2 - \lambda|\varphi|^4\,,\end{aligned} \tag{20}$$

where $W^a_{\mu\nu} = \partial_\mu W^a_\nu - \partial_\nu W^a_\mu + g\,\epsilon^{abc}\,W^b_\mu W^c_\nu$ is the field strength of the $\mathrm{SU}(2)_L$ group with their respective gauge bosons W^a_μ, $B_{\mu\nu} = \partial_\mu B_\nu - \partial_\nu B_\mu$ is of the $\mathrm{U}(1)_Y$ group with its respective gauge boson B_μ. Ψ_L is any of the fermion gauge doublets in Eq. (18), ψ_R are all the fermion $\mathrm{SU}(2)_L$ singlets, L_L is any of the leptonic doublets, ℓ_R any of the charged-lepton right-handed singlets, Q_L any of the quark doublets, D_R the down-quark right-handed singlets, U_R the up-quark right-handed singlets, $\tilde{\varphi} = i\sigma_2\varphi^*$, Y_ℓ, Y_D, Y_U are the charged-lepton, down-quark and up-quark Yukawa couplings, and D_μ is the covariant derivative of the $\mathcal{G}_{\rm EW}$ group:

$$D_\mu = \partial_\mu - i\,g W^a_\mu\,T^a_L - i\,g_Y B_\mu\,\frac{Y}{2}\,. \tag{21}$$

In an aim to explain to the potentially confused reader what is happening, let us briefly summarize what Eq. (20) is showing us: the first line is all the kinetic terms of all the particles: gauge bosons, fermions, and scalars, all including the necessary covariant derivatives that maintain the Lagrangian invariant under the $\mathcal{G}_{\rm EW}$ group; the second line is all the Yukawa couplings between fermions and the scalars; the third line is showing us the Higgs potential. We've included all the renormalizable terms, which Lorentz invariance, and the $\mathcal{G}_{\rm EW}$ allow us to have with the fields we have included. To not include any would either be a mistake[4] or would imply the existence of another symmetry, we usually call this the **totalitarian principle**.

2.3.1 Symmetry breaking and mass spectrum

The kinetic term of the Higgs potential will be the one responsible for giving the gauge bosons their masses:

$$\begin{aligned}|D_\mu\varphi|^2 &\supset \left|-\frac{i}{2}\begin{pmatrix} gW^3_\mu + g_Y B_\mu & g\,(W^1_\mu - iW^2_\mu) \\ g\,(W^1_\mu + iW^2_\mu) & -gW^3_\mu + g_Y B_\mu\end{pmatrix}\begin{pmatrix}0\\ \frac{v}{\sqrt{2}}\end{pmatrix}\right|^2 \\ &= \frac{1}{4}\frac{v^2}{2}\left[g^2\left(W^1_\mu\right)^2 + g^2\left(W^2_\mu\right)^2 + \left(g_Y B_\mu - gW^3_\mu\right)^2\right]\,,\end{aligned} \tag{22}$$

what we have found out is that there are two neutral bosons W^1_μ, W^2_μ with the same mass, which is equivalent to a charged boson. We can see this by using a different basis:

$$W^\pm_\mu = \frac{W^1_\mu \mp iW^2_\mu}{\sqrt{2}}\,, \tag{23}$$

[4] I remember one of my professors once saying that everything which you symmetries allow you include has to be included, otherwise ultraviolet completion will do it for you.

moreover, it seems that two different gauge bosons mix and do not have a defined mass. We can decouple them using the next transformation:

$$\begin{cases} Z_\mu = c_w W_\mu^3 - s_w B_\mu \\ A_\mu = s_w W_\mu^3 + c_w B_\mu \end{cases}, \tag{24}$$

where $c_w = \cos\theta_w, s_w = \sin\theta_w$ and $t_w = \tan\theta_w = g_Y/g$ is the tangent of the Weinberg angle. Then:

$$\mathcal{L}_{\text{mass}-\text{gauge}} = \frac{1}{4} g^2 v^2 W_\mu^+ W^{\mu-} + \frac{1}{8}\frac{g^2 v^2}{c_w^2} Z_\mu Z^\mu \,, \tag{25}$$

we now have a mass spectrum for the gauge bosons of the SM:

$$\begin{aligned} M_W &= \frac{1}{2} g v \,, \\ M_Z &= \frac{1}{2}\frac{g v}{c_w} \,, \end{aligned} \tag{26}$$

the key point to emphasize here: there is a direct relation between the masses of the W and the Z boson. We would be expecting:

$$\rho \equiv \frac{M_Z^2\, c_w^2}{M_W^2} = 1 \,, \tag{27}$$

the SM is already predicting that the mass of the Z boson will be bigger. How big it is depends, firstly on the value of θ_w, and, a little more subtly on the representation under which the scalar transforms. Indeed, had the scalar doublet actually been a triplet with $Y = 2$, the ρ-parameter would've actually been 2, but it if had been a triplet with hypercharge $Y = 0$ it would've been zero. This ρ-parameter functions as a probe of the quantum numbers of the scalar doublet. In reality, this factor is actually not exactly 1. Loop corrections to the mass of the W and Z bosons alter it slightly, which makes the ρ-parameter a powerful tool to constraint potential beyond-the-Standard-Model (BSM) physics which might change its value.

The Yukawa couplings, in the second line of Eq. (20) give mass to all the fermions:

$$\begin{aligned} \mathcal{L}_{\text{Yuk.}} &= -\sum_{\alpha,\beta} \bar{L}_{\alpha,L} \cdot \varphi \; (Y_\ell)_{\alpha\beta} \; \ell_{\beta,R} - \sum_{i,j} \left[\bar{Q}_{i,L} \cdot \varphi \, (Y_D)_{ij} D_{j,R} + \bar{Q}_{i,L} \cdot \varphi \, (Y_U)_{ij} U_{j,R}\right] + \text{h.c.} \\ &\supset -\frac{v}{\sqrt{2}} \sum_{\alpha,\beta} \bar{\ell}_{\alpha,L} \, (Y_\ell)_{\alpha\beta} \, \ell_{\beta,R} - \frac{v}{\sqrt{2}} \sum_{i,j} \left[\bar{D}_{i,L} \, (Y_D)_{ij} D_{R,j} + \bar{U}_{i,L} (Y_U)_{ij} U_{j,R}\right] + \text{h.c.} \end{aligned} \tag{28}$$

where the sub-indices α, β indicate different lepton generations, and i, j different quark generations. It is clear, as it was near the end of Section 2.2, that the masses of the fermions will be proportional to their Yukawa couplings times the SM vev, but the situation is different here: we have multiple generations, and the Yukawa couplings can mix different generations. Indeed, in general, the Yukawa matrices may not necessarily be diagonal.

But we can choose, without any loss of generality, to have some Yukawa matrices to be diagonal. Let's take the quark sector, if we ignore the Yukawa couplings, the Lagrangian is

invariant under the following global transformations:

$$\begin{aligned} U_L &\to V_Q^L\, U_L\,, \quad D_L \to V_Q^L\, D_L\,, \\ U_R &\to V_U^R\, U_R\,, \quad D_R \to V_D^R\, D_R\,, \end{aligned} \tag{29}$$

where all the V's are unitary transformations in the *flavor space* of quarks. We can then choose a V_Q^L and V_U^R such that diagonalizes Y_U, at the cost that Y_D may not necessarily be diagonal (if Y_D were diagonal it would mean that there is an amazing flavor symmetry in the quark sector). Or we could do it the other way around, we could choose Y_D to be diagonal and Y_U to not be diagonal. This means that we can choose one of them to be diagonal without any loss of generality. We will stick to convention and set Y_U to be diagonal.

We then have to perform a unitary transformation so that Y_D is diagonalized, we should only then rotate the down quark fields $D_L \to V_D^L\, D_L$, and $D_R \to V_D^R\, D_R$. It will not be the case that the rest of the Lagrangian will be invariant under this transformation, as we will see later, this will impact the interactions between quarks and charged gauge bosons, but not in interactions with neutral gauge bosons: decoupling quarks in Yukawa interactions will mix them in gauge interactions. This mixing will bring some interesting phenomenological implications like meson mixing, meson oscillations, and CP violation, which will be discussed a little bit more on the following pages.

We can perform the same argument in the lepton sector and actually choose Y_ℓ to be diagonal without any loss of generality, there will be no mixing between leptons because we did not include a right-handed neutrino field in the model. As far as we know, this seems to be the case with charged leptons, they do not seem to mix with one another, searches for processes that violate charged lepton flavor (or cLFV processes), like $\mu^- \to e^- e^- e^+$ or $\mu^- \to e^- e^+$ place very strong bounds on the mixing between charged leptons. The case with neutral leptons, however, is different and shall be discussed later on.

Let us now re-write the second line in Eq. (28) as:

$$\mathcal{L}_{\psi-\text{mass}} = -\frac{v}{\sqrt{2}} \sum_\alpha \bar{\ell}_{\alpha,L}\, (y_\ell)_\alpha \ell_{\alpha,R} - \frac{v}{\sqrt{2}} \sum_i \left(\bar{D}_{i,L}\ (y_D)_i\ D_{i,L} + \bar{U}_{i,L}\, (y_U)_i\, U_{i,L} \right)\,, \tag{30}$$

where much like before, $m_\psi = \frac{1}{\sqrt{2}}\, y_\psi v$.

The values of the masses of the different fermions can be seen in Fig. 1, the third generation of all particles have the highest values, which means that their Yukawa couplings have a bigger value than those of the second generation; and those higher than the ones of the first generation. Can we probe this? Is there a way to examine that it is actually the Higgs mechanism that is responsible for giving fermions their masses and the gauge bosons theirs?

As a matter of fact, there is. The coupling of the Higgs boson to a SM particle is proportional to their masses:

$$\mathcal{L}_{\text{Higgs}} = -\sum_\psi \frac{m_\psi}{v}\, \bar{\psi}\psi h + 2\, \frac{M_W^2}{v}\, W_\mu^+ W_\mu^- h + \frac{M_Z^2}{v}\, Z_\mu Z^\mu h\,, \tag{31}$$

so, if kinematically allowed, we would expect the decay width of the Higgs to a pair of fermions to be: $\Gamma(h \to \bar{\psi}\psi) \propto m_\psi^2$. For heavier particles, like the t-quark and gauge bosons, we can check

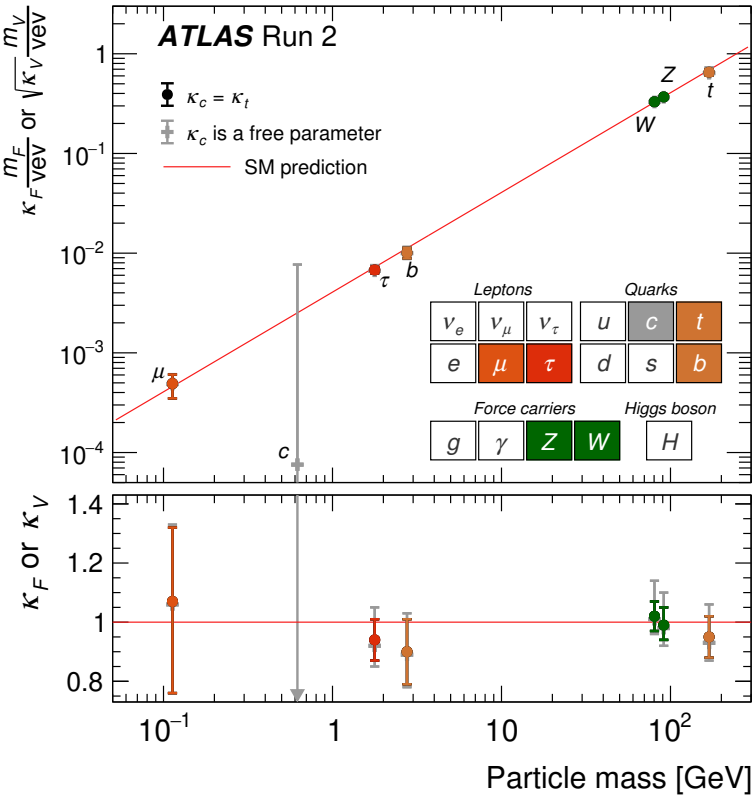

Figure 2: Measurement done by ATLAS of the couplings between Higgs and the rest of the SM particles as a probe of the Higgs mechanism. Plot obtained from [78].

the coupling, either by the production cross-section or decays through off-shell particles.

Have we measured all the couplings between the Higgs and SM particles? The Higgs boson was discovered in 2012 [76, 77], ever since we've tried relentlessly to measure all of its parameters in hopes of disproving the SM. Fig 2 shows the measurements of the Higgs couplings performed by ATLAS from [78]. The lighter particles are, the harder it is to probe the Higgs mechanism for them. Quarks are even harder to probe due to their subsequent hadronization after production and excessive amounts of background. But what is truly remarkable here is how accurate the Higgs mechanism and the SM seem to be, all of the couplings agree to a great extent with their SM predictions! How remarkable!

2.3.2 Interactions between gauge bosons and fermions

	t_L^3	q
U	$1/2$	$2/3$
D	$-1/2$	$-1/3$
ν	$1/2$	0
ℓ	$-1/2$	-1

Table 1: Values of t_L^3 and q for the different SM fermion fields

Now let us turn our attention to how fermions interact with gauge bosons. From the covariant

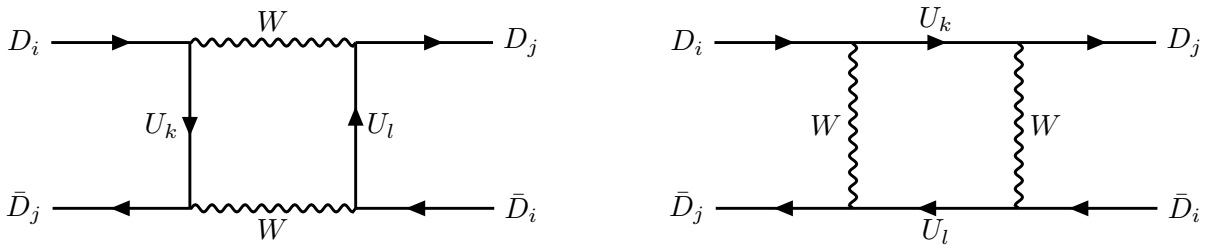

Figure 3: Loop-mediated meson oscillations: $M \leftrightarrow \bar{M}$.

derivative of both left-handed doublets and right-handed singlets, we arrive at:

$$\mathcal{L}_W = \frac{g}{\sqrt{2}} \sum_{\alpha} \bar{\nu}_\alpha \not{W}^+ P_L \, \ell_\alpha + \frac{g}{\sqrt{2}} \sum_{i,j} \bar{U}_i \not{W}^+ \left(V_{\rm CKM}\right)_{ij} P_L D_j + \text{h.c.}\,, \tag{32}$$

$$\mathcal{L}_{Z,A} = \frac{g}{c_w} \sum_{\psi} \left[\bar{\psi} \not{Z} \left(t_L^3 P_L - s_w^2 q\right) \psi\right] + \sum_{\psi} e \, \bar{\psi} \not{A} Q \psi\,, \tag{33}$$

where here the $V_{\rm CKM} = V_D^L$, the unitary matrix we used to help us diagonalize the down-quark Yukawa coupling, commonly known as the Cabibbo-Kobayashi-Maskawa (CKM) matrix, P_L and P_R and the left and right-handed projectors, t_L^3 is the value of the third weak-isospin of ψ, and q the value of the charge of ψ, the values for different fermions are summarized in Table 1.

Notice how the photon field couples to charged fermion proportional to the value of their charge times the constant e, as predicted from QED. Where did the e come from? As a matter of fact $e = g c_w$, or in other words:

$$\frac{1}{e^2} = \frac{1}{g^2} + \frac{1}{g_Y^2}\,, \tag{34}$$

this relationship is not an accident, and it can actually be inferred from Eq. (17) as it was proven in [79]. The general statement arises from the possibility of having a unified theory, let us assume that the relationship in Eq. (17) gets modified $Q = \sum_i C_i T_i$, where T_i and C_i is a constant, we write Q as the linear combination of generators of bigger gauge groups, then:

$$\frac{1}{e^2} = \sum_i \frac{C_i^2}{g_i^2}\,, \tag{35}$$

where g_i is the gauge coupling of those bigger gauge groups. This relationship will prove useful in the next section.

A key feature of the SM is the presence of P violation in interactions of fermions and a W-boson. This can be clearly seen from the P_L projectors in Eq. (32). The immediate consequence of this is that only left-handed particles and right-handed anti-particles will participate in weak interactions with a W-boson (these interactions are commonly called charged-current interactions or CC interactions). The discovery of parity violation in β-decays [5, 6] was perhaps one of the most important discoveries in particle physics.

The presence of $V_{\rm CKM}$ in Eq. (32) interactions has rich phenomenological implications, one of which is meson oscillations. Meson oscillations are loop-mediated transitions between a meson to its own anti-particle, their diagrams are shown in Fig. 3, and their probabilities can be properly understood from the amplitude transition that can be calculated from QFT. Such processes

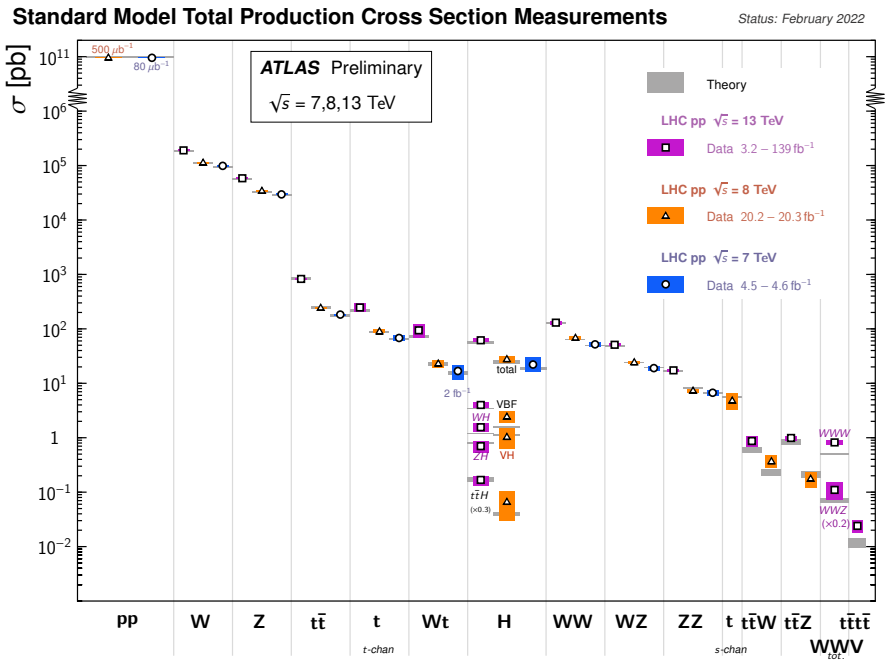

Figure 4: Measurement of the cross section for different SM processes compared to their prediction. Plot from [14].

would be impossible if the CKM matrix were diagonal. Moreover, the fact that the CKM matrix can be complex implies CP violation, one of its distinct features of it is that the transition $M \to \bar{M}$ has a different probability than $\bar{M} \to M$: weak interactions care about whether we're dealing with particles or anti-particles.

The possibility of seeing meson oscillations was first postulated in 1955 by non-other than Gell-Mann [80], and it inspired Bruno Pontecorvo to propose the possibility of oscillations between neutrinos[5] [83, 84]. But, according to the SM, neutrinos cannot oscillate. There is no mixing between neutrinos since there's no mass term that could induce mixing, or is there...?

2.4 Problems with the SM

The SM is a beautiful theory that models the interactions between fundamental particles. It is not beautiful for the shape, structure, or form it has, but rather because it accurately models reality, and what can be more beautiful than reality? Indeed, Fig. 4 shows the measurement of the cross-section of different processes compared to the predictions that the SM gives, and they all (with a few exceptions) give you a very accurate result.

But, for good or for evil, we know that the SM is not the final answer. There are a number of issues that SM cannot answer. We shall present some of them:

- **Neutrino masses and oscillations**: as we said before, the SM does not have a right-handed neutrino field, and therefore there is no neutrino mass term, no lepton mixing,

[5] Pontecorvo did other remarkable things, such as being the first to propose inverse-β decay to discover neutrinos [81] and was the first to suggest that there is a difference between electron and muon neutrinos [82]. He never won a Nobel Prize. As a matter of fact, the Nobel Prize for the discovery of the first neutrinos was given after the discovery of the muon neutrino, after his death. A former professor of mine claimed Pontecorvo never got a Nobel Prize because the academy didn't want to give it to a person who was a communist spy for the Soviet Union.

and no lepton oscillations. But as a matter of fact, we have already witnessed neutrino oscillations and transformations [16, 85, 86]. Indeed neutrino transformations due to propagation of neutrinos through matter [87, 88] witnessed from Solar Neutrino experiments are not predicted by the SM: for them to occur you require neutral current interactions that violate neutrino lepton flavor or neutrino masses. The discovery of neutrino oscillations by KamLAND showed us that neutrinos are massive.

- **Baryon asymmetry of the universe**: detailed studies of Big Bang Nucleosynthesis (BBN) [89] and the Cosmic Microwave Background (CMB) [21] indicate that there is an asymmetry between particles and anti-particles in the universe. Where did this asymmetry come from? Sakharov postulated three conditions that must be satisfied in order to generate baryon asymmetry [18]: baryon number non-conservation, C and CP violation, and thermal inequilibrium. The first condition is necessary, since if we had a universe that was baryon symmetric then baryon number violation is needed to generate it. The second condition is needed because if we had exact C and CP symmetries, then processes generating particles would occur at the same rate as anti-particles. And the third condition is necessary because if the universe were in thermal equilibrium, any process that can generate baryon asymmetry has an equal probability to the inverse process, thus any baryon asymmetry would be washed out. (a formal proof of the last condition can be found in any Cosmology book, see e.g., Chapter 11 of [90])

  The SM conserved both baryon number (B) and lepton number (L), but only on perturbative processes. The SM has non-perturbative terms which can generate B violating processes [22, 91]. As we saw in the previous section, there is CP violation in the SM, but it is actually not big enough for it to properly generate baryon asymmetry [92, 93]. Deviations from thermal equilibrium can only occur at very high energies [19]. The symmetry breaking related to the SM could've produced a first-order phase transition [91] had the Higgs boson been light enough [94]. The eventual discovery of the Higgs boson with its current mass falsified the SM as a source of thermal inequilibrium.

- **Dark Matter**: different astrophysical and cosmological observations indicate that the universe is not just made of SM particles, including the rotation curves of galaxies [95], the mass of galaxy clusters [20], bullet clusters [96] and the CMB itself [21]. We know that particle dark matter must follow a number of conditions for it to follow astrophysical observations, such as it being electrically neutral and stable. Neutrinos follow a lot of conditions and could be a viable dark matter candidate, but they do not comply with cosmological data. The density of neutrinos in the universe is not high enough to account for dark matter, they are not abundant enough or massive enough. The Standard Model does not account for dark matter.

- **Strong CP violation**: at its core, the so-called strong-CP problem is: why is the neutron dipole moment (nEDM) so small? The term generating the nEDM looks like $\mathcal{L} \sim d_n F_{\mu\nu} \bar{n} \sigma^{\mu\nu} i\gamma_5 n$. The explicit calculation that QCD (and by extension the SM) gives for d_n is $d_n = 3.2 \times 10^{-16}\, \theta\, \mathrm{e\,cm}$. (the explicit calculation can be found in Chapter 94 of [97]). The θ-parameter comes from the term $\mathcal{L} \sim \theta \epsilon^{\mu\nu\rho\sigma} G^a_{\mu\nu} G^b_{\rho\sigma}$ that was realized may

not necessarily be zero [98], satisfies all possible symmetries Yang-Mills symmetries and violates CP. The experimental value of $d_n \leq 1.8 \times 10^{-26}\,\mathrm{e\,cm}$ [99], which means that $|\theta| \lesssim 5 \times 10^{-11}$. This is the cusp of the problem strong CP problem, why is θ so small?[6]

- **Gravity**: the SM itself does not have a problem with gravity, but rather it is QFT itself that has a problem with gravity. It can easily be seen from the dimensions of the Newtonian Constant G, that a theory of gravity is non-renormalizable [7]. Non-renormalizable theories can be treated perturbatively until a certain energy scale. For processes with a center-of-mass energy above that energy scale, we must find a different theory that shall model interactions differently. For the non-renormalizable Fermi interaction which modeled β-decay, that energy scale was of the order of the SM vev, processes with high energy the W-boson revealed itself. The energy scale at which we can no longer treat Einstein's Theory in a perturbative way is above the Planck Scale $M_{\mathrm{PL}} \simeq 1 \times 10^{19}\,\mathrm{GeV}$, what will reveal itself at energies above?

2.5 Neutrino masses in the SM

What could possibly be the problem with introducing right-handed neutrino fields in the SM? Following the same procedure as before, let us add a right-handed neutrinos ν_R to Eq. (20) and (28):

$$\mathcal{L} = \mathcal{L}_{\mathrm{SM}} + \sum_{\alpha} i\,\bar{\nu}_{\alpha,R}\,\partial\!\!\!/\,\nu_{\alpha,R} - \sum_{\alpha,\beta} L_{\alpha,L}\cdot\tilde{\varphi}\,(Y_\nu)_{\alpha\beta}\,\nu_{\beta,R} + \mathrm{h.c.}\,, \tag{36}$$

much like in the quark case, this would induce mixing between different leptons and generate neutrino masses with $m_\nu \propto Y_\nu v$. Can we probe that the Higgs mechanism gives neutrinos their masses? A decay $\Gamma(h \to \nu\nu) \propto m_\nu^2/v^2$. Current bounds on neutrino masses have them at less that 1 eV. Seeing how we are yet to probe the Higgs mechanism even for electrons (see Fig. 2), it is unlikely that we would be capable of probing the Higgs mechanism for neutrinos. There is only one measurement for an invisible decay of the Higgs ($h \to ZZ^* \to \nu\nu\nu\nu$). To detect deviations from it would be unfeasible.

Eq. (36) has left us with a model for neutrino masses that proves itself very hard to probe. We can actually find a different mechanism that might be easier to probe. We have not written all the possible terms allowed in Eq. (36), we have missed one:

$$\mathcal{L} = \mathcal{L}_{\mathrm{SM}} + i\sum_{i} \bar{\nu}_{i,R}\partial\!\!\!/\,\nu_{i,R} - \sum_{\alpha,i} L_{\alpha,L}\cdot\tilde{\varphi}\,(Y_\nu)_{\alpha i}\,\nu_{i,R} - \frac{1}{2}\sum_{i,j}\bar{\nu}^C_{i,R}\,(M_R)_{i,j}\,\nu_{j,R} + \mathrm{h.c.}\,, \tag{37}$$

where M_R is a Majorana mass matrix, and the super-index C indicates charge-conjugated ($\psi^C = -i\gamma_2\psi^*$ in the chiral basis of Gamma matrices). This last term would not be allowed if we imposed a symmetry that conserves lepton number. How can this be any different from the usual SM

[6] There are some arguments against this is either a problem or not. What is the problem with it being so small? The Yukawa coupling of the electron is also quite small and that's not a problem [100]. We shall not address these debates anymore during this thesis.

[7] As a matter of fact, gravity is renormalizable at one-loop [101], but not at two-loops [25].

case? After SSB we will obtain:

$$\begin{aligned} -\mathcal{L}_{\text{mass}} &= \bar{\nu}_L M_D \nu_R + \frac{1}{2}\,\bar{\nu}_R^C\, M_R \nu_R + \text{h.c.} \\ &= \frac{1}{2}\begin{pmatrix}\bar{\nu}_L & \bar{\nu}_R^C\end{pmatrix}\begin{pmatrix}0 & M_D \\ M_D^T & M_R\end{pmatrix}\begin{pmatrix}\nu_L^C \\ \nu_R\end{pmatrix} + \text{h.c.}\,, \end{aligned} \tag{38}$$

where $M_D = \frac{1}{\sqrt{2}}\, v Y_\nu$ (do not confuse M_D with the mass matrix for down quarks!), is a mass term that we shall call *Dirac Mass Matrix*. The M_D^T term was obtained from the transpose of $\bar{\nu_L} M_D \nu_R$. Here it is quite clear that the mass terms of ν_L and ν_R mix with one another. They will have different masses. How can this be possible? How can it be possible that the right-chiral component and the left-handed component of the ν field to have different masses? These will actually be two different particles: two different Majorana particles. To avoid any potential confusion, we will now use N_R instead of ν_R.

We must diagonalize the matrix in Eq. (38) to obtain the mass spectrum. We will use a unitary matrix U:

$$U^\dagger \begin{pmatrix}0 & M_D \\ M_D^T & M_R\end{pmatrix} U^* = \begin{pmatrix}M_\nu & \\ & M_N\end{pmatrix}. \tag{39}$$

The most general form of U is:

$$U = \begin{pmatrix}c & s \\ -s^\dagger & \hat{c}\end{pmatrix} = \begin{pmatrix} \displaystyle\sum_{n=0}^{\infty} \frac{(-\Theta\Theta^\dagger)^n}{2n!} & \displaystyle\sum_{n=0}^{\infty} \frac{(-\Theta\Theta^\dagger)^n}{(2n+1)!}\Theta \\ -\displaystyle\sum_{n=0}^{\infty} \frac{(-\Theta^\dagger\Theta)^n}{(2n+1)!}\Theta^\dagger & \displaystyle\sum_{n=0}^{\infty} \frac{(-\Theta^\dagger\Theta)^n}{2n!} \end{pmatrix} \simeq \begin{pmatrix} I & \Theta \\ -\Theta^\dagger & I \end{pmatrix}, \tag{40}$$

where we will see later on the justification of the approximation in the last term to the right.

The diagonalization gives us the following relationships:

$$M_\nu = -M_D \frac{1}{M_N} M_D^T = -\Theta M_N \Theta^T\,, \tag{41}$$

with $M_N \simeq M_R$. This is the famous **Seesaw relationhip** [33, 34, 102], in its original conception we can easily see small neutrino masses naturally emerging: if $M_N \gg M_D$, then M_ν will be very small. This, in turn, will also make $\Theta = M_D\, M_N^{-1}$ very small.

M_ν may not necessarily be diagonal, but we can choose M_M (and thus M_N) to be so without any loss of generality. We must, therefore, also diagonalize M_ν with the neutrino-analog of the CKM matrix: V_ν, the Pontecorvo-Maki-Nakagawa-Sakata matrix (PMNS matrix). Thus:

$$V_\nu m_\nu V_\nu^T = -\Theta M_N \Theta^T\,, \tag{42}$$

where m_ν is a diagonal matrix. The diagonalization also implies mixing between the active neutrinos and the heavy singlets (which we will refer to as *heavy neutral leptons* or HNLs):

$$\begin{aligned} \nu_L &\to V_\nu \nu_L + \Theta N_L^C\,, \\ N_R &\to -\Theta^T V_\nu^* \nu_L^C + N_R\,, \end{aligned} \tag{43}$$

this mixing will thus produce interactions between HNLs and the rest of the SM particles, in exactly the same way that neutrinos interact with the rest of the SM particles, but suppressed by this mixing matrix Θ.

It is not clear how many of these singlets or *right-handed neutrino* fields we can add. In principle, we can add as many as we wish. If we added $\mathcal{N}$ of them, then M_M is a $\mathcal{N}\times\mathcal{N}$ matrix, M_D a $3\times\mathcal{N}$ matrix, U a $(3+\mathcal{N})\times(3+\mathcal{N})$ matrix and Θ a $3\times\mathcal{N}$ one.

We can write the interactions between neutral leptons and gauge bosons as [8]:

$$\mathcal{L}_W = \frac{g}{\sqrt{2}}\sum_{\alpha,i}\ell_\alpha \not{W}^- \,(\mathcal{U})_{i,\alpha}\, P_L n_i + \text{h.c.}\,, \tag{44}$$

$$\mathcal{L}_Z = \frac{g}{2c_w}\sum_{i,j}\bar{n}_i \not{Z}\,(\mathcal{C})_{i,j}\, P_L n_j\,, \tag{45}$$

where here n_i can be either an active neutrino mass state or an HNL, $\mathcal{U}$ is a $3\times(3+\mathcal{N})$ defined as $\mathcal{U} = \begin{pmatrix} V & \Theta \end{pmatrix}$, and $\mathcal{C} = \mathcal{U}^\dagger\mathcal{U}$.

Now we have a clear way to probe the mass generation of neutrinos: if we find an HNL, then we would say that neutrino masses are generated by the so-called **Type-I Seesaw matrix**. But there is an issue: let's take $m_\nu \simeq 1\,\text{eV}$ and $M_N \simeq 1\,\text{GeV}$, this implies $\Theta \simeq m_\nu/M_N \simeq 1\times10^{-9}$. Then, the decay $\Gamma(W\to N\ell) \simeq |\Theta|^2 \simeq 1\times10^{-18}$. It seems to be unprobable!

The above argument is true if we only had one HNL and one neutrino. If we add more generations of neutrinos and HNLs, then we would have more free parameters. Solving for Θ in Eq. (42) gives us:

$$\Theta = \pm iV\sqrt{m_\nu}\,O\frac{1}{\sqrt{M_N}}\,, \tag{46}$$

where O is a semi-orthogonal matrix of dimensions $3\times\mathcal{N}$. This is the so-called Casas-Ibarra parametrization [103]. This parametrization of Θ will always ensure the Seesaw relation. The freedom of the choice of this matrix O allows us to choose values of Θ that are probable. To see why, as an example, let's take the number of neutrinos and HNLs to be only two, then we can choose O as:

$$O_2 = \begin{pmatrix} \cos\omega & \sin\omega \\ -\sin\omega & \cos\omega \end{pmatrix}, \tag{47}$$

we can choose any value of ω and O_2 will be orthogonal, thus we can choose $\omega \simeq i\,\text{Im}(\omega)$, and if $\text{Im}(\omega) \gg 1$, then:

$$O_2 \simeq \frac{e^{\text{Im}(\omega)}}{2}\begin{pmatrix} 1 & i \\ -i & 1 \end{pmatrix}. \tag{48}$$

We can choose $\text{Im}(\omega)$ to be as big as we want to, as long as perturbativity allows for it. What is happening is that there is a symmetry, our choice of O and later of Θ imposes a lepton-number conserving symmetry. Neutrino masses are no longer kept small due to a difference between scales, but rather because a L-symmetry keeping them small.

There is an interesting phenomenological feature behind this, and it is that processes that violate lepton number (or LNV processes), like neutrinoless double-beta decay ($0\nu\beta\beta$), are sup-

[8] There are some technicalities with the Z vertex that are different between Dirac and Majorana particles that are addressed in Appendix A

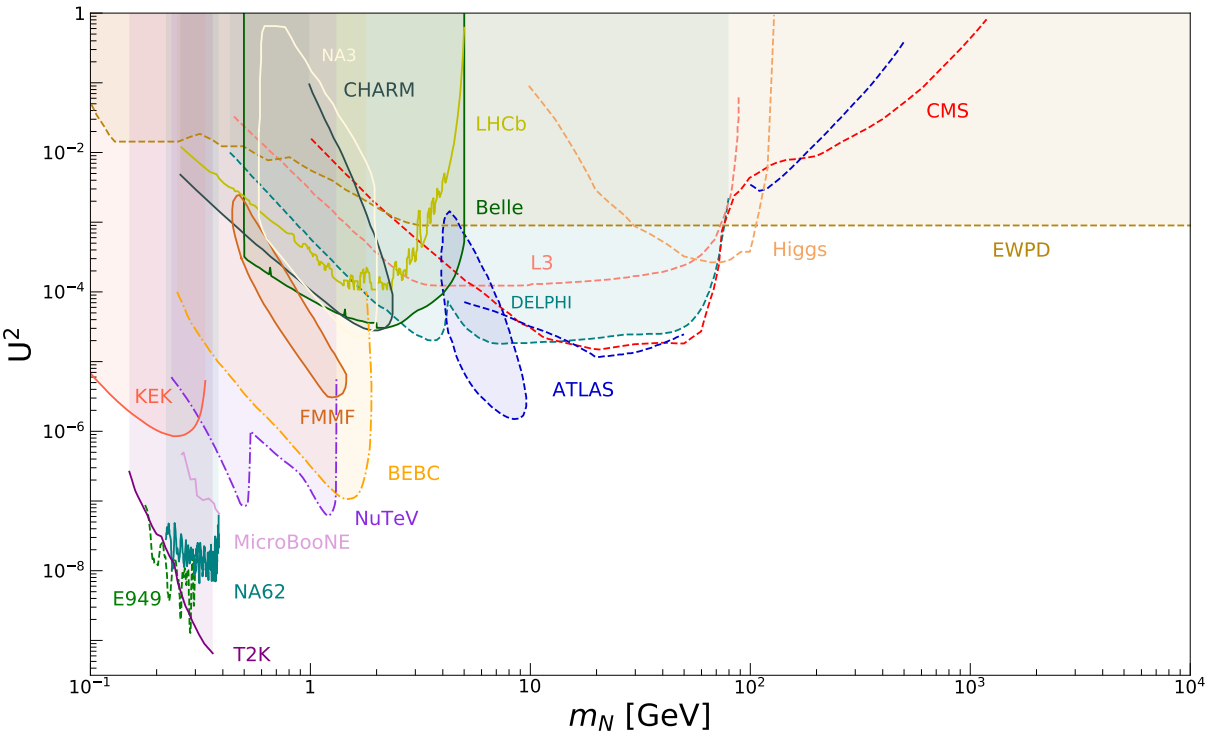

Figure 5: Constraints adapted from [104] (for the information on all the constraints and others, see all the references therein), the vertical axis is the Θ_μ coupling.

pressed to the order of neutrino masses.

Now we have a model of neutrino masses that we could probe. Multiple searches and different constraints have been performed throughout the years. BBN severely constrains them to be above the MeV scale [105, 106] (unless they have a very small coupling, indeed, keV HNLs dark matter candidates [105]), whereas other low-energy processes like cLFVs could constraint PeV HNLs [107]. We highlight the constraints from different experiments in Fig. 5.

Moreover, besides this model being a model for neutrino masses, the incorporation of two HNLs with almost degenerate masses can also generate baryon asymmetry of the universe [35, 108, 109], and as we mentioned in parenthesis in the paragraph above a keV HNL is a dark matter candidate. This is the most minimal model that can explain three of the problems the SM has: neutrino masses and oscillations, baryon asymmetry of the universe, and dark matter.

2.6 Other mass models for neutrinos

Let us briefly mention other mechanisms for the generations of neutrino masses. Besides the type-I Seesaw, we also have the so-called **Type-II Seesaw mechanism**. This mechanism adds a $\mathrm{SU}(2)_L$ triplet with $Y = 2$:

$$\Delta = \begin{pmatrix} \frac{\delta^+}{\sqrt{2}} & \delta^{++} \\ \delta^0 & -\frac{\delta^+}{\sqrt{2}} \end{pmatrix}, \qquad \Delta \to \mathbf{U}\Delta\mathbf{U}^\dagger, \tag{49}$$

where the second relations shows the transformation that Δ has that leaves the Lagrangian invariant, here $\mathbf{U} = e^{i\alpha(x)^a T_L^a}$. The addition of this triplet allows us the inclusion of the Yukawa

term:

$$\mathcal{L}_{Y,\Delta} = -\sum_{\alpha,\beta} \bar{L}^{C}_{L,\alpha} \left(Y_L\right)_{\alpha,\beta} \cdot \left(i\sigma^2 \cdot \Delta\right) \cdot L_{L,\beta} + \text{h.c.}\,. \tag{50}$$

This new scalar will acquire a different vev from the Higgs one, which we shall call v_L, and will sit at the component where δ^0 sits. After SSB we will get four different massive scalars, two doubly-charged scalars, one charged, and two neutral ones. All the scalars will have very similar masses m_Δ. The new Yukawa term will thus give a Majorana mass term to neutrinos:

$$M_\nu = \sqrt{2}\, Y_L v_L = Y_L \frac{\kappa v^2}{m_\Delta^2}\,, \tag{51}$$

where κ is a parameter with mass dimension one that enters the potential. This is also some sort of Seesaw mechanism: neutrino masses are small because of a difference of scales: we allow the triplet to have heavier masses compared to v^2, which will leave neutrino masses small. The curious reader can find more information on Type-II Seesaw from [110].

There are other *Seesaw mechanisms*, the type-III Seesaw involves the addition of lepton triplets [111], the inverse Seesaw and linear Seesaw requires the addition of more scalars, and the right-handed singlet field [112, 113],

Recently models where neutrinos obtain their masses due to a loop-mediated term have also acquired popularity in recent years [114]. The idea is self-explanatory: neutrinos are naturally light because they do not occur at tree-level. These models require the addition of further scalar and/or fermion fields, some of which are dark matter candidates (these models are usually called scotogenic models, scoto comes from the Greek for dark and genic from the word birth: neutrinos are born from darkness). There is a generic classification of these models depending on the topology of the loop-diagram involved [115]. These models are sometimes called type-IV, type-V, and type-VI Seesaws.

We can also generate neutrino masses from the appearance of bigger gauge groups, from a Grand Unified Theory (GUT) like SO(10), for example. Bigger GUT groups force us to include different fields and interactions which can generate neutrino masses at tree or loop-level. The following section will devote itself to one of these models.

We can parametrize all mechanisms for the generation of Majorana neutrino masses from the Weinberg Operator. Weinberg showed that the operator of the lowest dimension that gives you neutrino masses that also follows the symmetries of the $\mathcal{G}_{\text{EW}}$ is [116] without the additional fields to the original the SM has[9]:

$$\mathcal{L}_{5-dim} = \frac{1}{2}\frac{C^5_{\alpha\beta}}{\Lambda}\left[\bar{L}_{L,\alpha} \cdot \tilde{\varphi}\, \tilde{\varphi}^T \cdot L_{L,\beta}\right] + \text{h.c.}\,, \tag{52}$$

after SSB, we shall acquire a Majorana mass term: $M_\nu = C^5 v^2/\Lambda$. Here Λ is an energy scale where the Weinberg Operator will no longer be valid, and we ought to work with a more fundamental theory. Leaving $C^5 = 1$, one finds that $\Lambda \simeq 1 \times 10^{15}\,\text{GeV}$, which by complete numerical accident is the at the GUT scale (the energy scale of GUTs comes from constraints on proton decay). This implies that the mechanism which gives neutrinos their masses lies at the GUT

[9] An analog to Weinberg Operator for Dirac Neutrinos requires the addition of right-handed neutrino fields. The shape of the Dirac-Weinberg operator can be found in [117, 118].

scale unless the parameter C is very small. The GUT scale should rather only be taken as the upper value of the energy scale at which neutrinos acquire their masses.

2.7 Where to look for new physics?

Now that we've unveiled the fact that the SM is incomplete and needs extensions, it is natural to ask: where should we search for new physics?

We have two different frontiers to be explored, the **energy frontier** and the **intensity frontier**.

At the energy frontier, we are looking for new physics that would show itself at higher energy scales. The searches at the intensity frontier look for new physics that could be accessed at the current energy scale of experiments but has suppressed interactions due to a weak coupling. In some sense, the energy frontier aims for a higher Λ whereas the intensity frontier looks for a lower C in an Effective Operator that encompasses new physics like the Weinberg Operator in Eq. (52).

Searches at the energy frontier are typically done by high-energy colliders. The intensity frontier is probed by many different experiments, even high-energy colliders can probe it with higher values of luminosity, but as well with low-energy experiments, neutrino experiments, or fixed-target experiments, which look for tiny deviations from predictions of the SM from unbeknownst feebly interacting particles.

3 Left-Right Symmetric Model

Left-right symmetric models are based on an extension of the $\mathcal{G}_{\text{EW}}$ group:

$$\mathcal{G}_{\text{LRSM}} = \text{SU}(2)_R \times \text{SU}(2)_L \times \text{U}(1)_{B-L}\,, \tag{53}$$

where $B - L$ here is baryon number minus lepton number. Much like in the SM, the idea is to break this group, first to the SM group and subsequently to $\text{U}(1)_Q$:

$$\begin{array}{c} \text{SU}(2)_R \times \text{SU}(2)_L \times \text{U}(1)_{B-L} \\ \Big\downarrow v_R \\ \text{SU}(2)_L \times \text{U}(1)_Y \\ \Big\downarrow v \\ \text{U}(1)_Q \end{array} \tag{54}$$

There may have been a larger group for example, some symmetry-breaking patterns of SO(10) can lead to $\text{SU}(3)_C \times \mathcal{G}_{\text{LRSM}}$.

The idea behind gauge theories that follow $\mathcal{G}_{\text{LRSM}}$ comes from an aim to explain parity violation merely as a low-energy phenomenon. As soon as we turn up to a higher scale, parity will no longer be violated [30–34].

In addition to $\mathcal{G}_{\text{LRSM}}$ we also include a discrete symmetry to the theory, which comes in the form of a generalized charge ($\mathcal{C}$) or parity ($\mathcal{P}$) conjugation. Including one of these discrete symmetries reduces the number of free parameters in the theory and makes the particle content left-right symmetric.

From the symmetry breaking pattern in Eq. (54) we can notice some relationships between the different charges from different scales, analogous to Eq. (17):

$$\frac{Y}{2} = T_R^3 + \frac{B-L}{2}\,, \tag{55}$$

there will also be an analogous relationship between the gauge couplings like in Eq. (35) we have:

$$\frac{1}{g_Y^2} = \frac{1}{g_R^2} + \frac{1}{g_{B-L}^2}\,, \tag{56}$$

where g_R is the coupling of the $\mathcal{SU}(2)_R$ gauge group and g_{B-L} of the $\mathcal{U}(1)_{B-L}$ one.

3.1 Particle content

The particle content will also get extended, just as we had the left-handed doublet fields (see Eq. (18)), we will also have right-handed doublets:

$$\begin{aligned} &\text{Left-handed doublets:} \quad L_{L,\alpha} = \begin{pmatrix} \nu_{\alpha,L} \\ \ell_{\alpha,L} \end{pmatrix} , \quad Q_{i,L} = \begin{pmatrix} U_{i,L} \\ D_{i,L} \end{pmatrix} , \\ &\text{Right-handed doublets:} \quad L_{R,\alpha} = \begin{pmatrix} N_{\alpha,R} \\ \ell_{\alpha,R} \end{pmatrix} , \quad Q_{i,R} = \begin{pmatrix} U_{i,R} \\ D_{i,R} \end{pmatrix} , \end{aligned} \tag{57}$$

where left-handed doublets are $\mathrm{SU}(2)_R$ singlets and right-handed doublets are $\mathrm{SU}(2)_L$ singlets. Both lepton doublets have a $B - L$ of -1 and both quark doublet of $1/3$.

And for the scalar field, we will include three different scalar fields an SU_R triplet, an $\mathrm{SU}(2)_L$ triplet, and a bi-doublet, a doublet in the $\mathrm{SU}(2)_L$, and a doublet of $\mathrm{SU}(2)_R$, but the latter under its complex representation:

$$\Delta_{R,L} = \begin{pmatrix} \frac{\delta^+_{R,L}}{\sqrt{2}} & \delta^{++}_{R,L} \\ \delta^0_{R,L} & -\frac{\delta^+_{R,L}}{\sqrt{2}} \end{pmatrix} , \qquad \Phi = \begin{pmatrix} \phi_1^{0*} & \phi_2^+ \\ -\phi_1^- & \phi_2^0 \end{pmatrix} \tag{58}$$

where $\Delta_{R,L}$ are the triplets and Φ is the bi-doublet, both triplets have a $B - L = 2$, and the bidoublet $B - L = 0$. Δ_R. They transform under gauge transformations as:

$$\Delta_{R,L} \to \mathbf{U}_{R,L} \Delta_{R,L} \mathbf{U}^\dagger_{R,L} , \qquad \Phi \to \mathbf{U}_L \Phi \mathbf{U}^\dagger_R , \tag{59}$$

with $\mathbf{U}_{R,L} = \exp\Big(i\, \alpha^a_{R,L}\, T^a_{R,L} \Big)$. There is also, of course, the $\mathrm{U}(1)_{B-L}$ abelian transformations.

Furthermore, we will also have our gauge bosons. We will have the same three gauge bosons of the $\mathrm{SU}(2)_L$ group (we will call them $W^a_{L,\mu}$), and we will also have the three gauge bosons of the $\mathrm{SU}(2)_R$ group ($W^a_{R,\mu}$) and a gauge boson of the $\mathrm{U}(1)_{B-L}$ group ($B_{B-L,\mu}$).

At this point, we must emphasize something which we mentioned at the start of this section. We will also include a generalized discrete $\mathcal{P}$ or $\mathcal{C}$ conjugation, so we will require the Lagrangian to be invariant under:

$$\begin{aligned} \mathcal{P} &: \{\Phi, \Delta_L, \Delta_R\} \leftrightarrow \left\{ \Phi^\dagger, \Delta_R, \Delta_L \right\} , \\ \mathcal{C} &: \{\Phi, \Delta_L, \Delta_R\} \leftrightarrow \left\{ \Phi^T, \Delta^*_R, \Delta^*_L \right\} , \end{aligned} \tag{60}$$

for the scalar sector and:

$$\begin{aligned} \mathcal{P} &: \left\{ W^a_{L,\mu}, B_{\mu,B-L}, Q_L, L_L \right\} \leftrightarrow \left\{ W^a_{R,\mu}, B_{B-L,\mu}, Q_R, L_R \right\} , \\ \mathcal{C} &: \left\{ W^a_{L,\mu}, B_{B-L,\mu}, Q_L, L_L \right\} \leftrightarrow \left\{ -W^a_{R,\mu}, B_{B-L,\mu}, Q^C_R, L^C_R \right\} , \end{aligned} \tag{61}$$

for the gauge and fermion sector.

As it is clear from these transformations, these were inspired by the usual C and P conjugations. The imposition of either of these discrete symmetries forces us to make the particle content left-right symmetric, a right-handed triplet implies a left-handed one; three left-handed neutrinos imply three right-handed ones.

From this, we can now write our Lagrangian:

$$\begin{aligned}\mathcal{L}_{\text{LRSM}} = &-\frac{1}{2}\operatorname{tr}\left[\mathbf{W}_{R,\mu\nu}\mathbf{W}_R^{\mu\nu}\right] - \frac{1}{2}\operatorname{tr}\left[\mathbf{W}_{L,\mu\nu}\mathbf{W}_L^{\mu\nu}\right] - \frac{1}{4}B_{B-L,\mu\nu}\,B_{B-L}^{\mu\nu} \\ &+ i\sum \bar{\Psi}_L \not{D}\Psi_L + i\sum \bar{\Psi}_R \not{D}\Psi_R + \operatorname{tr}\left|D_\mu\Delta_L\right|^2 + \operatorname{tr}\left|D_\mu\Delta_R\right|^2 + \operatorname{tr}\left|D_\mu\Phi\right|^2 \\ &- \Big[\bar{Q}_L\cdot\left(Y_1^Q\Phi + Y_2^Q\tilde{\Phi}\right)\cdot Q_R + \bar{L}_L\cdot\left(Y_1^\ell\Phi + Y_2^\ell\tilde{\Phi}\right)\cdot L_R \\ &+ \frac{1}{2}\,\bar{L}_L^C\,Y_L\cdot(i\sigma_2\cdot\Delta_L)\cdot L_L + \frac{1}{2}\,\bar{L}_R^C\,Y_R\cdot(i\sigma_2\cdot\Delta_R)\cdot L_R + \text{h.c.}\Big] + V(\Delta_L,\Delta_R,\Phi)\,,\end{aligned} \tag{62}$$

where all the different Y are different Yukawa matrices, $W_R^{\mu\nu}, W_L^{\mu\nu}$ and $B_{B-L}^{\mu\nu}$ should be understood as the usual strength tensors, $\tilde{\Phi} = \sigma_2\cdot\Phi^*\cdot\sigma_2$, and $V(\Delta_L,\Delta_R,\Phi)$ is the scalar potential. There have been multiple studies done on the potential alone, its symmetries, structure, the mass spectrum of all scalar particles, the RGEs of their couplings, phenomenology... [119–125]. A complete review of it is beyond the scope of this thesis, and shall not be mentioned again.

The covariant derivatives look like:

$$D_\mu\Psi = \left[\partial_\mu - ig_L\,W_{L,\mu}^a T_L^a - ig_R\,W_{R,\mu}^a T_R^a - ig_{B-L}\,B_{B-L,\mu}\left(\frac{B-L}{2}\right)\right]\Psi\,, \tag{63}$$

$$D_\mu\Delta_{R,L} = \partial_\mu\Delta_{R,L} - ig_{R,L}W_{R,L;\mu}^a\left[T_{R,L}^a,\Delta_{R,L}\right] - ig_{B-L}B_{B-L,\mu}\Delta_{R,L}\,, \tag{64}$$

$$D_\mu\Phi = \partial_\mu\Phi - ig_L W_{L,\mu}^a T_L^a\Phi - ig_R W_{R,\mu}^a\Phi T_R^a\,. \tag{65}$$

This is a good point to stress one of the consequences of our $\mathcal{P}$ or $\mathcal{C}$ invariance. Thanks to it $g_L = g_R = g$. This can be seen from any of the kinetic terms, for example.

3.2 Symmetry breaking and gauge boson mass spectrum

As it was shown from the symmetry breaking pattern in (54), we will require a few vevs. The presence of these vevs will not only break $\mathcal{G}_{\text{LRSM}}$ but will also break the discrete symmetry. The vevs will be in the following positions of the scalars:

$$\begin{gathered}\langle\Delta_R\rangle = \frac{1}{\sqrt{2}}\begin{pmatrix}0 & 0\\ v_R & 0\end{pmatrix}\,, \qquad \langle\Delta_L\rangle = \frac{1}{\sqrt{2}}\,e^{i\beta_L}\begin{pmatrix}0 & 0\\ v_L & 0\end{pmatrix}\,, \\ \langle\Phi\rangle = \frac{1}{\sqrt{2}}\begin{pmatrix}v_1 & 0\\ 0 & v_2\,e^{i\alpha}\end{pmatrix}\,,\end{gathered} \tag{66}$$

in general, all vevs could be complex, but we can rotate away two complex phases from the gauge transformations, therefore, we can choose v_R and v_1 to be real, without any loss of generality. We can parameterize v_1 and v_2 in a different way:

$$\begin{aligned}v_1 &= v\,c_\beta\,,\\ v_2 &= v\,s_\beta\,,\end{aligned} \tag{67}$$

where v is the SM vev, $s_\beta = \sin\beta, c_\beta = \cos\beta$, and β is an arbitrary angle that dictates the direction of the vev. At this point we can answer a question that may or may not have crossed

the reader's mind: where is the SM Higgs? We can re-write the definition of the bi-doublet in Eq. (58) as it is composed of two $\mathrm{SU}(2)_L$ doublets explicitly[10]:

$$\Phi = \begin{pmatrix} i\sigma_2\,\varphi_1^* & \varphi_2 \end{pmatrix}, \tag{68}$$

with $\varphi_i = \begin{pmatrix} \phi_i^+ \\ \phi_i^0 \end{pmatrix}$.

The SM doublet, defined in Eq. (19), is a linear combination of both of these scalars:

$$\varphi_{\mathrm{SM}} = c_\beta\,\varphi_1 + s_\beta\,e^{-i\alpha}\,\varphi_2\,, \tag{69}$$

$$\varphi_{\mathrm{FV}} = -s_\beta e^{i\alpha}\,\varphi_1 + c_\beta\,\varphi_2\,. \tag{70}$$

The linear combination in the first line is our SM doublet, whereas the one in the second line is a different doublet. Notice how the SM doublet has a vev corresponding to the one the Higgs has, whereas the second doublet, φ_{FV} does not have a vev. The index FV will make sense as the text progresses.

There is a hierarchy concerning the doublets, we expect:

$$v_L \ll v \ll v_R\,, \tag{71}$$

because v_R is the scale of the LRSM, and v_L, as one could anticipate from the conversation in Section 2.6 with regards to the Type-II Seesaw with an $\mathrm{SU}(2)_L$ doublet, will be directly proportional to neutrino masses.

We can repeat the procedure we did with regard to the SM and aim to obtain the mass spectrum for gauge bosons. Without doing any calculations we can already predict that we will obtain a massless particle: the photon, the gauge particle related to the unbroken $\mathrm{U}(1)_Q$ group. The mass terms will once again come from the kinetic terms of the scalars after redefining them so that they have the appropriate vacuum. For the charged sector:

$$\mathrm{tr}\,|D_\mu \Delta_R|^2 \supset \frac{1}{2}\,g^2\,v_R^2\,W_{R,\mu}^+\,W_R^{-\mu}\,, \tag{72}$$

$$\mathrm{tr}\,|D_\mu \Phi|^2 \supset \frac{1}{4}\,g^2\,v^2\left[W_{L,\mu}^+\,W_L^{-\mu} + W_{R,\mu}^+\,W_R^{-\mu} - W_{L,\mu}^+\,W_R^{-\mu}\;s_{2\beta}\,e^{i\alpha} - W_L^{-\mu}\,W_{R,\mu}^+ s_{2\beta}\,e^{-i\alpha}\right], \tag{73}$$

where we shall neglect v_L. We can immediately notice that there is a mixing in the mass terms of W_L and W_R. We can more compactly parameterize the mass terms with a matrix:

$$\mathcal{L}_{W-\mathrm{mass}} = \frac{g^2}{4}\begin{pmatrix} W_{R,\mu}^+ & W_{L,\mu}^+ \end{pmatrix}\begin{pmatrix} 2\,v_R^2 + v^2 & -v^2\,s_{2\beta}\,e^{-i\alpha} \\ -v^2\,s_{2\beta}\,e^{i\alpha} & v^2 \end{pmatrix}\begin{pmatrix} W_R^{-\mu} \\ W_L^{-\mu} \end{pmatrix}, \tag{74}$$

the factor of 2 multiplying the v_R^2 stems from the fact related that the mass comes from a triplet, instead of a doublet, this is related to our discussion regarding the ρ parameter of the SM and how it probed the representation under which the scalar of the SM transforms. We need the

[10] We could also write them as two $\mathrm{SU}(2)_R$ doublets, but it would be with two-row vectors instead of two column vectors

eigenvalues to obtain the masses of our particles, these are:

$$M^2_{W_R} \simeq \frac{1}{2}\, g^2\, v_R^2\,, \qquad\qquad M^2_{W_L} \simeq \frac{1}{4}\, g^2\, v^2\,, \tag{75}$$

this mixing will also imply that the gauge bosons will mix at interactions. This mixing is dictated by a unitary matrix which also serves to diagonalize the matrix in Eq. (74):

$$\begin{pmatrix} W_R^{-\mu} \\ W_L^{-\mu} \end{pmatrix} \to \begin{pmatrix} \cos\xi_W & \sin\xi_W e^{-i\eta} \\ -\sin\xi_W e^{i\eta} & \cos\xi \end{pmatrix} \begin{pmatrix} W_R^{-\mu} \\ W_L^{-\mu} \end{pmatrix}\,, \tag{76}$$

with $\eta = \alpha$ and $\tan(2\xi_W) = \frac{v^2}{v_R^2}\, s_{2\beta}$. We can find an approximate expression for both $\cos\xi_W$ and $\sin\xi_W$ in the case where $v^2 \ll v_R^2$:

$$\cos\xi_W \simeq 1\,, \qquad \sin\xi_W \simeq \xi_W \simeq \frac{v^2}{2\, v_R^2}\, s_{2\beta} \simeq \frac{M^2_{W_L}}{M^2_{W_R}}\, s_{2\beta}\,. \tag{77}$$

The neutral sector of gauge particles will also mix, just as in the SM there was mixing between W_L^3 and B_Y, but in this case, we will have mixing between W_L^3, W_R^3 and B_{B-L}. We can easily repeat the procedure we did for the charged sector, there will be contributions from both v_R and v. Here the matrix looks like this:

$$\mathcal{L}_{\text{n-mass}} = \frac{1}{2}\begin{pmatrix} W^3_{R,\mu} & W^3_{L,\mu} & B_{B-L,\mu} \end{pmatrix} \begin{pmatrix} g^2\, v_R^2 + \frac{1}{4}\, g^2 v^2 & -\frac{1}{4}\, g^2 v^2 & -g\, g_{B-L} v_R^2 \\ -\frac{1}{4}\, g^2 v^2 & \frac{1}{4}\, g^2 v^2 & 0 \\ -g\, g_{B-L} v_R^2 & 0 & g^2_{B-L} v_R^2 \end{pmatrix} \begin{pmatrix} W_R^{3\mu} \\ W_L^{3\mu} \\ B^\mu_{B-L} \end{pmatrix}\,, \tag{78}$$

the eigenvalues give:

$$M^2_{Z_R} \simeq g^2\, v_R^2\, \frac{c_w^2}{c_{2w}}\,, \qquad\qquad M^2_{Z_L} \simeq \frac{1}{4}\frac{g^2\, v^2}{c_w^2}\,, \qquad\qquad M^2_A = 0\,, \tag{79}$$

where we have used the fact that $g_{B-L} = g\frac{c_w}{\sqrt{c_{2w}}}$, which can be inferred from Eq. (56). From here we can already make a similar prediction to what the SM predicted to be the relations between the masses of the Z and W boson. We would expect $M_{Z_R} \simeq 1.69\, M_{W_R}$. This prediction gives us a nice way to falsify this specific version of the LRSM, the inclusion of different representations of different scalars should change the relationship between M_{Z_R} and M_{W_R}, akin to how the SM ρ-parameter would change depending on the representation of the scalar multiplet. The diagonalization is carried out by using an orthogonal matrix, which will mix all neutral gauge bosons:

$$\begin{pmatrix} Z_R^\mu \\ Z_L^\mu \\ A^\mu \end{pmatrix} = \begin{pmatrix} \cos\zeta_Z & -\sin\zeta_Z & 0 \\ \sin\zeta_Z & \cos\zeta_Z & 0 \\ 0 & 0 & 1 \end{pmatrix} \begin{pmatrix} 1 & 0 & 0 \\ 0 & c_w & -s_w \\ 0 & s_w & c_w \end{pmatrix} \begin{pmatrix} c_R & 0 & -s_R \\ 0 & 1 & 0 \\ s_R & 0 & c_R \end{pmatrix} \begin{pmatrix} W_R^{3\mu} \\ W_L^{3\mu} \\ B^\mu_{B-L} \end{pmatrix}\,, \tag{80}$$

where $c_R = \cos\theta_R = \frac{\sqrt{c_{2w}}}{c_w}$ and $s_R = \sin\theta_R = t_w$. We can interpret these three matrices as follows: the one with θ_R decouples W_R and B_{B-L} to give us the Z_R and B_Y, the latter is the same SM gauge field related to the $\mathrm{U}(1)_Y$ group; the rotation with θ_w is the SM one that decouples W_L and

B_Y to obtain Z_L and the photon, A; the last rotation is there because there is mixing between Z_L and Z_R, their decoupling is proportional to the angle ζ_Z, which is proportional to $\frac{v^2}{v_R^2}$:

$$\cos\zeta_Z \simeq 1 \qquad\qquad \sin\zeta_Z \simeq \zeta_Z \simeq -\frac{c_{2w}^{3/2}}{4\,c_w^4}\frac{v^2}{v_R^2} \simeq -\frac{c_{2w}^{3/2}}{2\,c_w^4}\frac{M_{W_L}^2}{M_{W_R}^2}\,, \tag{81}$$

which, unlike the mixing of the W-bosons, this one does not depend on the parameter β.

3.3 Quark interactions with scalars and mass spectrum

Let's now concentrate specifically on the first term of the third line of Eq. (63):

$$-\mathcal{L}_{\mathrm{Q}-\Phi} = \sum_{i,j} \bar{Q}_{i,L}\cdot\left[\left(Y_1^Q\right)_{i,j}\Phi + \left(Y_2^Q\right)_{i,j}\tilde{\Phi}\right]\cdot Q_{j,R} + \mathrm{h.c.}\,, \tag{82}$$

if we impose the Lagrangian to be invariant under the $\mathcal{C}$ or $\mathcal{P}$ transformations in Eq. (60) and (61), then we get restrictions on the Yukawa matrices:

$$\mathcal{P}: Y_i^Q = \left(Y_i^Q\right)^\dagger\,, \qquad\qquad \mathcal{C}: Y_i^Q = \left(Y_i^Q\right)^T\,. \tag{83}$$

We can also decouple the SM Yukawa couplings from the Yukawa coupling in the LRSM Lagrangian:

$$\begin{aligned} Y_U &= c_\beta\, Y_1^Q + s_\beta\, e^{-i\alpha}\, Y_2^Q\,,\\ Y_D &= s_\beta\, e^{i\alpha}\, Y_1^Q + c_\beta Y_2^Q\,, \end{aligned} \tag{84}$$

now, writing Eq. (82) in term of $Y_U, Y_D, \varphi_{\mathrm{SM}}$ and φ_{FV}:

$$\begin{aligned} -\mathcal{L}_{Q-\Phi} = \sum_{i,j}\Bigg\{ &\bar{Q}_{i,L}\cdot\left[\tilde{\varphi}_{\mathrm{SM}}\, Y_U + \tilde{\varphi}_{\mathrm{FV}}\,\left(\frac{Y_D - e^{i\alpha}\, s_{2\beta}\, Y_U}{c_{2\beta}}\right)\right]_{i,j} U_{j,R}\\ &+\bar{Q}_{i,L}\cdot\left[\varphi_{\mathrm{SM}}\, Y_D + \varphi_{\mathrm{FV}}\,\left(\frac{Y_U - e^{-i\alpha}\, s_{2\beta}\, Y_D}{c_{2\beta}}\right)\right]_{i,j} D_{j,R}\Bigg\} + \mathrm{h.c.}\,, \end{aligned} \tag{85}$$

where we remind the reader that $\tilde{\varphi} = i\sigma_2\varphi^*$.

The subindex FV should now make some sense, it stands for flavor violating: the vertices with either φ_{FV} or $\tilde{\varphi}_{\mathrm{FV}}$ induce tree-level interactions which violate quark flavor. These flavor-changing scalars can mediate processes such as $B-\bar{B}$ oscillations or affect the $K-\bar{K}$ mixing at tree-level, therefore, they are very constrained. We would be expecting them of the order $\mathcal{O}(10\,\mathrm{TeV})$ [126].

Notice how the restrictions in Eq. (83) also affect Y_U and Y_D, in the case of $\mathcal{C}$ both will be symmetric, but in the case of $\mathcal{P}$ we won't have them to be entirely hermitian, due to the α phase that appears in the vev.

As in the SM, Y_U, and Y_D may not necessarily be diagonal. We can try to perform a similar argument as the one we did for the SM model: the Lagrangian is still invariant under the transformations in Eq. (29) with the condition that $V_U^R = V_D^R = V_Q^R$, due to the fact that the

right-handed counterpart now forms a doublet. Moreover, if we wish to preserve $\mathcal{P}$ or $\mathcal{C}$:

$$\mathcal{P} : V_Q^L = V_Q^R = V_Q \,, \qquad\qquad \mathcal{C} : V_Q^L = \left(V_Q^R\right)^* = (V_Q)^* \,. \tag{86}$$

In the case of $\mathcal{C}$ there is no issue here, both Y_U and Y_D are symmetric matrices so $V_Q^T\, Y_U\, V_Q$ and $V_Q^T\, Y_D\, Y_Q$ can be chosen to be diagonal, but in the case of $\mathcal{P}$ we have a problem: $V_Q^\dagger\, Y_U\, V_Q$ and $V_Q^\dagger\, Y_D\, V_Q$ may not necessarily be diagonal because Y_U or Y_D are, in general, not hermitian. We can work on the limit where $s_\beta s_\alpha$ is small enough that we can take them to be almost hermitian[11]. In this limit, we can consider one of the Yukawa matrices to be diagonal.

But, once again, due to the fact that we can only choose one of these matrices to be diagonal, we shall again consider Y_U to be diagonal, and the diagonalization of Y_D will induce mixing in interactions with charged gauge bosons, both in the left-sector where the mixing will give us the usual CKM matrix $V_{\rm CKM}^L$, and in the right-sector where there will be a *right-handed CKM matrix* $V_{\rm CKM}^R$. Both of these are related to one another due to the discrete generalized symmetries:

$$\mathcal{P} : V_{\rm CKM}^L \simeq V_{\rm CKM}^R \,, \qquad\qquad \mathcal{C} : V_{\rm CKM}^L = V_{\rm CKM}^{R*} \,, \tag{87}$$

up to some complex phases, in general, both matrices should have 9 different complex phases, but we can remove some of the phases by changing the phase of the spinor fields: the left-handed CKM will only have one complex phase for 3 generations of quarks, the rotation may not necessarily remove the same phases for the right-handed CKM matrix, and this will be the case of $\mathcal{C}$, where the right-handed CKM matrix will differ in having five more phases. In the case of $\mathcal{P}$, they will not differ in the number of phases.

3.4 Lepton interactions with scalars, mass spectrum and Seesaw mechanism

For leptons, we have three different terms: interactions with the bi-doublet and interactions with both triplets. We did not have the interactions between triplets and quarks because these interactions would violate $B - L$. Let's write both of these interactions separately:

$$-\mathcal{L}_{L-\Phi} = \sum_{\alpha,\beta} \bar{L}_{\alpha,L} \cdot \left[\left(Y_1^\ell\right)_{\alpha,\beta} \Phi + \left(Y_2^\ell\right)_{\alpha,\beta} \tilde{\Phi} \right] \cdot L_{\beta,R} + \text{h.c.} \,, \tag{88}$$

$$\begin{aligned} -\mathcal{L}_{L-\Delta} = \frac{1}{2} \sum_{\alpha,\beta} \Big[& \bar{L}^C_{\alpha,L} \left(Y_L\right)_{\alpha,\beta} \cdot (i\sigma_2 \cdot \Delta_L) \cdot L_{\beta,L} \\ & + \bar{L}^C_{\alpha,R} \left(Y_R\right)_{\alpha,\beta} \cdot (i\sigma_2 \cdot \Delta_R) \cdot L_{\beta,R} \Big] + \text{h.c.} \,, \end{aligned} \tag{89}$$

once again, due to the discrete symmetry we have, all the Yukawa couplings will have some restrictions:

$$\begin{aligned} &\mathcal{P} : Y_i^\ell = \left(Y_i^\ell\right)^\dagger \,, \quad \mathcal{C} : Y_i^\ell = \left(Y_i^\ell\right)^T \,, \\ &\mathcal{P} : Y_L = Y_R \,, \qquad \mathcal{C} : Y_L = Y_R^* \,. \end{aligned} \tag{90}$$

[11] See [124, 127] for the justification, an analysis of Yukawa couplings gives $t_{2\beta} s_\alpha < 2\frac{m_b}{m_t}$. Moreover, the difference between the right-handed and left-handed CKM matrices has been calculated to less than 1% difference [128].

We can decouple the Yukawa matrices of leptons in exactly the same way we did it for quarks:

$$\begin{aligned} Y_\nu &= c_\beta\, Y_1^\ell + s_\beta\, e^{-i\alpha}\, Y_2^\ell\,, \\ Y_\ell &= s_\beta\, e^{i\alpha}\, Y_1^\ell + c_\beta Y_2^\ell\,, \end{aligned} \tag{91}$$

and once again:

$$\begin{aligned} -\mathcal{L}_{L-\Phi} = \sum_{\alpha,\beta} \Bigg\{ \bar{L}_{\alpha,L} \cdot \left[\tilde{\varphi}_{\rm SM}\, Y_\nu + \tilde{\varphi}_{\rm FV} \left(\frac{Y_\ell - e^{i\alpha}\, s_{2\beta}\, Y_\nu}{c_{2\beta}} \right) \right]_{\alpha,\beta} N_{\beta,R} \\ + \bar{L}_{\alpha,L} \cdot \left[\varphi_{\rm SM}\, Y_\ell + \varphi_{\rm FV} \left(\frac{Y_\nu - e^{-i\alpha}\, s_{2\beta}\, Y_\ell}{c_{2\beta}} \right) \right]_{\alpha,\beta} \ell_{\beta,R} \Bigg\} + \text{h.c.}\,. \end{aligned} \tag{92}$$

There is almost no difference between the interactions of the quark fields with the bi-doublet, as with the interactions between the leptons and the bi-doublet: we will also have $\varphi_{\rm FV}$ mediate flavor-changing interactions at tree level, much like $\mu^- \to e^- e^- e^+$ decays or muonium-antimuonium oscillations for example, which once again confirms that the doublet must be quite massive, we are yet to see cLFV processes.

But there is a major difference in the mass generation, specifically with regard to the neutrally charged leptons. With the charged leptons, only Φ and v contribute to a mass term for leptons, so much like in the SM we will have that $M_\ell = \frac{1}{\sqrt{2}} v Y_\ell$, but for neutral leptons there will be contributions from both triplets. The entire mass term for neutral leptons is:

$$-\mathcal{L}_{\rm mass} = \sum_{\alpha,\beta} \left[\bar{\nu}_{\alpha,L}\, \left(M_D\right)_{\alpha,\beta}\, N_{\beta,R} + \frac{1}{2}\, \nu^C_{\alpha,L}\, \left(M_L\right)_{\alpha,\beta}\, \nu_{\beta,L} + \frac{1}{2}\, \bar{N}^C_{\alpha,R}\, \left(M_R\right)_{\alpha,\beta}\, N_{\beta,R} \right] + \text{h.c.}\,, \tag{93}$$

where $M_R = \frac{1}{\sqrt{2}}\, v_R\, Y_R$, $M_L = \frac{1}{\sqrt{2}}\, v_L\, e^{i\beta_L}\, Y_L$ and $M_D = \frac{1}{\sqrt{2}}\, v\, Y_\nu$. We have now three different mass terms. Notice this: the first and third are the ones that appear in the Type-I Seesaw mechanism (see Section 2.5) and the second term appears in the Type-II Seesaw mechanism (see Section 2.6). The Seesaw mechanism in the LRSM is a combination of both Seesaw mechanisms. We can once again re-write the mass terms as a matrix:

$$-\mathcal{L}_{\rm mass} = \frac{1}{2} \begin{pmatrix} \bar{\nu}_L & \bar{N}^C_R \end{pmatrix} \begin{pmatrix} M_L^\dagger & M_D \\ M_D^T & M_R \end{pmatrix} \begin{pmatrix} \nu^C_L \\ N_R \end{pmatrix} + \text{h.c.}\,. \tag{94}$$

The diagonalization of this matrix is done in exactly the same way as it was done before we will use the same unitary matrix as the one used in Eq. (40), then we obtain the Seesaw relation:

$$M_\nu \simeq -M_D\, \frac{1}{M_N}\, M_D^T + M_L^\dagger \simeq -\Theta\, M_N\, \Theta^T + M_L^\dagger\,, \tag{95}$$

with $M_N \simeq M_R$ and $\Theta \simeq M_D M_N^{-1}$. In LRSM we cannot take an arbitrary number of HNLs, we have three right-handed doublets and therefore we must have three HNLs. To reiterate what we've said before, we can think of the first term as the contribution from Type-I Seesaw and the second as the contribution from Type-II Seesaw. This equation also shows the usual "Seesaw behavior" one would expect $M_D \sim v$ and $M_N \sim v_R$, then $M_\nu \sim v^2/v_R + v_L$. This exemplifies what we've said before, it should be that $v_L \ll v$ because v_L directly contributes to neutrino

masses [12].

Naturally, a question should now arise which we must examine and consider, if $m_\nu \sim v^2/v_R$, does this mean that $v_R \sim v^2/m_\nu$? This is in accordance with the discussion we had about the Weinber Operator in Section 2.6, where we found that the energy scales responsible for neutrino masses sit near the GUT scale ($\sim 1\times 10^{15}\,\text{GeV}$), then, does v_R, the scale of the LRSM, also sit at the GUT scale? We must remember that we have a lot more parameters in this theory, we have the Yukawa couplings which may contribute to this suppression: Y_ν could be very small compared to Y_R, or it could be that there is coincidental cancellation between the Type-I and Type-II contributions. Therefore, the limit $v_R \sim 1\times 10^{15}\,\text{GeV}$ should only be taken as an upper bound.

We must also diagonalize the matrix M_ν and M_N, unlike in the minimal Type-I Seesaw, we cannot take M_N to be diagonal. Moreover, due to the restrictions due to the Yukawa matrices due to the discrete symmetry (see Eq. (90)), the Seesaw relations slightly change in the case of $\mathcal{P}$ or $\mathcal{C}$:

$$\mathcal{P}: V_\nu\, m_\nu\, V_\nu^T \simeq -M_D\, V_N\, \frac{1}{m_N}\, V_N^T\, M_D^* + \frac{v_L}{v_R}\, e^{-i\beta_L}\, V_N\, m_N\, V_N^T\,, \tag{96}$$

$$\mathcal{C}: V_\nu\, m_\nu\, V_\nu^T \simeq -M_D\, V_N\, \frac{1}{m_N}\, V_N^T\, M_D + \frac{v_L}{v_R}\, e^{-i\beta_L}\, V_N^*\, m_N\, V_N^\dagger\,, \tag{97}$$

where $M_\nu = V_\nu\, m_\nu\, V_\nu^T, M_N = V_N^*\, m_N\, V_N^\dagger$, where both m_ν and m_N are diagonal matrices; and V_N and V_ν are unitary matrices that diagonalize both matrices. The last term proportional to m_N is due to the restrictions regarding Y_L and Y_R in Eq. (90).

Notice that in the case where $M_D \simeq 0$, we have that $V_\nu = V_N$ for $\mathcal{P}$ and $V_\nu = V_N^*$ for $\mathcal{C}$, due to the restrictions in Eq. (90) and up to some phases, due to any potential redefinition in interactions with gauge bosons.

Remember that in the minimal Type-I Seesaw, we were capable of parametrizing Θ in terms of an arbitrary orthogonal matrix O. We cannot do this in the LRSM, because of generalized discrete symmetry in our model. In the case of $\mathcal{C}$, for example[13], M_D has an explicit solution:

$$\begin{aligned} M_D &\simeq \pm i\, V_N^* \sqrt{m_N} \left[\frac{1}{\sqrt{m_N}}\, V_N^T\, V_\nu\, m_\nu\, V_\nu^T\, V_N\, \frac{1}{\sqrt{m_N}} - \frac{v_L}{v_R} e^{-i\beta_L}\right]^{1/2} \sqrt{m_N}\, V_N^\dagger\,, \\ &\simeq \pm i V_N^* \sqrt{m_N} \left[\frac{m_\nu}{m_N} - \frac{v_L}{v_R} e^{-i\beta_L}\right]^{1/2} \sqrt{m_N}\, V_N^\dagger\,, \end{aligned} \tag{98}$$

where the second line was simplified in the case $V_\nu \simeq V_N^*$. We obtained this equation by some algebraic manipulations of Eq. (97): multiplying on the left of both parts by $m_N^{-1/2}\, V_N^*$ and on the right times $V_N\, m_N^{-1/2}$, then we the product of a matrix times itself and the solution then becomes obvious. This explicit solution of M_D fixes the O matrix in Eq. (46) to be of order one, and it cannot be arbitrarily large. What is of significance here, is that $M_D \sim \sqrt{m_\nu\, m_N}$ and therefore $\Theta \sim \sqrt{m_\nu/m_N}$, making all interactions mediated by Θ completely suppressed.

[12] Moreover, the potential also predicts $v_L \propto v^2/v_R$ [119]

[13] The case for $\mathcal{P}$ is much more delicate and was tackled in [129–131], we shall not repeat their calculation here, but the results are quite similar.

	t_R^3	t_L^3	q
U_i	$1/2$	$1/2$	$2/3$
D_i	$-1/2$	$-1/2$	$-1/3$
ν_α	0	$1/2$	0
N_α	$1/2$	0	0
ℓ_α	$-1/2$	$-1/2$	-1

Table 2: Quantum numbers for the different fermions in the LRSM

3.5 Interactions between gauge bosons and fermions

As in the SM, interactions between fermions and gauge bosons stem from the covariant derivatives. Now we shall have:

$$\mathcal{L}_{W_L} = \frac{g}{\sqrt{2}} \sum_{\alpha,i} \bar{n}_i \not{W}_L^+ \left(\mathcal{U}_L^*\right)_{\alpha,i} P_L \, \ell_\alpha + \frac{g}{\sqrt{2}} \sum_{i,j} \bar{U}_i \not{W}_L^+ \left(V_{\text{CKM}}^L\right)_{i,j} P_L D_j \tag{99}$$

$$+ \frac{g\,\xi_W}{\sqrt{2}} e^{i\alpha} \sum_{\alpha,i} \bar{n}_i \not{W}_L^+ \left(\mathcal{U}_R^*\right)_{\alpha,i} P_R \, \ell_\alpha + \frac{g\,\xi_W}{\sqrt{2}} e^{i\alpha} \sum_{i,j} \bar{U}_i \not{W}_L^+ \left(V_{\text{CKM}}^R\right)_{i,j} P_R D_j + \text{h.c.}\,,$$

$$\mathcal{L}_{W_R} = \frac{g}{\sqrt{2}} \sum_{\alpha,i} \bar{n}_i \not{W}_R^+ \left(\mathcal{U}_R^*\right)_{\alpha,i} P_R \, \ell_\alpha + \frac{g}{\sqrt{2}} \sum_{i,j} \bar{U}_i \not{W}_R^+ \left(V_{\text{CKM}}^R\right)_{i,j} P_R D_j$$

$$- \frac{g\,\xi_W}{\sqrt{2}} e^{-i\alpha} \sum_{\alpha,i} \bar{n}_i \not{W}_R^+ \left(\mathcal{U}_L^*\right)_{\alpha,i} P_L \, \ell_\alpha - \frac{g\,\xi_W}{\sqrt{2}} e^{-i\alpha} \sum_{i,j} \bar{U}_i \not{W}_R^+ \left(V_{\text{CKM}}^L\right)_{i,j} P_L D_j + \text{h.c.}\,, \tag{100}$$

$$\mathcal{L}_{Z_L} = \frac{g}{c_w} \sum_{\psi} \left[\bar{\psi} \not{Z}_L \left(t_L^3 P_L - s_w^2 q\right) \psi\right] - \frac{g\,c_w}{c_{2w}^{1/2}} \zeta_Z \sum_{\psi} \left[\bar{\psi} \not{Z}_L \left(t_R^3 P_R + t_w^2\, t_L^3 P_L - t_w^2 q\right) \psi\right]\,, \tag{101}$$

$$\mathcal{L}_{Z_R} = \frac{g\,c_w}{c_{2w}^{1/2}} \sum_{\psi} \left[\bar{\psi} \not{Z}_R \left(t_R^3 P_R + t_w^2\, t_L^3 P_L - t_w^2 q\right) \psi\right] + \frac{g}{c_w} \zeta_Z \sum_{\psi} \left[\bar{\psi} \not{Z}_R \left(t_L^3 P_L - s_w^2 q\right) \psi\right]\,, \tag{102}$$

$$\mathcal{L}_A = e \sum_{\psi} \bar{\psi} \not{A} q \psi \tag{103}$$

where $\mathcal{U}_L = \begin{pmatrix} V_\nu & \Theta\, V_N^* \end{pmatrix}$ and $\mathcal{U}_R = \begin{pmatrix} -\Theta^T V_\nu^* & V_N \end{pmatrix}$ are 3×6 matrices and n_i can be either an HNL or a neutrino: $P_L\, n \equiv \begin{pmatrix} \nu_L & N_R^C \end{pmatrix}$ and $P_R\, n \equiv \begin{pmatrix} \nu_L^C & N_R \end{pmatrix}$.

The terms equivalent to ξ_W and ζ_Z (defined in Eq. (77) and (81)) are due to the mixing between the left-handed and right-handed gauge bosons.

We're using a similar notation to define neutral current interactions to the one we used when defining SM interactions; t_R^3 is the third right-handed weak isospin of ψ, t_L^3 the third left-handed weak isospin and q its charge. We're adding overall fermions fields: $U_i, D_i, \ell_\alpha, \nu_\alpha$, and N_α. After diagonalizing the Seesaw matrix, we have to substitute $\nu_\alpha = \sum_{\alpha,i} \left(\mathcal{U}_L\right)_{\alpha,i} n_i$ and $N_\alpha = \sum_{\alpha,i} \left(\mathcal{U}_R\right)_{\alpha,i} n_i$. All of the values of the quantum numbers are in Table 2.

Considering the discussion we had in previous sections, we know that V_{CKM}^L and V_{CKM}^R are related to one another due to the discrete generalized symmetries. Moreover, we know that

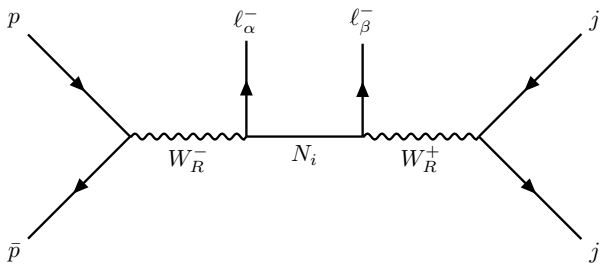

(a) LNV process

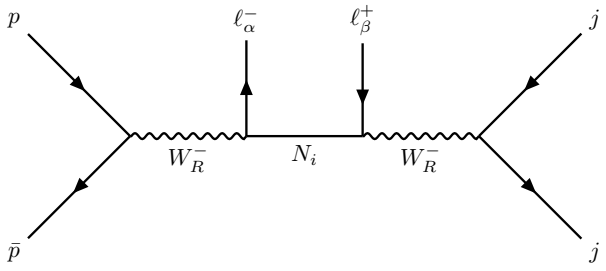

(b) LNC process

Figure 6: Hadron collider processes, diagram (a) shows a lepton number violating process (LNV process), and diagram (b) shows the lepton number conserving process (LNC).

interactions proportional to Θ should be suppressed, and therefore we can ignore interactions proportional to that parameter.

All the new interactions between SM fermions and the new gauge bosons can have significant effects on some observables, the most remarkable of them are meson oscillations. Take the diagrams in Fig. 3: the W_L vertex gets modified due to the ξ_W extra term, and we can also have additional diagrams with two W_R's or one W_L and a W_R. Moreover, there are tree-level contributions coming from the flavor-violating bi-doublet. All of these contributions place very strong constraints on the model, as a matter of fact, during the 80s these low-energy processes gave the strongest constraints on v_R setting it near the TeV-scale [41–43]. At the time, this demotivated the model because there was an unfeasible scale at colliders, but the theory has gained recent popularity due to the fact that the LHC can now probe comparable energies.

3.6 Hadron collider phenomenology and constraints

At the current time, the best constraints on the model are from the LHC. The most popular channel for LRSM searches at the LHC is the so-called Keung-Senjanovi process (KS process) [132]. The diagram of the process is the upper diagram in Fig. 6: it requires the production of a W_R which subsequently decays into a $N_i + \ell_\alpha$ and then the HNL decays into another lepton with the same charge. This process is a lepton number violating process (LNV process), which, in theory, should be background free; the SM process does not predict any process with a final state with same-sign (SS) leptons or LNV processes. Of course, there is an equivalent with opposite-sign (OS) leptons in the final state or lepton number conserving (LNC) process, which should not be as clean as the LNV process.

Such LNV processes are allowed due to the Majorana nature of HNLs: an on-shell HNL can undergo the decay $N \to \ell^- U \bar{D}$ and $N \to \ell^+ \bar{U} D$ with equal probability. But in the processes in Fig. (6), the HNL may or may not necessarily be on-shell.

Assuming we have enough energy, then if $m_N > M_{W_R}$ then the initial W_R should be mostly off-shell and the last W_R mostly on-shell. In the case $m_N < M_{W_R}$, then we produce both the initial W_R and N mostly on-shell, but the final W_R should be off-shell.

On-shell HNLs have equal probabilities of producing LNV and LNC processes, as long as their decay width, $\Gamma_N \ll m_N$; but if $\Gamma_N \sim m_N$ then LNC processes are preferred. On the other hand, if HNLs are off-shell then it is LNV processes that are dominant. The details of a very similar process in a different model can be found in [133]; but the idea is that for LNV processes mediated or caused by Majorana fermions are proportional to the mass of the Majorana fermion itself, so in off-shell processes where the dominant energy scale is m_N we have an enhancement of these processes, in off-shell processes where $\Gamma_N \sim m_N$ there is a cancellation in LNV processes that cannot be seen in LNC processes.

There are other processes where we can search for LRSM at hadron colliders, either involving the scalar sector or other gauge bosons. We also discussed low-energy processes, such as meson mixing, but there are other low-energy processes that would be affected by LRSM. So far no signal has been found, so we can only place bounds on the parameter space.

Current constraints

- Constraints from hadron colliders: Both ATLAS and CMS have done multiple searches for the KS process [134, 135, 146–153] to no avail. Besides the KS process, we can also obtain constraints from the *invisible KS process* [140], where the HNL is so light it doesn't decay inside the detector, and therefore we only see one of the final leptons. We expect to see a very highly energetic lepton with the energy of $M_{W_R}/2$. Both ATLAS [139] and CMS [138] already give us constraints from this process. We can also search for decays of an on-shell W_R into a pair of highly energetic jets, which provide constraints independent on the mass of HNLs; ATLAS and CMS data [136, 137] give a lower bound of $M_{W_R} \gtrsim 4\,\text{TeV}$.

- Constraints from low-energy processes: we've already discussed meson mixing and how it can constrain LRSM parameters. Current constraints on meson mixing [126] give a lower bound of $M_{W_R} \gtrsim 3\,\text{TeV}$. Moreover, LRSM also affects the probability of observing neutrino-less double beta decay ($0\nu2\beta$) [154–157][14].

  Most interesting is also the fact that in the case of $\mathcal{P}$, LRSM parameters affect the nEDM [37, 38, 158–163]. If the reader remembers our brief discussion on SM problems, the nEDM tells us how much CP violation there is in strong interactions. This observable actually gives the strongest constraints on $M_{W_R} \gtrsim 17\,\text{TeV}$, which is very much above the potential the LHC has to produce one directly.

Future constraints

[14] It is not hard to see that the KS process, the upper diagram in Fig. 6, is the same diagram for $0\nu2\beta$. Other diagrams also contribute, like triplet mediated diagrams, more information can be seen in the references given.

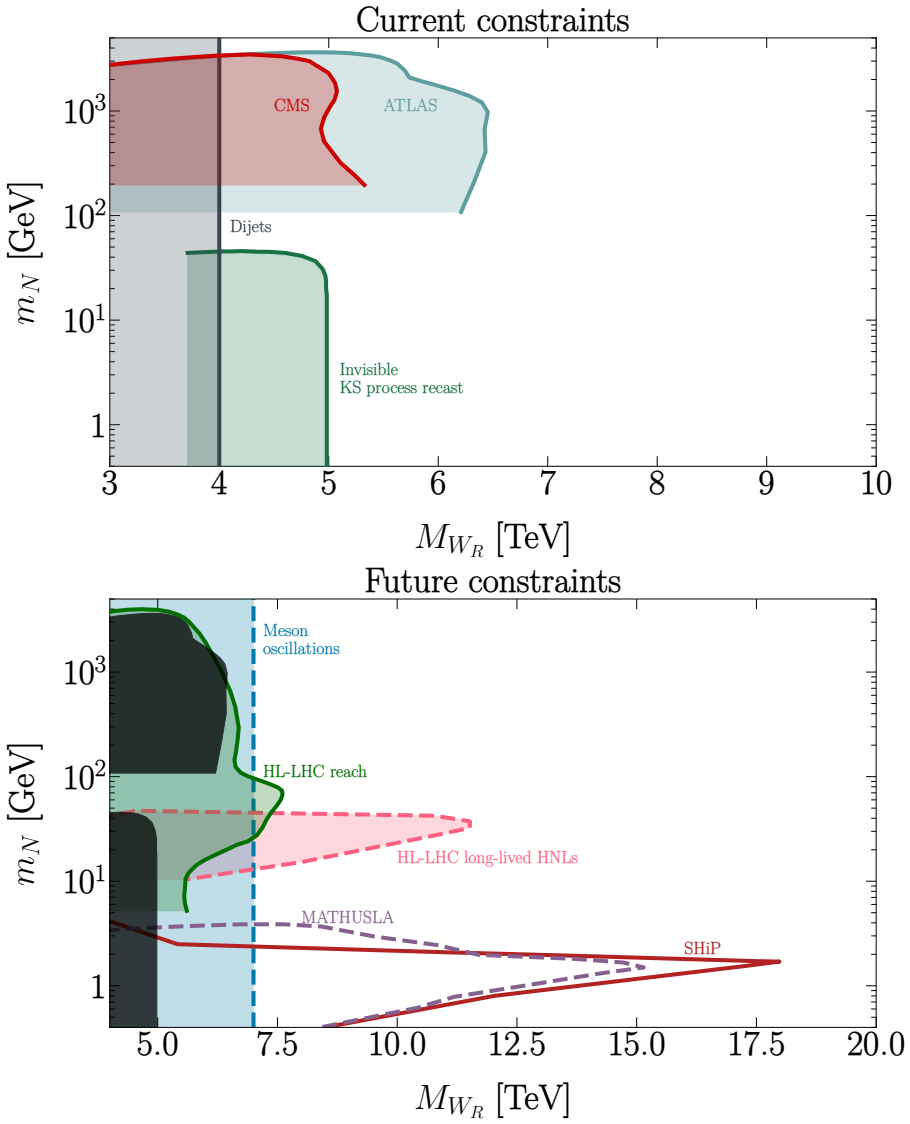

Figure 7: Current and future constraints of LRSM in a $m_N - M_{W_R}$ parameter space plot. We show the current constraints from ATLAS [134], CMS [135], di-jets signals [136, 137] which can interpreted a W_R decaying to a jet pair, and signals of high-energy leptons with missing energy [138, 139] which can be interpreted as a KS-process with an HNL so light it decays outside of the detector [140]. We also show the prospective bounds from the HL-LHC [140], a KS process with a displaced vertex [141], meson oscillations [126], SHIP [142–144] and MATHUSLA [62, 145].

- Hadron colliders: we expect the next LHC runs to have much more luminosity, and therefore have a higher probability of seeing LRSM signals. Most of the analysis has already been done in [140]. Although, it seems that their analysis underestimated the sensitivity in a very specific region of the parameter space [141]. It is a region of the parameter space where the HNL in the KS process is light enough to generate a displaced vertex, but heavy enough to decay inside the detector. These displaced vertices should be mostly, if not completely, background free. At the current time, neither ATLAS nor CMS have performed any searches on such displaced vertices.

- Low-energy processes: the next Belle-II and LHCb runs will have the potential to probe masses of M_{W_R} up to 7 TeV [126], which will surpass the potential the LHC has.

- High-intensity experiments: Future high-intensity experiments like SHIP [142] and MATHUSLA [145] will provide complementary constraints to the ones from hadron colliders. High-intensity experiments aim to search for displaced vertices from long-lived particles and will be particularly sensitive to HNLs with lower masses and W_R with higher masses than the ones from hadron colliders. Both SHIP [142–144] and MATHUSLA [62, 145] which have sensitivities up to $M_{W_R} \simeq 18\,\text{TeV}$ and $m_N \simeq 5\,\text{GeV}$.

We show most of these constraints in a $m_N - M_{W_R}$ parameter space plot in Fig. 7.

3.7 Can the LRSM solve the problems the SM has?

The model we've described at length can solve some of the problems we've discussed in Sec. 2.4. We've already mentioned how we can accommodate small neutrino masses into the model from the Seesaw mechanism. The model can also give rise to BAU (see [164] for a review on the subject of the generation of BAU in LRSM), we can also have one of our HNLs as a dark matter particle [39, 140] as long as their masses have masses in the order of keV. We've also briefly discussed how nEDM gives us constraints on LRSM parameters in the case of $\mathcal{P}$: indeed, the LRSM also provides a solution for the strong CP problem (see details in the references above, or in [165] for a pedagogical review on the subject).

It seems like the LRSM can solve most of our problems, but the issue is that the region in the parameter scale where the LRSM can solve most of our problems lies completely outside the experimental reach of most experiments. For example, [39] claims that we require $M_{W_R} \gtrsim 17\,\text{TeV}$ in order to have HNLs as dark matter so as to not disrupt BBN. And in [166], it was claimed that the minimal mass W_R can have to successfully generate BAU is 18 TeV. It seems that it is the case that if we find LRSM in the LHC, we have actually proved that it cannot solve the problems the SM has and that we must require even more physics to do so.

4 Proposals for future lepton colliders

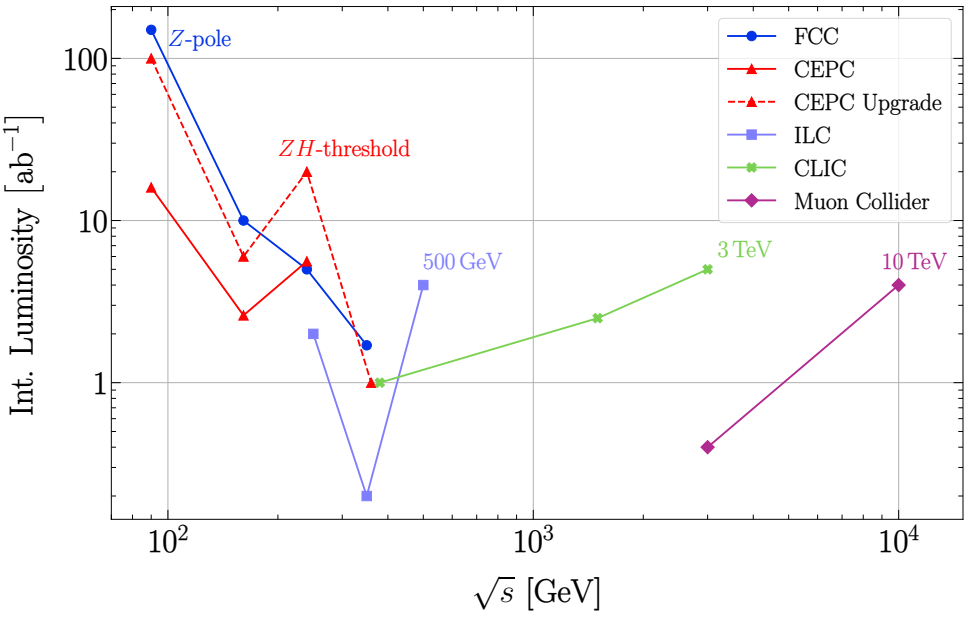

Figure 8: The running plan of several collider proposals in integrated luminosity and center of mass energy, $\sqrt{s}$ for the FCC-ee [44], CEPC [48], the recently proposed CEPC upgrade [167], ILC (plan H20 of [168, 169]) and CLIC [56]. The benchmark points for the muon collider were taken from [60], where they claim that it should be possible to achieve the integrated luminosity plots per year. See Table 3 for the exact values.

We briefly mentioned at the end of the last section the proposal of high-intensity experiments like SHIP and MATHUSLA. The aim of these experiments is mainly to search for long-lived particles which can escape the reach of detectors of particle accelerators. There is a list of much many current forward experiments at CERN that are also searching for such particles. The proposal for experiments like this is quite numerous, there is a huge incentive from the particle physics community to search in this area as it probes areas of the parameter space of different models which other experiments cannot easily probe. This is one of the types of experiments we briefly talked about before that searches for physics at the intensity frontier.

Much like flowers bloom and flowers fade, the LHC will eventually fade after its bloom. We expect the LHC to cease operations by December of 2041 [170]. This has placed the particle physics community at its crossroads: what should we do next? What should be our next experiment? How can we keep probing the energy frontier?

As things seem to stand, the preferred direction of the particle physics community is to build a lepton collider. We will demarcate them into three different categories: circular colliders, linear colliders, and muon colliders.

4.1 Circular colliders

FCC-ee: the Future Circular Collider (FCC) [44–47] is a proposed 90 km circular collider. The current proposed plan of the experiment is first it to collide electron positron pairs, in this first stage the project has the name *FCC-ee*; then it is meant to upgrade to a hadron collider, which

will be capable of reaching higher energies up to 100 TeV; and in its final stage, it is proposed to also use it as an electron-hadron collider.

The first stage, the FCC-ee will be run at much lower energies than the FCC-hh will, but the FCC-ee will have much higher luminosity. The high luminosity reach of the FCC-ee will allow it to probe the intensity frontier, as opposed to the FCC-hh which aims to probe mostly the energy frontier. This is part of the common lore of collider physics: ee colliders are meant for precision measurements, whereas hadron colliders are meant for probing higher energy scales. This is due primarily because electrons are harder to accelerate because of energy losses due to synchroton radiation; hadrons are heavier and therefore can reach higher energies, but since they are composite particles and subject to complicated QCD interactions, are subject to more uncertainties and thus more imprecise measurements.

The goals in energy and integrated luminosity for the FCC-ee are plotted in Fig. 8 and shown in Table 3. The impressive reach in luminosity on all different scales of energy will allow the FCC-ee to produce 10^{12} Z bosons, 10^8 W's, 10^6 Higgses and 10^6 top quarks.[15]

At the current time, it seems like the FCC-ee is the preferred proposal, it is planned to be built in CERN, between France and Switzerland. The construction of a hypothetical FCC-ee should be around 10.5 BCHF (billion Swiss Francs) [16].

CEPC: the Circular Electron Positron Collider [48, 49, 171] is a proposed 100 km circular collider. It will run at the same benchmark points in energy as the FCC-ee, but with different luminosity benchmarks, which are shown in Fig. 8 and Table 3. New benchmark points were proposed only recently, where they aim to reach integrated luminosities comparable to the ones the FCC-ee aims to reach [167].

Much like FCC, the CEPC could be upgraded to a hadron collider which would now be called the Super Proton-Proton Collider (SPPC). Unlike the FCC, it very much seems like construction will start soon, sometime in this decade in China, and will begin to see operations sometime in 2030. The estimate cost of the construction the CEPC is around 5–6 BUSD (billion US Dollars) [172].

4.2 Linear Colliders

ILC: the International Linear Collider [50–53] is a proposed electron-positron linear collider planned to have an approximate stretch of 20 km. Linear colliders have the advantage that it is easier for them to accelerate electrons because there are no energy losses due to synchrotron radiation, therefore they should be more capable of probing the energy frontier than circular colliders. This is why the energy benchmarks shown in Fig. 8 and Table 3 are higher for the ILC than for the other circular collider proposals.

There have also been suggestions to run the ILC of center-of-mass energies than the ones shown in Table 3, namely $\sqrt{s} \simeq 1\,\text{TeV}$ with an integrated luminosity of $\sim 8\,\text{ab}^{-1}$, as well as lower center-of-mass energies 90 GeV at the Z-pole and 160 GeV at the WW-threshold [168, 169].

[15] Here we are of course referring to the SM gauge bosons, and not to any of the new gauge bosons that the LRSM proposes.

[16] At the time of writing: 1 CHF $\simeq$ 7.73 DKK $\simeq$ 1.17 USD $\simeq$ 1.04 EUR.

Experiment	Energy (GeV)	Luminosity (ab^{-1})
FCC-ee	90, 161, 240 and 350	150, 10, 5 and 1.7
CEPC	90, 161 and 240	16, 2.6 and 5.6
CEPC upgrade	90, 161, 240 and 360	100, 6, 20 and 1
ILC	250, 350 and 500	2, 0.2 and 4
CLIC	380, 1500 and 3000	1, 2.5 and 5
Muon Collider	3000 and 10 000	0.4 and 4 (per year)

Table 3: The exact values plotted in Fig. 8.

Initially, the ILC was meant to reach 1 TeV, but the strategy after the discovery of the Higgs in 2012, and $\sqrt{s} \sim 250$ GeV, above the ZH threshold, to make the experiment a Higgs factory.

The experiment has been proposed to both Japan and CERN. The preferred option for scientists in Europe is the FCC-ee, and it is unclear whether the Japanese government would be willing to build the ILC alone without any outside help from European countries which most likely would spend their money building the FCC-ee. The ILC would have a total cost of 7.8 BILCU (billion ILC Currency Units) [17].

CLIC: the Compact Linear International Collider [54–56] is a proposed linear collider which aims to a have a stretch between 11 km and 50 km. Being a linear collider, CLIC aims to reach a higher center of mass energies than circular colliders.

CLIC has been proposed to CERN, and it is another option in case the FCC-ee is not built. CLIC would have a cost of 6 BCHF.

4.3 Muon collider

Muon colliders offer the best of both ee and pp colliders: muons are heavier than electrons and should be easier to accelerate at higher energies than electrons; muons are elementary particles, since hadrons are not elementary particles the entire center-of-mass energy is distributed between the partons in the hadrons, muons should therefore have a higher energy reach than protons at the same center-of-mass energy.

There are, however, several technical difficulties regarding the construction of a muon collider: muons are unstable particles, they have a lifetime of 2.2 μs in their own rest-frame; muons are produced from pions, therefore we must first produce the pions from proton collisions with a specific target: muons will be tertiary particles. Both of these issues provide several engineering problems, from the cooling of muons to the acceleration of them; there are other non-engineering problems, like the fact that muon decays will also provide huge amounts of background and the decay of muons with TeV energies will generate several high energy electrons and neutrinos, the neutrinos specifically can affect infrastructure far away from the place where the muon collider would be. More details on the advantages and disadvantages of muon colliders can be found in [173].

Some of the solutions to some of these difficulties have begun to see small steps towards solutions, which is why there has been a surge in popularity for the construction of a muon collider, particularly with physicists residing in the US [57–61].

[17] The ILCU is defined as the price of a 1 USD in 2012.

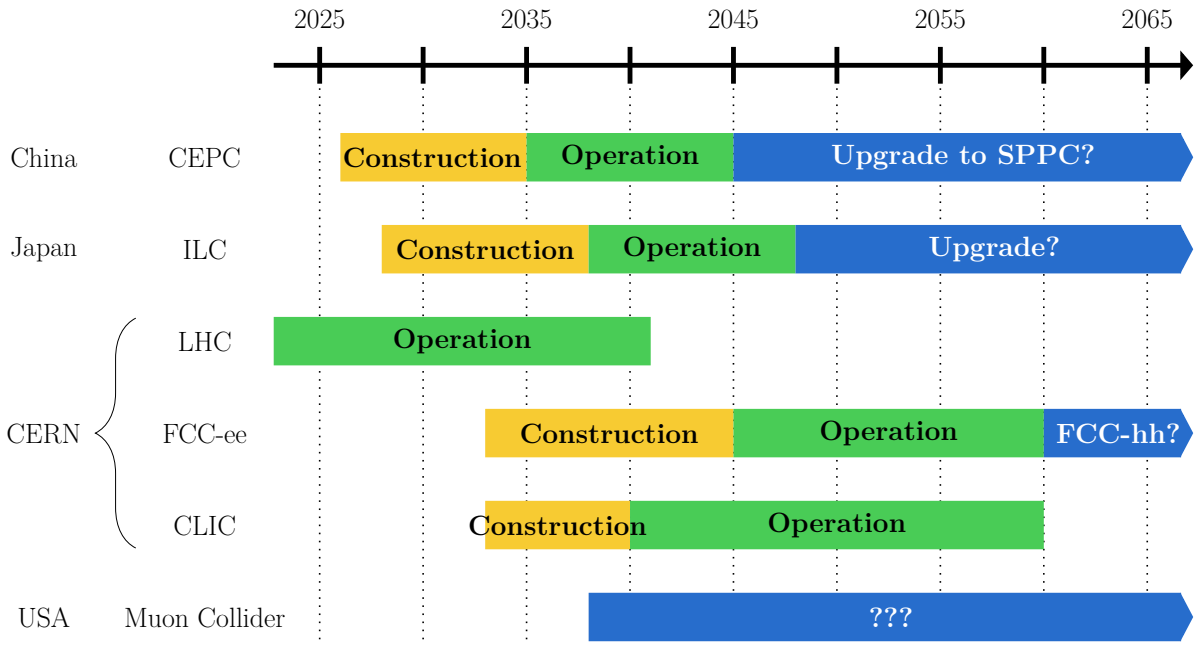

Figure 9: Possible timeline on the construction of the colliders. The timeline is adapted from the information of the operation and construction given by the FCC-ee [45, 174], CEPC [175], ILC [168], and CLIC [56]. The LHC is expected to shutdown by 2041 [170]. The estimate time for the construction of all colliders depends of numerous factors impossible to predict. It is very unlike for CERN to build both the FCC-ee and CLIC. Plot adapted slightly adapted from [176].

4.4 The future?

Are all of these projects possible? In Fig. 9 we show a very optimistic timeline for the possible construction and operation times for the experiments we've described above. There are still questions regarding each and every experiment; for example, there is still not an agreed-upon place where to build the CEPC, and it is still quite uncertain whether the ILC will even be built in Japan if at all [177, 178], and even though the FCC is the most likely candidate for the next big experiment on CERN, it still remains uncertain whether there will be an ee phase before a pp phase since there are some scientists who would prefer to jump straight into the energy frontier. CLIC should only be considered in case the FCC is not built in CERN.

As we mentioned before, there are still numerous difficulties regarding muon colliders. It remains uncertain whether these difficulties will ever be completely conquered.

5 HNL-LRSM phenomenology at lepton colliders

Two sections ago we devoted our discussion to the theory of the LRSM and a little bit of the phenomenology of LRSM at hadron colliders, as well as the relevant phenomenology of low-energy processes that gives rise to constraints on LRSM parameters. And the previous section was devoted to the different proposals for different lepton lepton collider experiments. Our discussion will now shift to the phenomenology of the LRSM in these experiments.

The material we're about to present in this section can be found in the literature [179–186]. This was initially unbeknownst to us, all of what we're about to present are re-derivations of previously known results.

5.1 Main channels for the production of HNLs

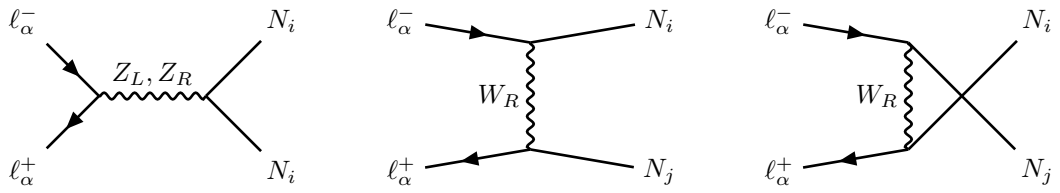

(a) s-channels (b) t-channel (c) u-channel

Figure 10: Diagrams showing the production of two-HNLs at linear colliders.

We will focus on the simultaneous production of two HNLs. We shall work in the simplified setting where Θ is negligible, for the reasons we've discussed in Sec. 3.4, that it is proportional to $\Theta \sim m_\nu/m_N$, and therefore should be very small.

There are four main different channels for the production of two HNLs in lepton colliders: an s-channel mediated by a Z_L, another by Z_R, and a t and u-channel mediated by a W_R. The diagrams of these processes are drawn in Fig. 10.

For the s-mediated channels we can only produce the same generation of HNLs. But for the W_R mediated channels, we can produce two different HNLs. We will work in the simplified case where $V_N = I$, and therefore there is no mixing between HNLs and charged fermions in interactions mediated by charged gauge bosons.

There are other channels that can produce two HNLs. We will explain in the following subsection why they are negligible.

We've calculated the amplitude and cross-section of the four main diagrams, as well as the interference that is between all of them.

We calculated the cross-sections with the help of `FeynCalc` [187] and `FeynArts` [188], `Mathematica` packages that help with the manipulation and calculation of the amplitudes of different Feynman Diagrams. We used the implementation of LRSM for `FeynRules` from [189]. `FeynRules` [190] is another `Mathematica` package that translates Lagrangians into package files which can be used for Monte-Carlo simulators like `MadGraph` or `WHIZARD`, as well with other software to do analytical computations, like `CalcHep` or `FeynArts`.

The amplitudes are for the process $\ell^-(p_1) + \ell^+(p_2) \to N(k_1) + N(k_2)$ are:

$$i\mathcal{M}_{Z_L} = i\,\frac{g^2\,\zeta_Z}{2c_{2w}^{1/2}}\,\frac{\left[\bar{v}(p_2)\,\gamma^\mu\left[\left(-\frac{1}{2}+s_w^2\right)P_L + s_w^2 P_R\right]u(p_1)\right]\left[\bar{u}(k_2)\gamma_\mu\left[P_R - P_L\right]v(k_1)\right]}{s - M_{Z_L}^2 + i\Gamma_{Z_L}\,M_Z}\,, \tag{104}$$

$$i\mathcal{M}_{Z_R} = -i\,\frac{g^2\,c_w^2}{2\,c_{2w}}\,\frac{\left[\bar{v}(p_2)\,\gamma^\mu\left[\left(-\frac{1}{2}+t_w^2\right)P_L + t_w^2 P_R\right]u(p_1)\right]\left[\bar{u}(k_2)\gamma_\mu\left[P_R - P_L\right]v(k_1)\right]}{s - M_{Z_R}^2 + i\Gamma_{Z_R}\,M_{Z_R}}\,, \tag{105}$$

$$i\mathcal{M}_{t,W_R} = -i\,\frac{g^2}{2}\,\frac{\left[\bar{u}(k_1)\,\gamma^\mu P_R\,u(p_1)\right]\left[\bar{v}(p_1)\gamma_\mu P_R\,v(k_2)\right]}{t - M_{W_R}^2}\,, \tag{106}$$

$$i\mathcal{M}_{u,W_R} = i\,\frac{g^2}{2}\,\frac{\left[\bar{u}(k_2)\,\gamma^\mu P_R\,u(p_1)\right]\left[\bar{v}(p_1)\gamma_\mu P_R\,v(k_1)\right]}{u - M_{W_R}^2}\,, \tag{107}$$

where $t = (p_1 - k_1)^2, u = (p_1 - k_2)^2$ and Γ_{Z_L} and Γ_{Z_R} are the decay widths of Z_L and Z_R respectively. It is necessary to include the decay widths of both s-channels in the case $s = M_{Z_L}^2, M_{Z_R}^2$ we're hitting the pole of either of them. We did not include the decay width of the W_R because particles in the t-channel cannot be on-shell.

Another important characteristic to notice is the fact that the spin-structure of the vertices $Z_L NN$ and $Z_R NN$ we're showing in the amplitudes in Eq. (104) and (105) is not aligning with the ones shown in the Lagrangian in Eq. (101) and (102). Indeed, according to (101) and (102) the spin-structure should've been $\gamma_\mu\,P_R$, but the amplitudes show $\gamma_\mu\,(P_R - P_L)$. The reason has to do with the fact we're dealing with Majorana particles: the same Majorana particle cannot interact with itself and a vector current γ_μ, therefore only the axial-current survives $\gamma_\mu\,\gamma_5$ (see Appendix A).

Due to the different spin structures between Dirac of Majorana, there will be a discrepancy in the cross-section of the s-channel. This discrepancy will be negligible for particles with much smaller masses than the intermediate boson, but if HNLs had masses comparable to the Z_L or Z_R, then there will be a suppression compared to the Dirac case [191].

A second difference that arises from calculations regarding Majorana particles, as opposed to Dirac, is that we have both a t and a u channel. In the case of Dirac HNLs, we would only have one of them. The interference between the t and the u channel reduces the Majorana cross-section compared to the Dirac case.

We shall not present the formula of the entire cross-section here, but we provided a summary of the calculation in Appendix C.1. The plot of the tree-level cross-section as a function of $\sqrt{s}$ for different values of M_{W_R} and m_N is plotted if Fig. 11. We shall now provide a brief analysis of the behavior of the cross-section.

Notice that in the case that $\sqrt{s} \ll M_{W_R}$, the cross-sections of the different channels will have a similar dependence on M_{W_R}: $\sigma \propto M_{W_R}^{-4}$, either because of the mediating particle (remember $M_{Z_R} \simeq 1.69\,M_{W_R}$ in this model), or because of the $Z_L - Z_R$ mixing angle $\zeta_Z \propto M_{W_R}^{-2}$. There are two notable features in this range of energies: first is the easy-to-see Z_L-pole, when $\sqrt{s} \simeq M_{Z_L}$ then the Z_L channel will dominate, and second is the behavior that the t and u channels have

in this energy range:

$$\sigma(\ell^-\ell^+ \to NN) \simeq \frac{3\,g^4}{512}\frac{s-m_N^2}{M_{W_R}^4}\sqrt{1-\frac{m_N^2}{4s}}\,, \qquad \text{for } \sqrt{s} \ll M_{W_R} \text{ and } \sqrt{s} \neq M_{Z_L}\,. \tag{108}$$

This result implies that the cross-section grows quadratically with center-of-mass energy for $\sqrt{s}$, when $\sqrt{s} \ll M_{W_R}$. This will actually be a very remarkable result! It means that the cross-section will grow with energy in a specific region of the parameter space, so if we have two colliders, one running at $\sqrt{s} \simeq 100\,\text{GeV}$ and another running at $\sqrt{s} \simeq 1\,\text{TeV}$, then the latter will have a cross-section 100 times bigger than the former for the same value of M_{W_R}. As we will see later on, this very important feature will allow us to probe higher values of M_{W_R} without $\sqrt{s}$ necessarily reaching M_{W_R}.

Some readers may object to these results. It cannot be the case that cross-sections increase with energy, which violating perturbativity and the unitarity of the S-matrix (see [192] for a recent pedagogical review). Indeed, the usual upper bound for cross-sections in order for them not to break perturbative unitarity is $\sigma \leq 4\pi s^{-1}$ [193, 194], this means that perturbatively would begin to break down when $\sqrt{s} \sim M_{W_R}$. The result we gave in Eq. (108) is only valid in the case $\sqrt{s} \ll M_{W_R}$, so there is no problem with us potentially breaking perturbativity.

Indeed, in the case $\sqrt{s} \to \infty$ once again only the W_R mediated channels dominate. The cross-section in this case looks like this:

$$\sigma(\ell^-\ell^+ \to NN) \simeq \frac{g^4}{32\pi M_{W_R}^2}\,, \qquad \text{for } \sqrt{s} \to \infty\,, \tag{109}$$

which perfectly aligns itself with the known result that non-abelian gauge theories that undergo spontaneous symmetry that cross-sections cannot arbitrarily grow with energy [195–197].

Before finishing off the topic regarding the double production of HNLs, we have to same some words about the Z_R-pole. At the Z_R-pole is the energy where the cross-section does not behave as $\sigma \propto M_{W_R}^{-4}$: the Z_R becomes on-shell and $\sigma \propto M_{Z_R}^{-2}\Gamma_{Z_R}^{-2}$. We show our calculation of Γ_Z Appendix C.4, but it should be sufficient to say here that it is much smaller than M_{Z_R}. At the Z_R pole the cross-section dramatically increases, as one would usually expect.

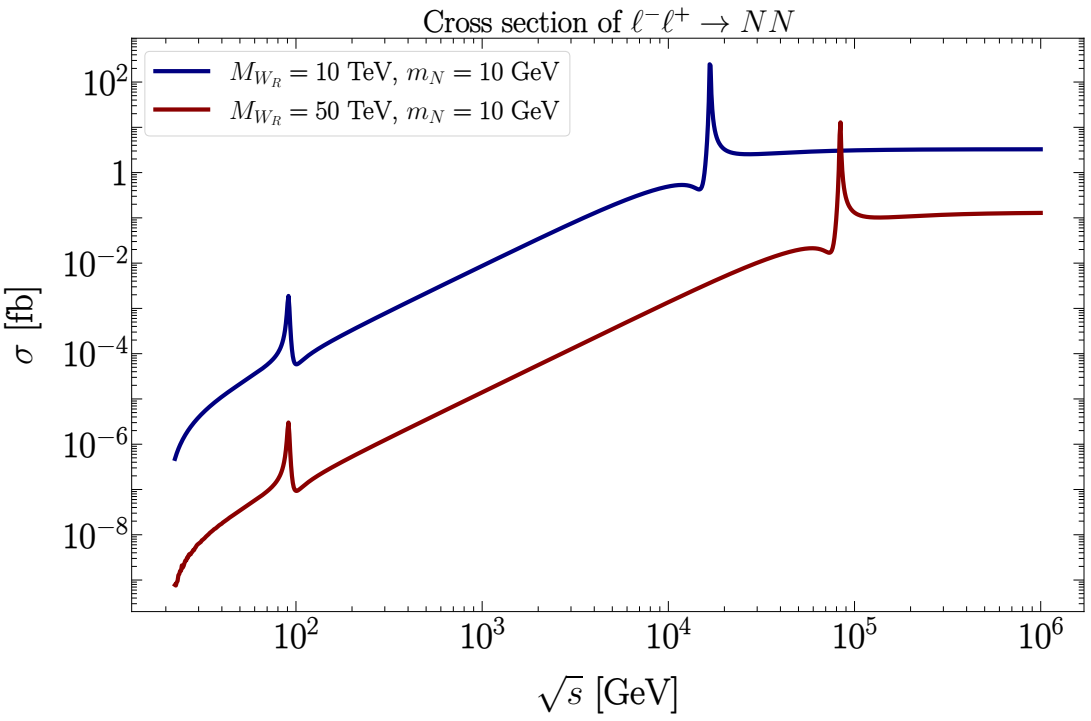

Figure 11: Plot of the cross-section as a function of $\sqrt{s}$ for different values of M_{W_R} and m_N shown in the plot. The two peaks correspond to the Z_L and Z_R poles.

5.2 Other HNL production channels

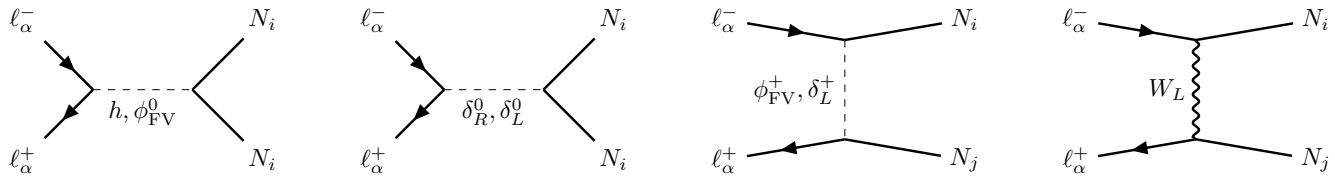

(a) Doublet mediated (b) Triplet mediated (c) Charged scalar mediated (d) W_L mediated

Figure 12: Other channels for the production of two HNLs. Here we are taking $\delta^0_R = \text{Re}\{\delta^0_R\}$, the real component of the δ^0_R shown in Eq. (58).

There are other channels for producing an HNL pair, shown in Fig. 12. Notice that we did not include any of the Goldstone bosons that are to be eaten by the gauge bosons, such as $\text{Im}\{\delta^0_R\}, \delta^\pm_R$ or the SM ones, these could be contained within the gauge bosons themselves in the Unitary Gauge. All the channels in Fig. 12 are suppressed compared to the ones described in:

- A SM Higgs, h, mediated s-channel (Diagram (a) in Fig. 12) is suppressed because the Higgs boson almost doesn't interact with light fermions as we said at the end of Sec. 2.3.1.

  A decay of an SM Higgs might initially seem suppressed because the coupling between two HNLs is proportional to ΘM_D, but we have another possible vertex. Much like there is mixing between $Z_L - Z_R$ and $W_L - W_R$, there is mixing between δ^0_R and h. The $h - \delta^0_R$ mixing is proportional to $s_\theta \propto v^2/v_R^2$ (see Appendix B). This fact was used as an advantage to estimate the sensitivity of the LRSM parameter for Higgs decays at the LHC [198]. It

could be interesting to analyze the potential this would have for Higgses produced in Higgsstrahlung processes instead of in the s-channel. We will not analyze this possibility.

- The neutral flavor violating scalar, $\phi^0_{\rm FV}$, mediated s-channel (shown in Diagram (a) in Fig. 12) would be proportional to lepton masses and the Dirac mass.
- The right-handed neutral triplet Higgs, δ^0_R, s-channel (shown in Diagram (b) of Fig. 12) can only happen due to the $h - \delta^0_R$ mixing s_θ. This implies that the process is twice-suppressed: the production is proportional to lepton masses times the mixing angle. Again, maybe a Higgsstrahlung-like process would be more interesting but we will not explore that possibility.
- The left-handed neutral triplet Higgs, δ^0_L, mediated process (in Diagram (b) of Fig. 12) can only occur due to the mixing between neutrinos and HNLs, the amplitude would be proportional to Θ^2.
- The charged flavor violating scalar, $\phi^\pm_{\rm FV}$, t-channel (in Diagram (c) of Fig. 12) is also suppressed for the exact same reasons as to why the $\phi^0_{\rm FV}$ mediated channel also is.
- The charged left-handed scalar triplet, $\delta^\pm_L$, mediated t-channel (shown in Diagram (c) of Fig. 12) is suppressed for the exact same reasons as to why the δ^0_L mediated channel also is.
- The $W^\pm_L$ mediated channel (shown in Diagram (c), Fig. 12), is suppressed because the cross-section is proportional to $\sigma \propto \xi^4_W$, which is suppressed compared to the channels described in the previous subsection.

All the diagrams are shown in Fig. 10 and 12 can produce a single HNL and a neutrino. One of the few advantages of this process is that we will have less phase space suppression, but most of these diagrams will have huge suppressions.

The diagrams in Fig. 10 will all be suppressed because their amplitude will either be proportional to Θ or to ξ_W. Whereas the diagrams in Fig 12 will still be suppressed, some a bit less, but still suppressed enough for us to consider them negligible.

The only diagram which might give us something interesting would be the W_L mediated channel, in the case β is big enough (remember ξ_W is proportional to the mixing of the vev of the bi-doublets). This process, being a t-channel, has its cross-section behaving similarly to the W_R mediated channels in the last subsection. As we saw, there will be a cross-section in energy until $\sqrt{s} \sim M_{W_L}$, and it plateaus for higher $\sqrt{s}$, which could be interesting for colliders with relatively low energies but very high luminosity. Even though it might be an interesting perspective, we shall not evaluate it further.

The list of diagrams we've given so far is by no means exhaustive. We already briefly mentioned the possibility of producing Higgs via Higgsstrahlung and then having them decay into a pair of HNLs. There's also the possibility of producing a $W_L W_L$ pair. Other potential processes do not have the adequate motivation to be examined, like the production of multiple heavy gauge bosons like two W_R or a W_L, W_R pair, given how the latter is suppressed by ξ_W.

Even though our list is not exhaustive, we're confident we're showing the most relevant contributions that can be searched for.

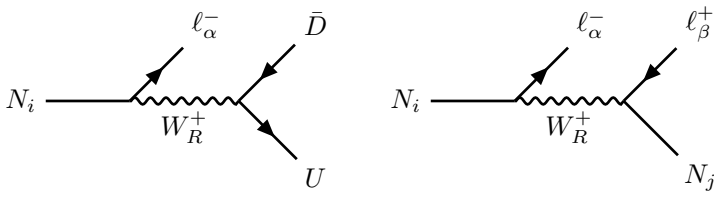

W_R mediated decays

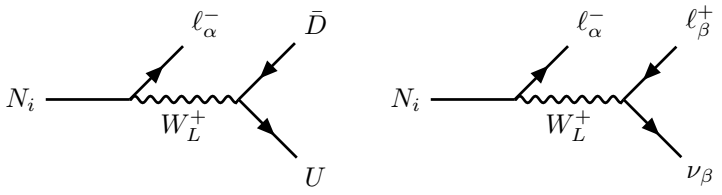

W_L mediated decays

Figure 13: Main HNL decay channels.

5.3 Main HNL decay channels

Now that we've discussed the production of HNLs, we can discuss the possible signals we would obtain from HNLs. The diagrams of the main decay channels we're considering are in Fig. 13, either a W_R or a W_L mediated channel. The latter can only happen if $\beta \neq 0$.

There are a few points we have to mention about these channels. If $m_N \ll M_{W_R}, M_{W_L}$ then both intermediate gauge bosons would be mostly off-shell. If not, then we would have to consider possible on-shell effects of the intermediate bosons.

Also, even though both channels could have the same final state ($N_i \to \ell_\alpha^- U \bar{D}$) they do not interfere with one another: the quarks will have different chiralities for different channels.

The decay $N_i \to \ell_\alpha^- \ell_\beta^+ N_j$ is only possible if $i \neq j$ and if kinematically allowed: the HNL with the lowest mass cannot decay into another HNL

HNLs, since they are Majorana particles, can decay with equal probabilities to particles as well as to anti-particles (see Appendix A) or: $\Gamma(N \to \ell_\alpha^- W_R^+) = \Gamma(N \to \ell_\alpha^+ W_R^-)$, where W_R can either be on-shell or of-shell, the only thing that will distinguish both of them will be the kinematic distribution (as well as the charge, obviously).

Once again, we calculated the decay widths within the simplified scenario that $V_N = I$, and we considered only the decay of the *lightest HNL*, meaning no HNLs decaying into another HNL. We shall only give the final result of the calculation of the decay widths in this section. The details of the computations are in Appendix. C.2.

In the case $M_{W_R}, M_{W_L} \gg m_N$ and where we have negligible masses of the final particles,

then:

$$\Gamma(N \to \ell_\alpha^- U_i \bar{D}_j) = \Gamma(N \to \ell_\alpha^+ \bar{U}_i D_j) \simeq \begin{cases} \dfrac{G_F^2 m_N^5}{64\pi^3} \dfrac{M_{W_L}^4}{M_{W_R}^4} \left|V_{i,j}^{\rm CKM}\right|^2, & \text{for the } W_R \text{ mediated channel}, \\ \dfrac{G_F^2 m_N^5}{64\pi^3} \xi_W^2 \left|V_{i,j}^{\rm CKM}\right|^2, & \text{for the } W_L \text{ mediated channel}, \end{cases} \tag{110}$$

$$\Gamma(N \to \ell_\alpha^- \ell_\beta^+ \nu_\beta) = \Gamma(N \to \ell_\alpha^+ \ell_\beta^- \nu_\beta) \simeq \frac{G_F^2 m_N^5}{192\pi^3} \xi_W^2 \,, \tag{111}$$

where here we've taken the left-handed and the right-handed CKM matrices to be equal, remember that in the case of $\mathcal{P}$ they are equal up to some phases, and in the case of $\mathcal{C}$ they are the transpose of one another up to some signs, the difference between both should vanish when we take the absolute value.

The difference between leptonic and semi-leptonic decays resides in a factor of three coming from quark colors. If we only consider decays to light quarks (u, d, c, s, b) and leptons, then our total decay width, Γ_N, is:

$$\Gamma_N \simeq \frac{G_F^2 m_N^5}{16\pi^3} \left[\frac{M_{W_L}^2}{M_{W_R}^2} + \frac{3}{2}\xi_W^2\right], \tag{112}$$

we can slightly generalize this formula to also include effects from an on-shell M_{W_L}. In this case, we cannot ignore the transferred momentum or the decay width of W_L, then we can generalize Eq. (112):

$$\Gamma_N \simeq \frac{G_F^2 m_N^5}{16\pi^3} \left[\frac{M_{W_L}^2}{M_{W_R}^2} + \frac{3}{2}\xi_W^2 I(m_N, M_{W_L}, \Gamma_{W_L})\right], \tag{113}$$

where Γ_{W_L} is the total decay width of the W_L and I is a dimensionless function that comes from the phase-space integration of the three-body decay which we are defining as:

$$I(m_N, M_{W_L}, \Gamma_{W_L}) = \frac{1}{2}\int_0^1 \frac{(1-x)^2(1+2x)}{(1 - x\, m_N^2/M_{W_L}^2)^2 + \Gamma_{W_L}^2/M_{W_L}^2}\,. \tag{114}$$

We've plotted the decay width for HNLs in Eq. (113) in Fig. 14 for two cases, where $\beta = 0$ (where $\xi_W = 0$) and for $\beta = \frac{\pi}{4}$, where ξ_W^2 is maximum. There is a difference between both plots at low masses due to the extra decay channels, as well as for heavier HNLs due to on-shell decays into a W_L-boson.

Notice that in both cases we shall have that $\Gamma_N \ll m_N$, this is a nice advantage because it allows us to use the so-called Narrow Width Approximation (NWA). The NWA allows us to consider intermediate particles with very small widths compared to their masses to be considered mostly on-shell if the center-of-mass energy allows for the on-shell production (see e.g., Chapter 9 of [199]).

The NWA is a crucial tool for us if we want to calculate the cross-section of the entire process:

$$\sigma(\ell^-\ell^+ \to NN \to [\ell^- U\bar{D}][\ell^+\bar{U}D]) \simeq \sigma(\ell^-\ell^+ \to NN) \times \text{Br}(N \to \ell^- U\bar{D}) \times \text{Br}(N \to \ell^+\bar{U}D)\,, \tag{115}$$

where Br is the branching ratio of a process: the decay width of a specific process divided by the total decay width. If we didn't have this option we would have to calculate a $2 \to 6$ process. Not

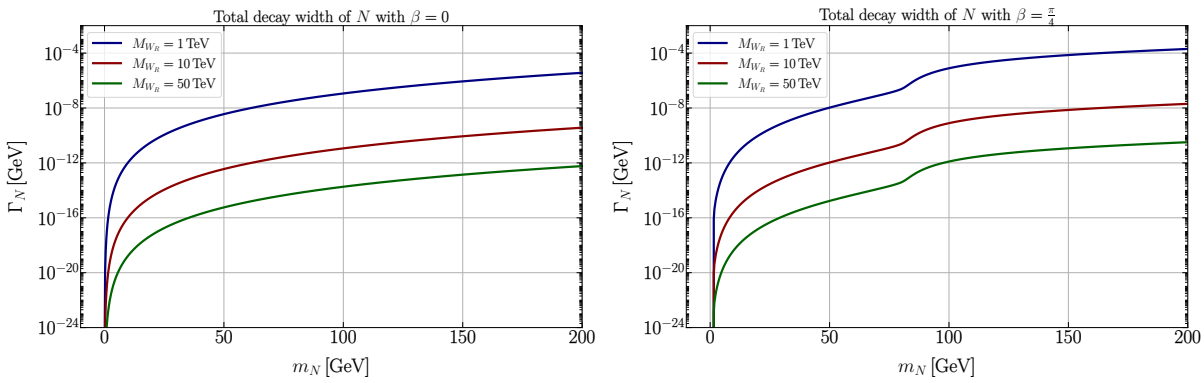

Figure 14: Plot of the decay width of an HNL in terms of its mass in GeV. For $\beta = 0$ (left) and $\beta = \pi/4$ (right).

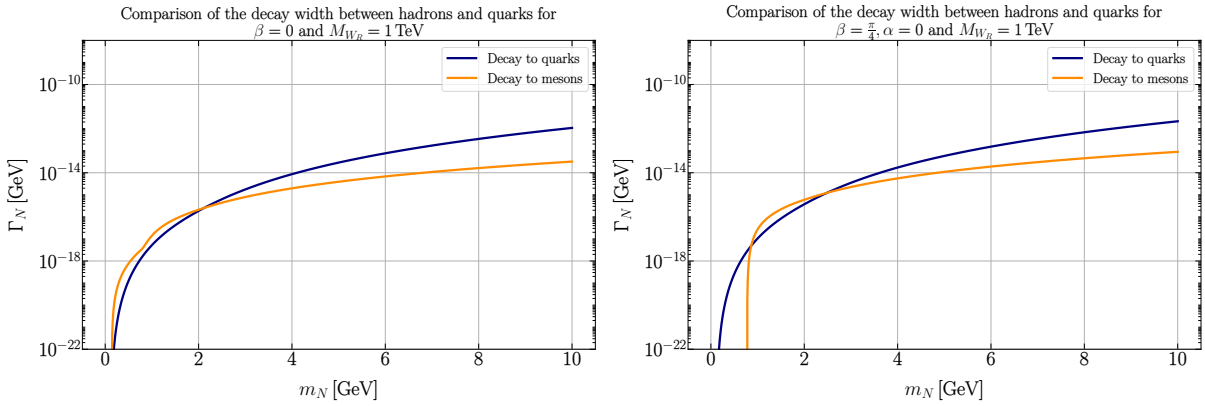

Figure 15: Plot comparing the semi-leptonic decay widths of N into either quarks themselves or composite mesons for $M_{W_R} = 1\,\text{TeV}$ and $\beta = 0$ at the left and $\beta = \frac{\pi}{4}, \alpha = 0$ on the right.

only is the calculation of the total amplitude square difficult, but the phase-space integration also could probably not be analytical and will require the use of Monte Carlo tools to do these integrals (see [200] for more details on these methods). Some tools rely on these methods to do simulations and estimate cross-sections of multiparticle processes, like `MadGraph` [201] or `WHIZARD` [202].

There is another interesting feature of having a small decay width: it means that HNLs can have a relatively long lifetime. Indeed, the lifetime of a particle is inversely proportional to the total decay width: $\tau_N \propto \Gamma_N^{-1}$. This won't be the case when the mass of the HNL is not that much smaller than the mass of W_R, then any HNL would decay quickly enough.

Before moving forward, let's discuss a final possibility, which is the decay of HNLs into composite states: either spin-0 pseudo-scalar or spin-1 vector mesons. Indeed, for sufficiently light HNLs, with masses lower than the QCD phase transition $\Delta_{\text{QCD}} \simeq \mathcal{O}(\text{GeV})$ HNLs will mostly decay into composite QCD quark states rather than the quarks themselves [203].

The decay width to either a pseudo-scalar or a vector meson should be well-known in the literature, but we've repeated the calculation in Appendix C.3. These decays are also mediated by the diagrams shown in Fig. 13 with quarks in the final state. Notice, however, that here there will be an interference between the W_L and W_R mediated diagrams, the final composite states will be the same in both cases, there is no difference in chirality as in the case of decays to quarks

themselves. Neglecting the mass of the final charged lepton:

$$\Gamma(N \to \ell_\alpha^- P^+) = \Gamma(N \to \ell_\alpha^+ P^-) \simeq \frac{G_F^2\, m_N^3}{16\,\pi}\, f_P^2\, \left|V_{i,j}^{\rm CKM}\right|^2 \left|\frac{M_{W_L}^2}{M_{W_R}^2} - \xi_W\, e^{i\alpha}\right|^2 \left(1 - \frac{m_P^2}{m_N^2}\right)^2 , \quad (116)$$

$$\Gamma(N \to \ell_\alpha^- V^+) = \Gamma(N \to \ell_\alpha^+ V^-) = \frac{G_F^2\, m_N^3}{16\,\pi}\, f_V^2\, \left|V_{i,j}^{\rm CKM}\right|^2 \left|\frac{M_{W_L}^2}{M_{W_R}^2} + \xi_W\, e^{i\alpha}\right|^2 \left(1 + 2\,\frac{m_V^2}{m_N^2}\right) \left(1 - \frac{m_V^2}{m_N^2}\right)^2 , \quad (117)$$

where $V_{i,j}^{\rm CKM}$ is the CKM matrix component of particles that compose the meson, m_P, and m_V are the masses of the pseudo-scalar and the vector respectively, and f_P and f_V their decay constants. The values of the masses and decay constants for different mesons are in Appendix D.

What is most interesting here is that if $s_{2\beta} c_\alpha$ is not negligible, to either prefer to decay to pseudo-scalars or vectors, depending on the value of α.

From Eq. (116) and (117) we can calculate the total decay width of HNLs decaying to mesons and a charged lepton:

$$\Gamma(N \to \ell + \text{mesons}) = 2 \sum_P \Gamma(N \to \ell_\alpha^- P^+) + 2 \sum_V \Gamma(N \to \ell_\alpha^- V^+) , \quad (118)$$

where the factor of two comes from the Majorana nature of HNLs.

We've compared the total decay width of both possible semi-leptonic decays, either to quarks themselves or to mesons in Fig. 15. The plot is in agreement with the usual expectation that for HNLs with masses above the $\mathcal{O}(\text{GeV})$ scale should mostly decay to quarks. Notice, however, how different both plots are for $\beta = 0$ on the left and $\beta = \pi/4, \alpha = 0$ on the right. The difference is once again due to the interference between W_L and W_R: there is suppression for pseudo-scalar decays but an enhancement for vector decays.

The plots also tell us that we should only really worry about decays into composite states for HNLs with masses below $\sim 2 - 3\,\text{GeV}$. Heavier HNLs mostly decay into quarks themselves.

5.4 Other possible decay channels

HNLs can also have decays mediated by a neutral current or by the scalar sector.

Decays mediated by a neutral current are suppressed since these decays could only be proportional to Θ. Whereas decays through intermediate scalars are all suppressed for very similar reasons as to why the cross-section production through intermediate scalars is suppressed: either the couplings are too small.

5.5 HNL lifetime and decay length

Now that we've talked about the decay width, we will have a brief discussion about the lifetime of our HNLs. It is well known that the lifetime of a particle is inversely proportional to its decay width. With this we can obtain the decay length of an HNL in frame where it has an energy E_N:

$$L_N = \beta_N\, \gamma_N\, \tau_N = \frac{\sqrt{E_N^2 - m_N^2}}{m_N}\, \frac{1}{\Gamma_N} , \quad (119)$$

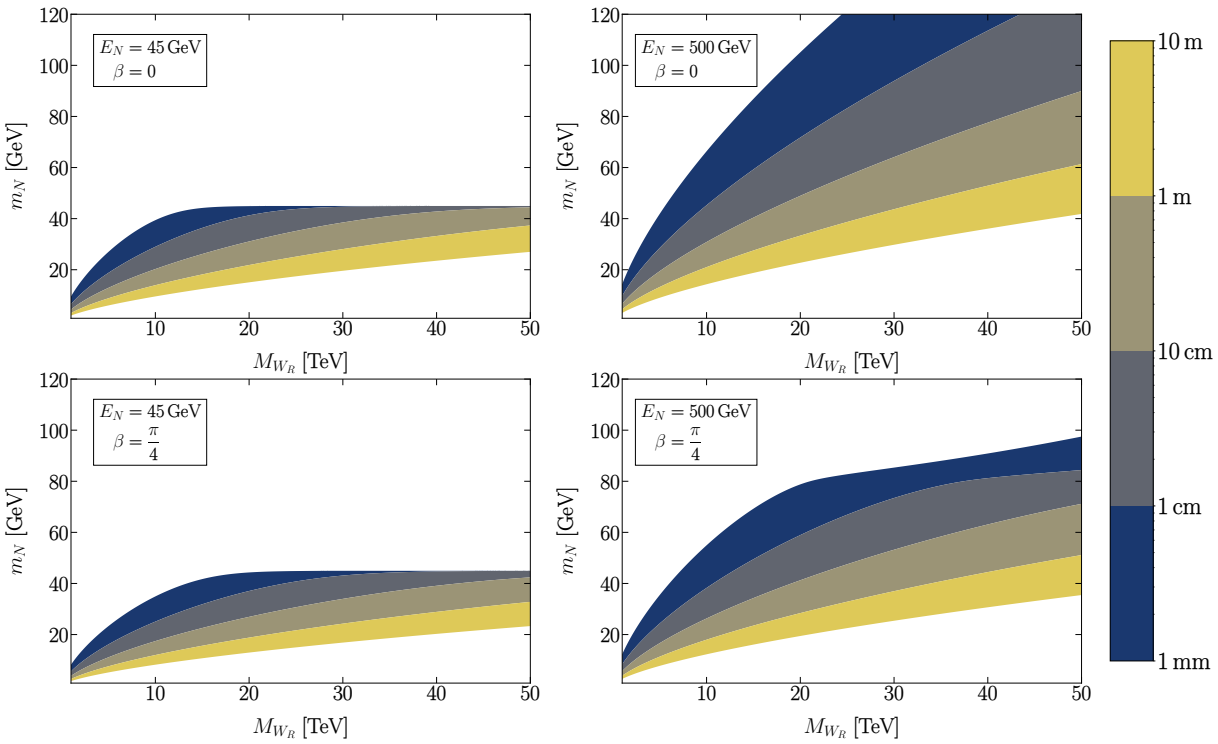

Figure 16: Decay length for different HNL energies E_N and values of β as a function of M_{W_R} and m_N. The different colors indicate the decay length shown in the color-bar on the right.

where β_N is the speed of the HNL, γ_N is its relativistic factor and τ_N is its lifetime. Of course, in the context of a pair of HNLs produced in a collider $E_N = \sqrt{s}/2$, half the center-of-mass energy.

From Eq. (113) we can immediately see that the decay width is inversely proportional to M_{W_R} and proportional to M_N. Therefore, the lighter N is and the heavier M_{W_R} is, the bigger lifetime and decay length N will have.

It is also entirely possible to have a relatively heavy and long-lived HNL as long as $\beta \ll 1$ and as long as W_R is sufficiently heavy. If this were not the case, the lifetime will be short due to decays to on-shell W_L bosons. We've plotted the decay-length of HNLs with different energies and different values of *beta* in a $m_N - M_{W_R}$ parameter space plot in Fig. 16.

5.6 How much can lepton colliders actually see?

Let's assume that the discovery of LRSM becomes significant when we've seen a specific number of signals, $\mathcal{N}_{\text{events}}$, which is equal to:

$$\mathcal{N}_{\text{events}} = \mathcal{L}_{\text{int.}} \cdot \sigma(\ell^-\ell^+ \to NN)\,, \tag{120}$$

where $\mathcal{L}_{\text{int.}}$ is the integrated luminosity of the collider at hand.

We can find what the maximum value of M_{W_R} can a specific collider probe for a specific value of $\sqrt{s}$ by solving for M_{W_R} in Eq. (120). For lepton colliders at the Z_L-pole we would have to use the value of the cross section at that energy; for much higher energies we can use Eq. (109), which is the maximum cross section (outside the Z_R-pole). This will overestimate the actual capacity of the lepton collider, but should be good enough as a first approximation.

The maximum probe of m_N is a simple matter of kinematics, the biggest value we can reach of $\sqrt{s}/2$, but the lowest value is not entirely simple. If HNLs are very light, they might not escape inside the detector and then we might never detect them. The minimum value we could probe of HNLs would actually come from Eq. (119), we would need to solve for m_N, here we can safely use Eq. (112). For the new generation of lepton colliders, their geometries will allow more or less a decay length of 3-5 m (more on the next section).

We should make a statement about background free processes, we can have displaced vertices as well as LNV processes. Displaced vertices can be considered to be almost background free for displacements above 5 mm. For lower lengths, there are a meson and τ decays would induce background [204, 205]. LNV signals in the form of a SS final lepton state, which correspond to half the total signal, should be background free: the SM does not have any LNV signal.

In practice there will be some complications to both of them, for displaced vertices we must take into consideration the possible suppression we might get from not properly reconstructing displaced vertices. Prompt SS processes can actually have SM backgrounds, not due to LNV processes, but rather because an additional neutrino would be produced that would not actually be seen. At the LHC, for example, the main sources of background for LNV processes come from SM diboson events [134, 206].

6 Sensitivity of lepton colliders on LRSM parameters

There have already been multiple studies on the potential that lepton colliders have in searches regarding the extended scalar sector of the LRSM [62–66]. We will map the sensitivity that the multiple proposals for lepton colliders have for HNLs and right-handed gauge bosons.

In the last section, we commented on the analytical computations we made for the production and decay of HNLs. The production cross-section calculations will not be enough: there are collider effects that we have to take into account to get a better estimate of the sensitivity.

One of these effects is Initial State Radiation (ISR), where we must consider second-order QED effects. Moreover, linear colliders are intent on polarizing their beams [207], which means that the initial leptons will have a defined distribution on helicity. Both will impact the cross-section, ISR will suppress the cross-section whereas beam polarization can negatively or positively increase the polarization. The latter is because of how left and right-chiral leptons interact with LRSM gauge particles: W_R will mostly interact with left-chiral anti-particles and right-chiral particles. Therefore a polarized beam with positive helicity particles and negative helicity anti-particles will enjoy a bigger cross section in the production of HNLs than one that isn't. The effect of a polarized beam is one of the few things recognized in the literature for the potential next generation of lepton colliders [67].

We did not consider these effects analytically (the details regarding the analytical computation of ISR see Chapter 20 of [208], and for polarized lepton beams see [207]), but rather, we used an event simulator to help us obtain how much would the cross sections change. We used `WHIZARD` [202] to model both effects, with the Universal FeynRules Output (UFO) files from [189].

ILC parameters				
$\sqrt{s}$ [GeV]	$\mathcal{L}_{\text{int.}}$ [ab^{-1}] for each $P(e^-, e^+) = (\pm 0.8, \pm 0.3)$			
	$(-,+)$	$(+,-)$	$(+,+)$	$(-,-)$
250	1.35	0.45	0.1	0.1
350	0.135	0.45	0.01	0.01
500	1.6	1.6	0.4	0.4

Table 4: Proposed beam polarizations and respective integrated luminosities for the ILC plan H20 [168, 169].

CLIC parameters		
$\sqrt{s}$ [GeV]	$\mathcal{L}_{\text{int.}}$ [ab^{-1}] for each $P(e^-, e^+) = (\pm 0.8, 0)$	
	$(-,0)$	$(+,0)$
380	0.5	0.5
1500	2.0	0.5
3000	4.0	1.0

Table 5: Proposed beam polarizations and respective integrated luminosities for CLIC [209].

6.1 Sensitivity to displaced vertices

To obtain the sensitivities we must first cut on HNLs that are not displaced enough to be considered prompt and cut on HNLs that are too displaced so that they decay outside the

detectors. We already said in the last section that we will consider displaced any particle whose decay length is above 5 mm, whereas the maximum displacement that HNLs can decay to depends on the geometry of the detector. We can filter on the particles with the desired decay length by multiplying times the decay probability in Eq. (120):

$$\mathcal{N}_{\text{events}} \simeq \mathcal{L}_{\text{int}} \cdot \sigma(\ell^-\ell^+ \to NN) \cdot P_{\text{dec.}} \cdot \epsilon \tag{121}$$

where here ϵ is the detection efficiency, $P_{\text{dec.}}$ is the decay probability:

$$P_{\text{dec.}} = \frac{1}{\pi}\int_0^\pi \mathrm{d}\theta \left[e^{-L_{\text{min.}}/L_N} - e^{-L_{\text{max.}}(\theta)/L_N}\right], \tag{122}$$

where L_N is defined in Eq. (119)[18]. Here we will set $L_{\text{min.}} = 5\,\text{mm}$ but $L_{\text{max.}}(\theta)$ for a cylindrical geometry is equal to:

$$L_{\text{max.}}(\theta) = \begin{cases} \dfrac{z}{2\,\cos\theta}\,, & \text{for } 0 < \theta < \arctan\left(\dfrac{2r}{z}\right), \\ \dfrac{r}{\sin\theta}\,, & \text{for } \arctan\left(\dfrac{2r}{z}\right) < \theta < -\arctan\left(\dfrac{2r}{z}\right), \\ \dfrac{-z}{2\,\cos\theta}\,, & \text{for } \arctan\left(\dfrac{2r}{\ell}\right) < \theta < \pi\,, \end{cases} \tag{123}$$

where r is the radius of the detector and z is the total *height* of the cylinder. To a very good approximation, we can use the average maximum length, rather than integrate the entire probability: the average maximum length is:

$$\langle L_{\text{max.}}\rangle = \frac{2}{\pi}\left[\frac{z}{2}\log\left(\frac{2r+\sqrt{z^2+4\,r^2}}{z}\right) + r\log\left(\frac{z+\sqrt{z^2+4\,r^2}}{2r}\right)\right]. \tag{124}$$

There are several proposals for different detectors for all colliders. We will consider only two of them as benchmark points. We will consider the geometry of the IDEA detector [45, 210] for circular and muon colliders; and the geometry of the SiD detector [211] for linear colliders. We will only consider HNLs that decay before reaching the muon system. The geometric values of both detectors are in Table 6.

Detector	z [cm]	r [cm]	$\langle L_{\text{max.}}\rangle$ [cm]
IDEA	1100	450	556.59
SiD	600	250	306.56

Table 6: Geometric values for the IDEA [45] and SiD [169] detectors.

We will want the number of events detected such that there is at least a 2σ significance of the discovery. Given how we will consider displaced particles to be background-free this will come from only $\mathcal{N}_{\text{eve.}} = 4$. We plotted the constraints from the best runs for each experiment in Fig 17 for the case $\beta = 0$.

The FCC-ee and CEPC give their best constraints in their runs at the Z_L-pole; whereas the

[18] We've checked with `WHIZARD` whether the momentum for distribution for HNLs would change due to ISR or any other effect, and we found no significant difference.

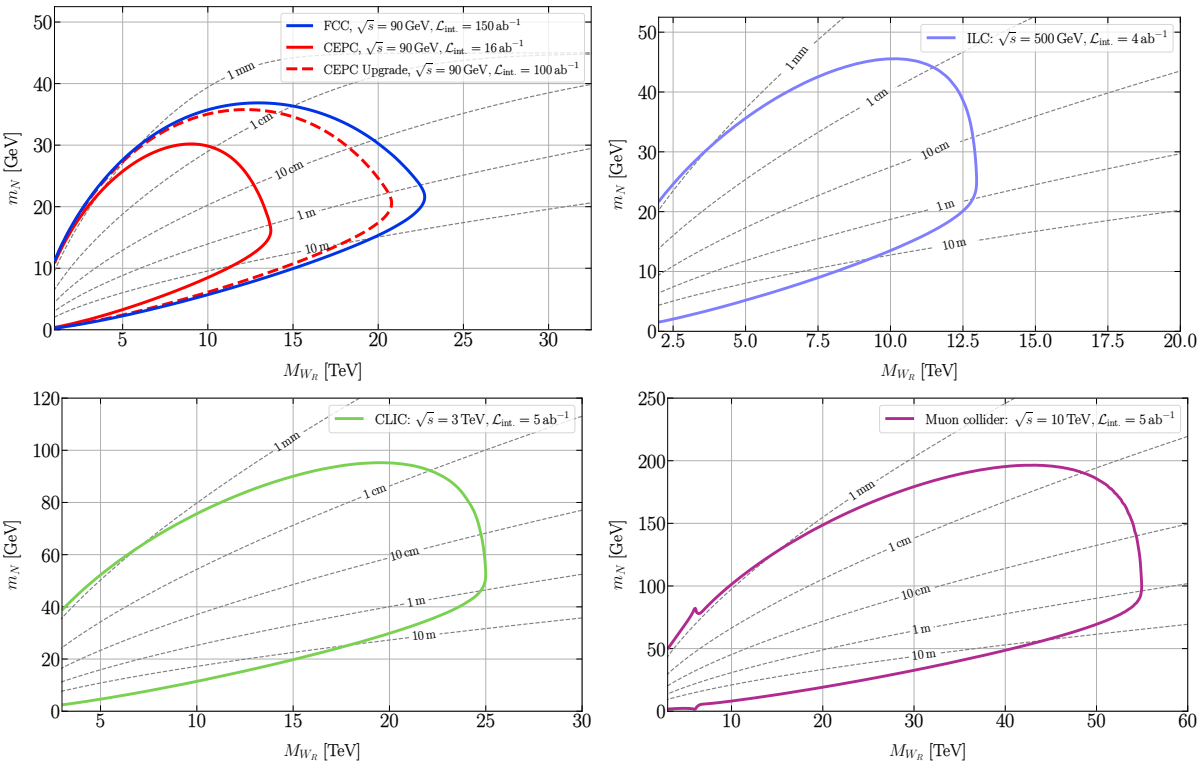

Figure 17: Sensitivity of the different experiments assuming $\epsilon = 1$ and $\mathcal{N}_{\text{eve.}} = 4$. The benchmark points are the ones shown in Table 3 with geometries in Table 6. For ILC and CLIC we took the values of beam polarization and their corresponding luminosities from Tables 4 and 5 respectively.

rest of the experiments give their best constraints for their runs at their highest energies.

We also plotted if Fig. 17 how displaced, on average, each HNL would be. We should state that those lines are on average, decays are processes that are due to quantum interactions and are therefore probabilistic, this is why we're sensitive to HNLs that can decay on average to 10 m despite the fact that they would decay outside the detector. Some of them won't.

The sensitivity that displaced searches have managed to reach a W_R with a mass in the order of $\mathcal{O}(10\,\text{TeV})$. If the reader remembers our discussion on whether the LRSM can solve some of the problems that the SM has, the lack of a mechanism to generate BAU, the lack of a dark matter candidate, and the strong-CP problem in Section 3.7, all require a W_R with at least $\sim 17\,\text{TeV}$. With the exclusion of the ILC, all of these experiments will be capable of probing certain regions of the parameter space where we could solve some of these problems. Moreover, a dark matter keV HNL will require another in the GeV region: all of these experiments will be capable of probing regions of the parameter space that meet both requirements. If we discover an HNL in this region of the parameter space, we will then only require to discover a keV HNL in order to make the discovery of dark matter.

How realistic in an $\epsilon \simeq 1$? There have been numerous previous studies on the sensitivity of long-lived HNLs in the context of the minimal Type-I Seesaw, and they all assumed $\epsilon \simeq 1$ [212–214]. [214] made a specific study on the potential detection efficiency for long-lived HNLs and argued it should be very close to it being 1 for semi-leptonic HNL decays. Semi-leptonic HNL decays for both models should be almost identical to one another with a difference perhaps in the angular distribution of both particles due to the different chiral structure. The big difference

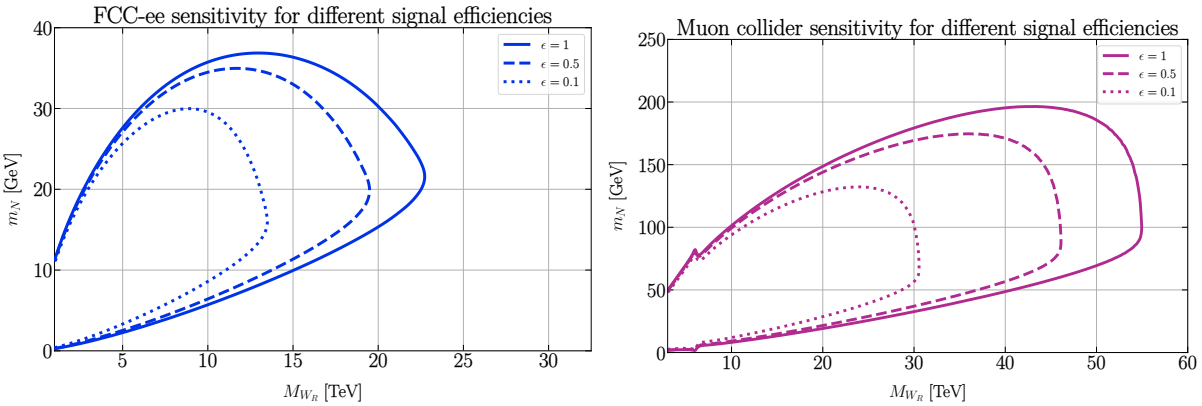

Figure 18: Re-calculation of the sensitivity of the FCC-ee and a muon collider with different overall efficiencies.

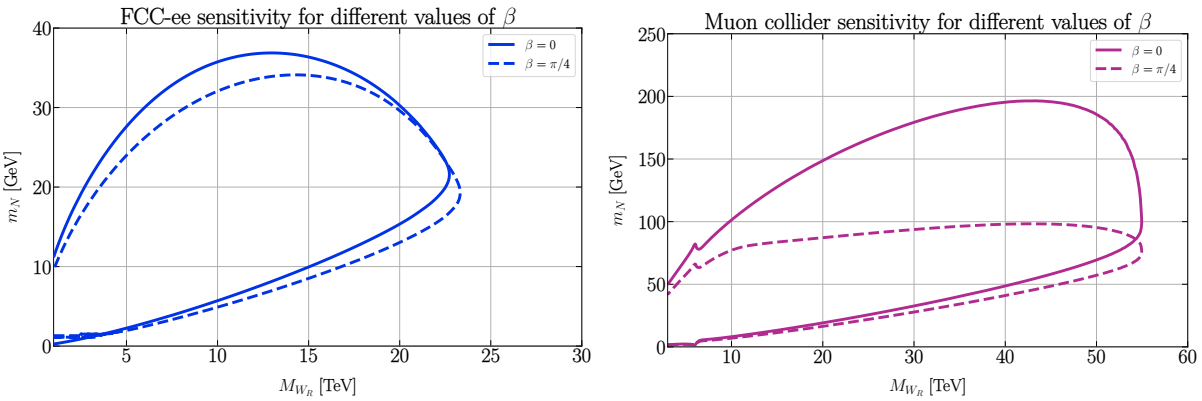

Figure 19: Sensitivity the FCC-ee and a muon collider would have to long-lived HNLs for different values of β.

in both models lies in the fact that we're producing two long-lived HNLs and not only one. We have to ask the question of whether we would still have a good efficiency if we manage to tag on two long-lived HNLs rather than one.

The reconstruction efficiency for long-lived particles at the LHC is typically above 0.1 for long-lived particles [204, 205]. The efficiency typically decreases linearly with decay length most of the time, but new clever techniques are being developed, for example, particles that decay inside the hadronic calorimeter (HCAP) can enjoy a better reconstruction than ones that decay in the electromagnetic calorimeter (ECAP): the ratio of energy deposited in the ECAP over than the one in the HCAP is much lower than what a jet would [215]. We can only hope that better and better techniques will be developed for the LHC that will serve as experience for detections in lepton colliders.

Having said this, we will take into consideration the possibility of having efficiencies lower than 1. In Fig. 18, we've plotted the sensitivity that the FCC-ee and a muon collider would have with an efficiency of $\epsilon = 0.5$ and $\epsilon = 1$ compared with the results in Fig. 17.

Finally, we should also mention the parameter β. In the case it is not zero, we will allow decays mediated by a W_L which will severely change the sensitivity of displaced searches for heavy HNLs due to the possibility of having on-shell W_L decays which will give heavy HNLs a much shorter displacement. It will also affect, to a lower degree, the sensitivity of lighter HNLs

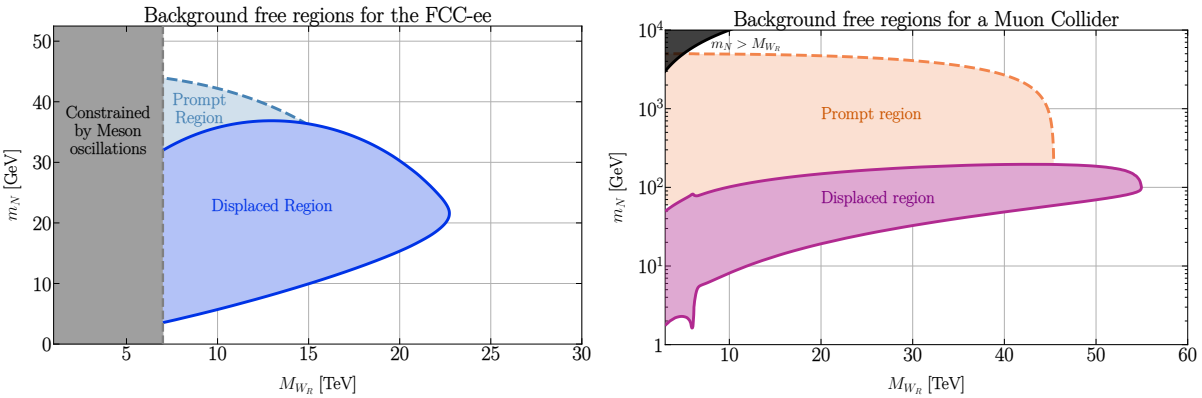

Figure 20: Overall sensitivity to both prompt and displaced searches for the FCC-ee at the Z_L-pole (left) and for a Muon Collider with $\sqrt{s} = 10\,\text{TeV}$.

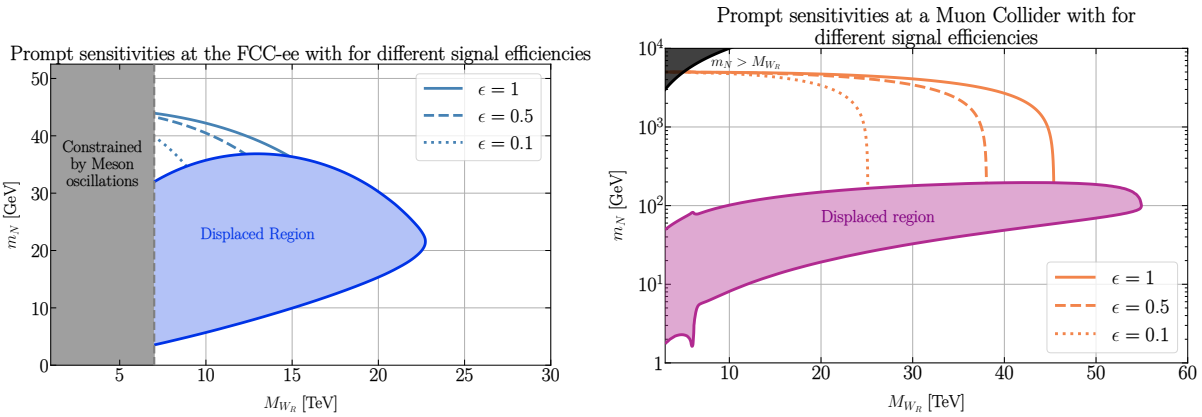

Figure 21: Effect of an overall sensitivity to the results obtained in Fig. 20.

since it will open more decay channels. The difference is shown in Fig. 19.

A different study recently proposed a different detector for lepton colliders called HECATE [216], which, if built, will give a 4π solid angle coverage in the cavern walls. It will effectively increase the maximum decay length to either 15 m or to 25 m. This will increase sensitivity to lighter HNLs, we show how much this will change in Appendix E.

6.2 Sensitivities to prompt HNLs

As we said in the previous section, we can also have background-free prompt HNL processes when we have SS leptons in the state, which will cut the total signal in half. We can perform the same analysis we did in the previous subsection to find the sensitivity, this time it will be simpler:

$$\mathcal{N}_{\text{events}} = \frac{1}{2}\,\mathcal{L}_{\text{int.}} \cdot \sigma(\ell^-\ell^+ \to NN) \cdot \epsilon\,, \tag{125}$$

We show the sensitivity we would get only for both the FCC-ee and for a Muon Collider for both prompt and displaced searches with an efficiency $\epsilon = 1$ in Fig. 20. We're only showing the values in $\sqrt{s}$ and $\mathcal{L}_{\text{int.}}$ that would give the sensitivities.

We're comparing the sensitivity the FCC-ee would have with the constraints we would get from meson oscillation from the next run of Belle-II and LHCb. There is a small additional region of the parameter space we're covering due to prompt LNV processes. On the other hand,

a 10 TeV muon collider will have much better sensitivity, potentially covering a huge region of the parameter space, especially with regards to $\mathcal{O}$(TeV) HNLs. This should not be surprising: a bigger center-of-mass energy will improve the sensitivity to heavier HNLs.

Prompt searches will also have the potential to make statements regarding the status of LRSM with regards to BAU, dark matter, and strong-CP violation due to the fact that they'll also be capable of probing W_R's in the proper region of the parameter space.

Of course, there will also be the question of the efficiency due to potential backgrounds, for example, multi-SM gauge boson production or particle misidentification could contribute to a background. The last ATLAS search gave an efficiency between 0.5 and 0.1 to the KS-process for different regions of the parameter space [134]. A full study of the background of SS-lepton signal is beyond the scope of this work. To have an idea of how much sensitivity we would lose, we plotted the sensitivity for $\epsilon = 0.5$ and $\epsilon = 0.1$ in Fig. 21.

7 Conclusions and future avenues of research

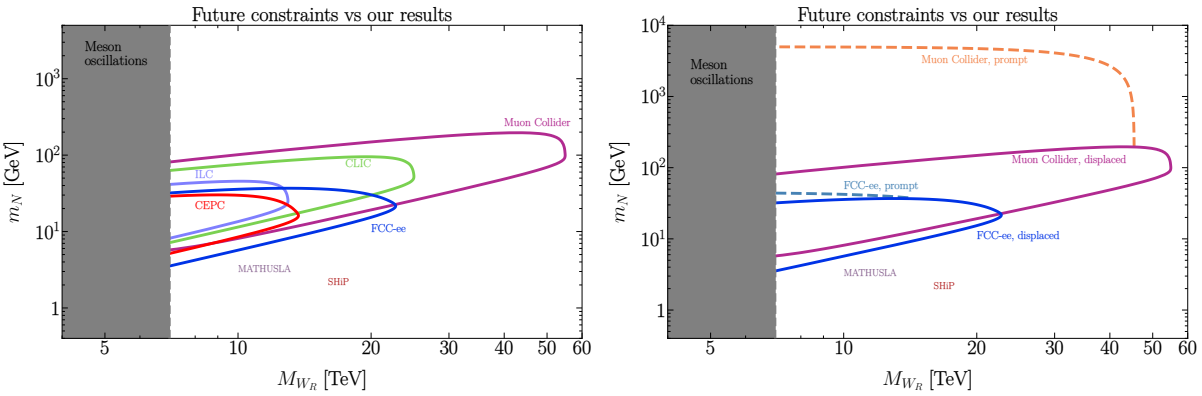

Figure 22: Comparison between our results obtained in Fig. 17 and 20 and the sensitivity of future experiments shown in Fig. 7. We did not include the constraints of the proposed upgrade to the CEPC, but the sensitivities should be very similar.

We've studied the production and decay of LRSM HNLs in lepton colliders and then analyzed the potential sensitivity that different proposals for lepton colliders have on LRSM parameters. The signals LRSM HNLs give us are, theoretically, background-free; either in the shape of displaced vertices or lepton number violating processes. We find that our constraints cover regions of the parameter space that would've been deemed unreachable by other means. Displaced vertex searches are more sensitive to lighter HNLs and heavier W_R's, whereas lepton number searches have a much higher sensitivity to heavier HNLs.

The sensitivity of W_R with masses in the $\mathcal{O}(10\,\text{TeV})$ we will be capable of probing a mechanism for the generation of the BAU, a potential probe for dark matter and an explanation for the lack of CP violation in strong interactions. Moreover, the discovery of this specific branch of LRSM will also give an indirect probe for the generation of neutrino masses (to properly probe it, we would need to see a signal proportional to Θ).

This study on the sensitivity that lepton colliders have on LRSM parameters is the first of its kind and is open to many avenues of potential future studies: a proper analysis of the background of SS leptons and an analysis of the reconstruction efficiency for double-displaced vertices. Moreover, there is a question on whether the Seesaw mechanism and the origin of neutrino masses could be actually probed. Also, whether there could be a probe of the mixing matrix of HNLs, given how our study only did a simplified analysis assuming they do not mix.

Appendices

Appendix A Majorana particles

[19] In 1937 Ettore Majorana published a paper that contained his famous equation [220]. He found a different equation than the Dirac Equation for relativistic neutral fermions. The main difference is that it had fewer degrees of freedom: the Majorana equation models particles that are their own antiparticles. Or in other words, any fermion field which follows:

$$\psi = \psi^C \,, \tag{126}$$

with $\psi^C = -i\gamma_2\,\psi$ (in the chiral basis of Gamma matrices) being the charge conjugated field. Much like we can decompose Dirac fields as a sum of their right and left-chiral components, we can do the same for Majorana particles:

$$\psi = \psi_L + \psi_L^C \,, \tag{127}$$

where ψ_L^C will actually be right-chiral [20].

The expansion of a Majorana field in terms of the Fourier coefficients will be different from the Dirac usual expansion. We will present both for comparison:

$$\psi_D = \int \frac{\mathrm{d}^3\,p}{(2\pi)^3\,2E_p} \sum_{h=\pm 1} \left[c_p^h\, u_p\, e^{-ip\cdot x} + d_p^{h\dagger}\, v_p\, e^{ip\cdot x} \right] , \tag{128}$$

$$\psi_M = \int \frac{\mathrm{d}^3\,p}{(2\pi)^3\,2E_p} \sum_{h=\pm 1} \left[a_p^h\, u_p\, e^{-ip\cdot x} + a_p^{h\dagger}\, v_p\, e^{ip\cdot x} \right] , \tag{129}$$

where ψ_D is a Dirac field, and ψ_M is a Majorana field. c_p^h and d_p^h are the annihilation operators for particles and anti-particles respectively for Dirac fields, and a_p^h is the annihilation operator for Majorana fields. Of course, we do not need two different operators for Majorana fields since they're their own anti-particle. u and v are the usual spinors.

We have the following anti-commutation relations from canonical quantization for the creation/annihilation operators of Majorana fields:

$$\begin{aligned} \left\{ a_p^h, a_q^{h'\dagger} \right\} &= 2\,E_p\,\delta_{h,h'}\,\delta^3(p-q)\,, \\ \left\{ a_p^h, a_q^{h'} \right\} &= \left\{ a_p^{h\dagger}, a_q^{h'\dagger} \right\} = 0\,. \end{aligned} \tag{130}$$

All of these relations can be derived from the condition in Eq. (126), but they can also be derived from the free Majorana Lagrangian and solving the Majorana equation. The free

[19] The curious reader can find a more detailed discussion on Majorana particles and the phenomenological difference between Majorana and Dirac Neutrinos in [217–219]

[20] This is easily seen from the fact that γ_5 and γ_2 anti-commute

Majorana Lagrangian looks like this:

$$\begin{aligned}\mathcal{L}_{\text{Maj.}} &= \frac{1}{2}\bar{\psi}\left(i\partial\!\!\!/ - m\right)\psi\,, \\ &= i\,\bar{\psi}_L\,\partial\!\!\!/\,\psi_L - \frac{1}{2}\,m\left(\bar{\psi}_L\,\psi_L^C + \bar{\psi}_L^C\,\psi_L\right)\,,\end{aligned} \tag{131}$$

the factor of $1/2$ makes sure we have the appropriate value of mass when obtaining the equations of motion. It is convenient to write the Lagrangian as we did in the last equation since this form will have a direct application when considering Majorana neutrinos: since we only have a left-handed neutrino field in the SM, the kinetic term looks the same in this shape.

The mass term is what really makes the difference between Dirac and Majorana fields. The free Dirac Lagrangian has a global U(1) symmetry, but not the free Majorana Lagrangian. In the SM without Majorana neutrinos, this is translated into a $U(1)$ symmetry whose conserved charge is lepton number, neutrinos with a Majorana field will thus violate lepton number.

If neutrinos were Majorana particles, then we should have processes that violate lepton number (LNV processes). A popular example of LNV processes is neutrinoless double beta decay ($02\nu\beta$), we would also have collider examples like same-sign di-lepton signal which was amply discussed in the main text[21].

There is a caveat to LNV processes mediated by neutrinos. Due to the structure of interactions of the SM and to the lightness of neutrinos, interactions that distinguish between Dirac and Majorana neutrinos are suppressed. This is part of the so-called *Practical Dirac-Majorana confusion theorem* [222–224] (see [225] for a recent review). This is, in particular, the case of all interactions mediated by charged currents, but with neutral currents, the situation might be a bit different.

Neutral current interactions between Dirac neutrinos and Majorana neutrinos are actually different. Let's take the Z-vertex, for example:

$$\mathcal{L}_{Z\nu\nu} = \frac{g}{2\,c_w}\bar{\nu}\,Z\!\!\!/\,P_L\,\nu\,. \tag{132}$$

Now, let's calculate the matrix element of $\langle\nu|\colon\mathcal{L}_{Z\nu\nu}\colon|\nu\rangle$ in the case of Dirac neutrinos (see Eq. (128)) and for Majorana neutrinos (see Eq. (129)). Both will be different due to the fact that we will associate neutrinos to u and $\bar{u}$ because only $c/c^\dagger$ can annihilate/create neutrinos; but since $a/a^\dagger$ can annihilate/create both neutrinos and anti-neutrinos, we will have contributions from both u and v:

$$\begin{aligned}&\text{Dirac}: && \langle\nu|\colon\mathcal{L}_{Z\nu\nu}\colon|\nu\rangle \propto \bar{u}\gamma^\mu\,P_L u\,, \\ &\text{Majorana}: && \langle\nu|\colon\mathcal{L}_{Z\nu\nu}\colon|\nu\rangle \propto \bar{u}\gamma^\mu\,P_L u + \bar{v}\gamma^\mu\,P_L v\,, \\ & && \qquad = \bar{u}\gamma^\mu\,(P_L - P_R)u\,,\end{aligned} \tag{133}$$

where the last equality comes from $v^C = u$. What this means is that two Majorana fields do not couple themselves to a vector current. This will have consequences in the cross-section or decay width of processes as well as the angular distribution. The differences in cross-section

[21] We should not assume that LNV processes are immediately associated with Majorana neutrinos or Majorana particles. [221] proposed a neutrinoless quadruple beta decay as a probe for Dirac Neutrinos in certain extensions of the SM. Even within the LRSM, we have LNV processes mediated by the doubly-charged triplets.

are negligible for very light Majorana particles. Neutrino experiments are not sensitive to this difference[22].

The fact that Majorana particles do not couple with neutral current vector currents explains the shape of the amplitude in Eqs. (104) and (105).

Before we finish this appendix, we will make a small comment on the fact that an on-shell HNL, a Majorana particle in our model, can both decays $N \to \ell^- U \bar{D}$ and $N \to \ell^+ \bar{U} D$. One can see this from the evaluation of both amplitudes, both are identical. What will differ between both of them is only the angular distribution of the decay product. For decays mediated by W_R, final leptons would be right-handed and final anti-leptons would be left-handed. [229] pronounced a similar statement in the case of HNLs in the minimal Type-I SeeSaw.

Appendix B Scalar potential and mass spectrum

The most general scalar potential in Eq. (63), without $\mathcal{C}$ or $\mathcal{P}$ can be found in [230]. The case for both $\mathcal{P}$ and $\mathcal{C}$ can be found in [119, 122].

We do not wish to show the full expression of the potential to the reader, lest we scare their poor soul. Let the brave enough and curious readers venture into the references provided. We shall only share the leading term in mass for the scalar sector and the $h - \delta_R^0$ mixing angle in terms of the terms in the potential, both of which can be found in [124].

The scalar sector will induce mixing between $h - \delta_R^0$, just as there mixing between $W_L - W_R$ and $Z_L - Z_R$:

$$h \to c_\theta \, h - s_\theta \, \delta_R^0 \,, \tag{134}$$

$$\delta_R^0 \to s_\theta \, h + c_\theta \, \delta_R^0 \,, \tag{135}$$

where here we're referring to δ_R^0 as the real component, the massive Higgs scalar rather than the imaginary part of this field which is the Goldstone boson that would be eaten by Z_R. We have that:

$$c_\theta \simeq 1 \qquad\qquad s_\theta \simeq \frac{\alpha}{2\rho_1} \frac{v}{v_R} \,, \tag{136}$$

And the mass spectrum is shown in Table 7. The parameters $\Lambda_\Phi, \alpha, \rho_i$ and α_3 in Eq. (136) and in Table 7 are all parameters or combination of parameters that appear in the scalar potential.

Appendix C Phase space integration and computation of cross-sections and decay widths

We will begin with a discussion that resembles the ones in Chapter 2 of [200]. We know that the cross-section of a given process is related to the probability of it occurring. Let's consider a process with two initial particles scattering into n final particles: $p_a + p_b \to p_1 + \cdots + p_n$. Due

[22] The CHARM-II experiment was the first experiment to make measurements of the neutral current couplings of neutrinos [226–228], but was only sensitive to $g_v + g_A$, the sum of the vector and axial contributions, not individual ones. This is also the case with current experiments, such as IceCube.

Particle	Mass^2
h	$4\,\left[\Lambda_\Phi - \alpha^2/(4\,\rho_1)\right]\,v^2$
δ_R^0	$4\,\rho_1\,v_R^2$
$\delta_R^{\pm\pm}$	$4\,\rho_2\,v_R^2$
δ_L	$(\rho_3 - 2\,\rho_1)\,v_R^2$
$\varphi_{\rm FV}$	$\alpha_3/(c_{2\beta})\,v_R^2$

Table 7: Mass spectrum of the scalar sector. See details in the text. Here δ_R^0 is once again the real component, δ_L encompasses all the fields in the left-handed triplet and $\varphi_{\rm FV}$ all of the ones in the flavor violating doublet.

to energy-momentum conservation, we shall have that:

$$p_a + p_b = p_1 + \cdots + p_n\,, \tag{137}$$

where all the p denote the four-momenta of a given particle. Without energy-momentum conservation, we wouldn't have a restriction on the possible configuration of the final particles in the final state.

As we usually know from QFT books (see, e.g. Chapter 5 of [208]), we know that the differential cross-section is:

$$\mathrm{d}\sigma = \frac{1}{2\,\sqrt{\lambda(s, m_a^2, m_b^2)}}\,|\mathcal{M}|^2\,\mathrm{d}\Pi_n\,, \tag{138}$$

where λ is the Källén function $\lambda(a,b,c) = (a-b-c)^2 - 4bc$, m_a is the mass of the particle with four-momenta p_a, and m_b likewise; $s = (p_a + p_b)^2$ is the center-of-mass energy squared. Here $|\mathcal{M}|^2$ contains in itself the information regarding the transition probability from an initial to a final state and $\mathrm{d}\Pi_n$ is the differential Lorentz Invariant Phase Space, defined as:

$$\begin{aligned}\mathrm{d}\Pi_n &= (2\pi)^4\,\delta^4(p_a + p_b - p_1 - \cdots p_n)\prod_{i=1}^{n}\frac{\mathrm{d}^4 p_i}{(2\pi)^4}\,\delta(p_i^2 - m_i^2)\,\Theta(p_i^0)\,,\\ &= (2\pi)^4\,\delta^4(p_a + p_b - p_1 - \cdots p_n)\prod_{i=1}^{n}\frac{\mathrm{d}^3 p_i}{(2\pi)^3}\,\frac{1}{2E_i}\,,\end{aligned} \tag{139}$$

where $\Theta(p)$ is the Heaviside function. All of the functionals appearing in the Lorentz Invariant Phase Space place restrictions on the final particles. It ensures that energy-momentum is conserved, places all final particles on-shell, and ensures they have positive energies.

Decay processes, such as $p \to p_1 + \cdots p_n$, are described using the differential decay width, which is written in a very similar way to the differential cross section:

$$\mathrm{d}\Gamma = \frac{1}{2\,m}\,|\mathcal{M}|^2\,\mathrm{d}\Pi_n\,, \tag{140}$$

where m is the mass of the particle with four-momentum p.

To obtain the cross section or decay width one must integrate the right-hand-side of Eq. (138) or Eq. (140). As one can imagine, the complexity of the integral increases with a bigger n. Phase-space integration for larger n's requires different techniques that can be found in [94]. These

techniques usually require the use of clever and obscure techniques such that the integrals are done with appropriate variables which usually involve the heavy use of Gram determinants. Monte Carlo methods are the best way one can solve these integrals, which modern event simulators typically use.

For the problems required in this thesis, we mostly worked with simple processes like $2 \to 2, 1 \to 3$ and $1 \to 2$ processes, all of which can easily be integrated. There was the possibility, however, to calculate a $2 \to 6$ process which we manage to simplify with the help of the Narrow Width Approximation (NWA).

We typically use the NWA to simplify the computation of hard multi-particle processes where we have an intermediate unstable particle. Take the Breit-Winger distribution of a particle that can be allowed to be produced on-shell (i.e., not in a t-channel), then we can use the following approximation:

$$\frac{1}{(p^2 - m^2) + \Gamma^2 m^2} \xrightarrow{\Gamma m \to 0} \frac{\pi}{\Gamma m} \delta(p^2 - m^2) \,. \tag{141}$$

Let's now imagine a process where we produce an unstable particle that undergoes a specific decay, the NWA allows us to approximate the cross-section of the process to:

$$\sigma \simeq \sigma_P \frac{\Gamma_D}{\Gamma} = \sigma_P \, \mathrm{BR}_D \,, \tag{142}$$

where σ_P is the cross-section required for the production of the unstable particle, Γ_D is the decay width of the decay we're considering, and BR_D is the branching ratio of this decay. A detailed proof of it can be found in [231] for a scalar unstable particle and in [232] for fermions and vector particles.

C.1 Calculation of the $\ell^- \ell^+ \to NN$ cross section

As we mentioned in the main text, the calculations of the cross sections were done with the help of the `Mathematica` packages `FeynCalc` and `FeynArts`, as well as the `FeynRules` files for the LRSM model in [189]. We shall provide a code that calculates the entire cross-section:

```
        Calling FeynCalc and FeynArts:

In[1]:= $LoadAddOns={"FeynArts"};
        <<"FeynCalc`";
        $FAVerbose=0;

        Generating diagrams
        Excluding particles that have a supressed cross section

In[2]:= diags=InsertFields[CreateTopologies[0,2→2],
        {F[2,{1}],-F[2,{1}]}→{F[5,{4}],F[5,{4}]},
        InsertionLevel→{Classes},Model→"mLRSM",
        ExcludeParticles→{S[1],S[2],S[3],S[4],S[9],S[10],S[11],S[12],
        S[13],S[14],V[3]}];
```

```
Generating amplitudes
Neglecting electron masses
Adding decay width to intermediate particles in the s-channel

In[3]:= amp[0]=FCFAConvert[CreateFeynAmp[diags],IncomingMomenta→{p1,p2},
OutgoingMomenta→{k1,k2},SMP→True,UndoChiralSplittings→True,
Contract→True,FinalSubstitutions→{Me→0,MN4→m_N^4,
MZ→√(SMP["m_Z"]^2-i Γ_Z SMP["m_Z"]),MZ2→√(m_ZR^2-i Γ_ZR m_ZR),MW2→m_WR^2}];

Defining the relevant dot products of the particles

In[4]:= FCClearScalarProducts[];
SetMandelstam[s,t,u,p1,p2,-k1,-k2,0,0,m_N^2,m_N^2];

Calculating the total amplitude squared in terms of Mandelstam variables

In[5]:= amp[1]=FullSimplify[(TrickMandelstam[#1,{s,t,u,2 m_N^2}]&)
[FeynAmpDenominatorExplicit[DiracSimplify[
(FermionSpinSum[#1,ExtraFactor→1/4]&)
[amp[0] ComplexConjugate[amp[0]]]]]]]

Defining the limits of integration of the phase space

In[6]:= tUpper=m_N^2-1/2 s (1-√(1-4 m_N^2/2));
tLower=m_N^2-1/2 s (1+√(1-4 m_N^2/2));

Integrating the differential cross section

In[7]:= σ[0]=(∫_tLower^tUpper amp[1] dt)/(8 π s^2)
```

This code should generate the entire cross-section. In practice we did not write the code like this, we separated the amplitude squared for the different contributions and integrated them individually, lest it takes 5 hours of computation.

The shape of the differential cross section in terms of the Mandelstam variable t, as well as the limits of integration are very well known and can be found either in Chapter 4 of [200] or in Chapter 49 of [233]. There's an extra factor of 1/2 in the final step to account for identical particles in the final state.

C.2 Three-body decay calculation

The calculation of the average amplitude square was done with the help of `Mathematica`, but the integration of the differential decay width was done by hand.

The `Mathematica` code was much simpler than the one described for the calculation of the cross-section. We shall consider a process $N(p) \to \ell^-(p_1) + U(p_2) + \bar{D}(p_3)$:

```
In[1]:=  Needs["FeynCalc`"];

In[2]:=  ampWR[0]=-(i SMP["g"]^2)/(2 m_WR^2) SpinorUBar[p1,m1].GA[μ,6].SpinorU[p,mN]
         SpinorUBar[p2,m2].GA[μ,6].SpinorV[p3,m3];

In[3]:=  FCClearScalarProducts[];
         SetMandelstam[m12,m13,m23,p1,p2,p3,-p,m1,m2,m3,mN];

In[4]:=  ampWR[1]=Simplify[DiracSimplify[(FermionSpinSum[#1,
         ExtraFactor→1/4]&)[ampWR[0] ComplexConjugate[ampWR[0]]]]]

Out[4]=  g^4 (m1^2-m12+m2^2) (m12-m3^2-mN^2)/(4 m_WR^4)
```

where $m1^2 = m_\ell^2$ is the mass of the lepton, $m2^2 = m_U^2$ is the mass of the up-type quark, and $m3^2 = m_D^2$ is the mass of the down-type quark. $m12 = (p_1 + p_2)^2 \equiv m_{12}^2$ is the invariant mass squared of the up-type quark and the lepton. This result gives us the following differential decay width:

$$\frac{\mathrm{d}\Gamma}{\mathrm{d}m_{12}^2 \mathrm{d}m_{23}^2} = \frac{g^4}{512\,\pi^3\,M_{W_R}^2}\left|V_{i,j}^{\mathrm{CKM}}\right|^2 \frac{\left(m_N^2 + m_D^2 - m_{12}^2\right)\left(m_{12}^2 - m_U^2 - m_\ell^2\right)}{m_N^3}\,, \tag{143}$$

with the limits of integration (see Chapter 5 of [200]):

$$(m_{23}^2)^- < m_{23}^2 < (m_{23}^2)^+\,, \tag{144}$$

$$(m_\alpha + m_U)^2 < m_{12}^2 < (m_N - m_D)^2\,, \tag{145}$$

with:

$$\left(m_{23}^2\right)^+ - \left(m_{23}^2\right)^- = \frac{\sqrt{\lambda(m_{12}^2, m_N^2, m_D^2)}\,\sqrt{\lambda(m_{12}^2, m_U^2, m_\ell^2)}}{m_{12}^2}\,. \tag{146}$$

The subsequent integration leaves:

$$\Gamma = \frac{G_F^2\,m_N^5}{192\pi^3}\,\frac{M_{W_L}^4}{M_{W_R}^4}\left|V_{i,j}^{\mathrm{CKM}}\right|^2 \mathcal{I}(x_U^2, x_D^2, x_\ell^2)\,, \tag{147}$$

with $x_U = m_U/m_N, x_D = m_D/m_N, x_\ell = m_\ell/m_N$, and where we define the $\mathcal{I}$ function as:

$$\mathcal{I}(x_U^2, x_D^2, x_\ell^2) = 12\int_{(x_U+x_\ell)^2}^{(1-x_D)^2} \frac{\mathrm{d}x}{x}\,(x - x_U^2 - x_\ell^2)(1 + x_D^2 - x)\sqrt{\lambda(1, x, x_D^2)\,\lambda(x, x_\ell^2, x_U^2)}\,, \tag{148}$$

which in the case of massless final particles $\mathcal{I}(0,0,0) = 1$, which is its maximum value.

In the case of the decays mediated by the W_L, the integration formula changes slightly, in this case:

$$\Gamma = \frac{G_F^2\,m_N^5}{192\pi^3}\,\xi_W^2\left|V_{i,j}^{\mathrm{CKM}}\right|^2 \mathcal{I}(x_D^2, x_U^2, x_\ell^2)\,, \tag{149}$$

due to the coupling, the mass of the intermediate particle, and due to the different spin-structure

in the amplitude: W_L couples to left-handed quarks and right-handed anti-quarks; W_R is the opposite.

For leptonic decays, it is sufficient to do the substitutions $x_D \to x_\ell$, $x_U \to 0$, and to set the CKM matrix element to 1.

Before we finalize the discussion on the calculations of three-body decays, let us finally do the computation in the case we cannot neglect the mass of the W_L-boson. The amplitude will now include the momentum of the W_L in the propagator, as well as the decay width, in this case:

$$\frac{\mathrm{d}\Gamma}{\mathrm{d}m_{12}^2\,\mathrm{d}m_{13}^2} = \frac{G_F^2\,M_{W_L}^2}{16\pi^3}\xi_W^2\,\frac{m_{13}^2\,(m_N^2 - m_{13}^2)}{(m_{23}^2 - M_{W_L}^2)^2 + \Gamma_{W_L}^2\,M_{W_L}^2}\,, \tag{150}$$

with integration limits:

$$0 < m_{13}^2 < m_N^2 - m_{23}^2\,, \tag{151}$$

$$0 < m_{23}^2 < m_N^2\,, \tag{152}$$

which leaves the answer and from it we derived Eq. (113).

C.3 Two-body decay calculation

For the two-body meson, let us consider the low-energy four-fermion effective operator which mediates the decay:

$$\mathcal{L} = -\frac{g^2}{4\,M_{W_R}^2}V_{i,j}^{\mathrm{CKM}}\left[\bar{U}\,\gamma^\mu(1+\gamma_5)D\right]\left[\bar{\ell}\,\gamma_\mu P_R N\right]\,. \tag{153}$$

Remember that we obtain the probability of a process from the S-matrix, so for an HNL decay to a meson, M and a lepton ℓ we have that $\langle f|S|i\rangle = \langle M,\ell|S|N\rangle$. Remember that the S-matrix is proportional to the Lagrangian (or the Hamiltonian), so we will need:

$$\langle M,\ell|\mathcal{L}|N\rangle = -\frac{g^2}{4\,M_{W_R}^2}V_{i,j}^{\mathrm{CKM}}\,\langle M|\left[\bar{U}\,\gamma^\mu(1+\gamma_5)D\right]|0\rangle\,\langle\ell|\left[\bar{\ell}\,\gamma_\mu P_R N\right]|N\rangle\,, \tag{154}$$

where we will have two contributions, a vector contribution, V, and a pseudo-scalar contribution, P, both will be different mesons:

$$\langle P|\bar{U}\,\gamma^\mu\,\gamma_5\,D|0\rangle = -if_P\,p_P^\mu\,, \tag{155}$$

$$\langle V|\bar{U}\,\gamma^\mu\,D|0\rangle = -i\frac{f_V}{m_V}\,\epsilon_V^{*\mu}\,, \tag{156}$$

with p_P being the four momentum of the pseudo-scalar meson, ϵ_V^μ the polarization vector of the vector meson, f_P is the decay constant of the pseudo-scalar and f_V of the vector.

The decay constants encapsulate all of the unknowns of the dynamics behind QCD. These decay constants can be calculated using lattice QCD methods. The reason for the p_P^μ in Eq. (155) comes from the fact we need a vector quantity to preserve Lorentz Invariance, and this is the only vector quantity available to us. But we cannot have p_V^μ on the right-hand side of Eq. (156), we know that final vector particles must be proportional to their helicity vector $\epsilon_V^{*\mu}$.

Particle type	g_R	g_L
U	$\frac{1}{2} - \frac{2}{3}\, t_w^2$	$-\frac{1}{6} t_w^2$
D	$-\frac{1}{2} + \frac{1}{3}\, t_w^2$	$-\frac{1}{6} t_w^2$
ℓ	$-\frac{1}{2} + t_w^2$	$\frac{1}{2}\, t_w^2$
ν	$-\frac{1}{2}\, t_w^2$	$\frac{1}{2}\, t_w^2$
N	$\frac{1}{2}$	$-\frac{1}{2}$

Table 8: Values for g_R and g_L for different particle types.

The $1 \to 2$ decays do not require any integration, this is because from the Phase Space integration, we can see that we have to perform six integrals, but we also have a four-dimensional Dirac Delta, which leaves us with only two integrals. If we evaluate the integral in the frame of the decaying particle, then the amplitude will actually not depend on any of these two final variables due to the O(3) symmetry in the initial state. For these processes, the decay width is:

$$\Gamma = \frac{\sqrt{\lambda(1, x_\ell^2, x_M^2)}}{16\pi\, m_N} \left|\mathcal{M}\right|^2 , \tag{157}$$

where $x_M = m_M/m_N$, with m_M being the mass of the final lepton.

As we mentioned in the main text, there will be an interference term coming from both the left-handed and the right-handed currents. This interference can either be destructive or constructive for processes with pseudo-scalars or vectors, and it entirely depends on the value of α. The total decay width for both processes is:

$$\Gamma(N \to \ell^- P^+) = \frac{G_F^2\, f_P^2\, m_N^3}{16\pi} \left|V_{i,j}^{\rm CKM}\right|^2 \left|\frac{M_{W_L}^2}{M_{W_R}^2} - \xi_W\, e^{i\alpha}\right|^2 \left[(1 - x_\ell^2)^2 - x_P^2\,(1 + x_\ell^2)\right] \sqrt{\lambda(1, x_\ell^2, x_P^2)}\,, \tag{158}$$

$$\Gamma(N \to \ell^- V^+) = \frac{G_F^2\, f_V^2\, m_N^3}{16\pi} \left|V_{i,j}^{\rm CKM}\right|^2 \left|\frac{M_{W_L}^2}{M_{W_R}^2} + \xi_W\, e^{i\alpha}\right|^2 \left[x_V^2\,(1 + x_\ell^2) + (1 - x_\ell^2)^2 - 2\, x_V^2\right] \sqrt{\lambda(1, x_\ell^2, x_V^2)}\,. \tag{159}$$

C.4 Calculation of the decay width of Z_R

We calculated the total decay width of Z_R only considering the channels which are not proportional to any mixing angle, neither the $Z_L - Z_R$ mixing or the $\nu - N$ mixing; and only decays to fermions. Therefore we will only consider the first term in Eq. (101), the amplitude will be parameterized as:

$$i\mathcal{M}(Z_R \to \bar\psi\psi) = i \frac{g\, c_w}{c_{2w}^{1/2}} \bar u_\psi \not{Z}_R \left[g_R\, P_R + g_L\, P_L\right] v_\psi\,, \tag{160}$$

the values of g_L and g_R are in Table 8 for all fermion types.

The decay width is also very simple to calculate, neglecting fermion masses we get:

$$\Gamma(Z_R \to \bar{\psi}\psi) = N_\psi \frac{g^2\, c_w^2}{24\,\pi\, c_{2w}} M_{Z_R} \left(g_L^2 + g_R^2\right) , \tag{161}$$

where N_ψ is equal to 3 for quarks to account for color, 1 in the case of charged leptons, and 1/2 in the case of Majorana particles to account for same-particles in the final state.

As a first approximation, we added overall particle types: three leptons, six quarks, three neutrinos, and only one HNL. The total decay width gives:

$$\Gamma_{Z_R} = \frac{g^4\, m_{Z_R}}{384\,\pi} \frac{55\, c_{4w} - 36\, c_{2w} + 69}{c_w^2\, c_{2w}} . \tag{162}$$

Appendix D Constants used on calculations

For relevant calculations, the values of the CKM matrix and masses of elementary particles and mesons from [233]. Most of the decay constants for vector mesons have not been measured experimentally, so for most of them, we shall give theoretical estimates derived from Lattice QCD or by other methods. Moreover, the vector meson $B_C^{*\pm}$ has not been discovered yet, so we provide the theoretical estimate of its mass derived from Lattice QCD.

The values of the masses and decay constants we used for the calculations are:

Quark content	Particle	Mass [MeV]	f_P [MeV]
ud	$\pi^\pm$	139.570 39 [233]	130.56 [233]
us	$K^\pm$	193.677 [233]	155.7 [233]
cd	$D^\pm$	1869.66 [233]	212.0 [233]
cs	$D_s^\pm$	1968.35 [233]	249.4 [233]
ub	$B^\pm$	5279.34 [233]	190.0 [233]
cb	$B_c^\pm$	6274.47 [233]	434 [234]

Table 9: Mass and decay constants of pseudo-scalar mesons.

Quark content	Particle	Mass [MeV]	f_V [MeV]
ud	$\rho^\pm$	775.26 [233]	210 [235]
us	$K^{*\pm}$	891.67 [233]	155.7 [235]
cd	$D^{*\pm}$	2010.26 [233]	223.5 [236]
cs	$D_s^{*\pm}$	2112.2 [233]	268.8 [236]
ub	$B^{*\pm}$	5324.71 [233]	186.4 [236]
cb	$B_c^{*\pm}$	6328 [237]	422 [234]

Table 10: Mass and decay constants of vector mesons.

Appendix E Additional plots

This appendix contains the sensitivity to all the runs shown in Table 3, for both displaced vertices and prompt LNV signals. All of the plots in this section were done using only the analytical estimation of the cross-section, we did not include ISR or polarization effects.

We also estimated the sensitivity that HECATE and THUNDERDOME [216] would have. HECATE has the potential of seeing decay widths up to 25 m and THUNDERDOME up to 100 m[23].

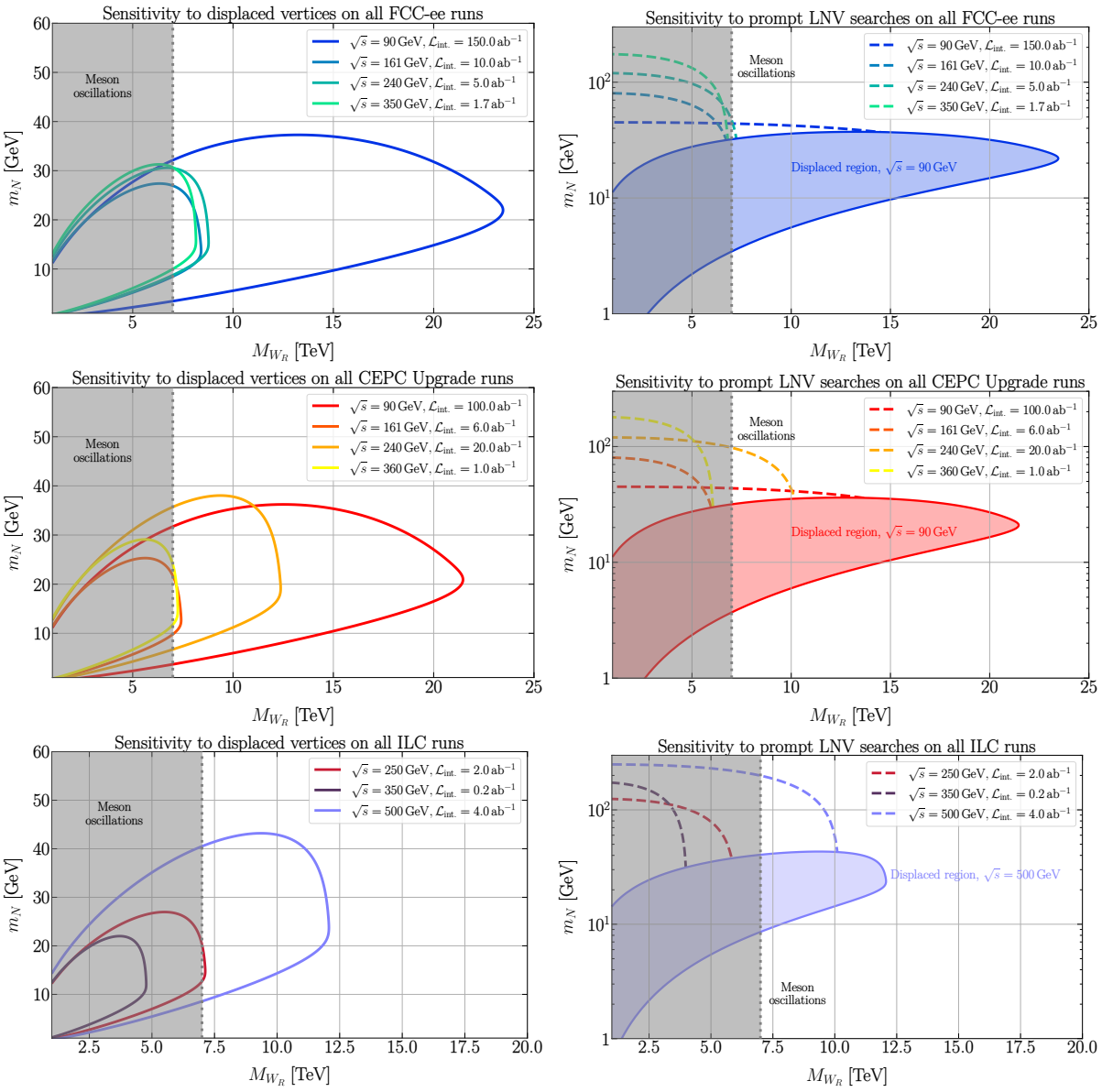

Figure 23: Additional plots

[23]THUNDERDOME stands for *Totally Hyper-UNrealistic DE-tectoR in a huge DOME*. The unrealistic part should not be understated.

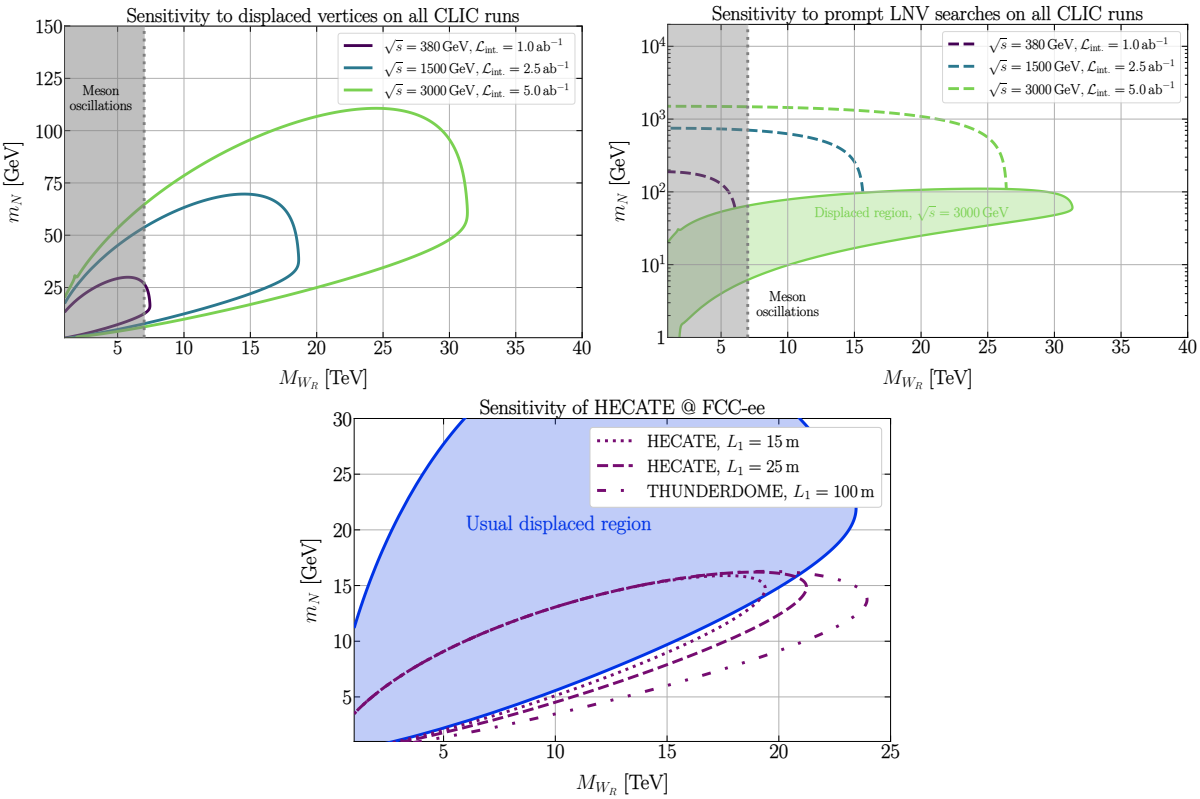

Figure 24: Additional plots

Bibliography

[1] S. L. Glashow, Nucl. Phys. **22**, 579 (1961).

[2] S. Weinberg, Phys. Rev. Lett. **19**, 1264 (1967).

[3] E. Rutherford, The London, Edinburgh, and Dublin Philosophical Magazine and Journal of Science **47**, 109 (1899), https://doi.org/10.1080/14786449908621245 .

[4] T. D. Lee and C.-N. Yang, Phys. Rev. **104**, 254 (1956).

[5] C. S. Wu, E. Ambler, R. W. Hayward, D. D. Hoppes, and R. P. Hudson, Phys. Rev. **105**, 1413 (1957).

[6] C.-N. Yang and R. L. Mills, Phys. Rev. **96**, 191 (1954).

[7] L. D. Faddeev and V. N. Popov, Phys. Lett. B **25**, 29 (1967).

[8] G. 't Hooft and M. J. G. Veltman, Nucl. Phys. B **44**, 189 (1972).

[9] Y. Nambu and G. Jona-Lasinio, Phys. Rev. **122**, 345 (1961).

[10] J. Goldstone, A. Salam, and S. Weinberg, Phys. Rev. **127**, 965 (1962).

[11] P. W. Higgs, Phys. Rev. Lett. **13**, 508 (1964).

[12] F. Englert and R. Brout, Phys. Rev. Lett. **13**, 321 (1964).

[13] G. S. Guralnik, C. R. Hagen, and T. W. B. Kibble, Phys. Rev. Lett. **13**, 585 (1964).

[14] G. Aad *et al.* (ATLAS), *Standard Model Summary Plots February 2022*, Tech. Rep. (CERN, 2022).

[15] Y. Fukuda *et al.* (Super-Kamiokande), Phys. Rev. Lett. **81**, 1562 (1998), arXiv:hep-ex/9807003 .

[16] Q. R. Ahmad *et al.* (SNO), Phys. Rev. Lett. **87**, 071301 (2001), arXiv:nucl-ex/0106015 .

[17] M. H. Ahn *et al.* (K2K), Phys. Rev. Lett. **90**, 041801 (2003), arXiv:hep-ex/0212007 .

[18] A. D. Sakharov, Pisma Zh. Eksp. Teor. Fiz. **5**, 32 (1967).

[19] V. A. Kuzmin, Pisma Zh. Eksp. Teor. Fiz. **12**, 335 (1970).

[20] F. Zwicky, Helv. Phys. Acta **6**, 110 (1933).

[21] N. Aghanim *et al.* (Planck), Astron. Astrophys. **641**, A6 (2020), [Erratum: Astron.Astrophys. 652, C4 (2021)], arXiv:1807.06209 [astro-ph.CO] .

[22] G. 't Hooft, Phys. Rev. Lett. **37**, 8 (1976).

[23] H. S. Snyder, Phys. Rev. **71**, 38 (1947).

[24] B. S. DeWitt, Phys. Rev. **160**, 1113 (1967).

[25] M. H. Goroff and A. Sagnotti, Phys. Lett. B **160**, 81 (1985).

[26] A. Crivellin, in *8th Symposium on Prospects in the Physics of Discrete Symmetries* (2023) arXiv:2304.01694 [hep-ph] .

[27] T. Asaka and M. Shaposhnikov, Phys. Lett. B **620**, 17 (2005), arXiv:hep-ph/0505013 .

[28] H. Georgi and S. L. Glashow, Phys. Rev. Lett. **32**, 438 (1974).

[29] H. Fritzsch and P. Minkowski, Annals Phys. **93**, 193 (1975).

[30] J. C. Pati and A. Salam, Phys. Rev. D **10**, 275 (1974), [Erratum: Phys.Rev.D 11, 703–703 (1975)].

[31] R. N. Mohapatra and J. C. Pati, Phys. Rev. D **11**, 2558 (1975).

[32] G. Senjanovic and R. N. Mohapatra, Phys. Rev. D **12**, 1502 (1975).

[33] R. N. Mohapatra and G. Senjanovic, Phys. Rev. Lett. **44**, 912 (1980).

[34] R. N. Mohapatra and G. Senjanovic, Phys. Rev. D **23**, 165 (1981).

[35] M. Fukugita and T. Yanagida, Phys. Lett. B **174**, 45 (1986).

[36] E. Ma and U. Sarkar, Phys. Rev. Lett. **80**, 5716 (1998), arXiv:hep-ph/9802445 .

[37] K. S. Babu and R. N. Mohapatra, Phys. Rev. D **41**, 1286 (1990).

[38] S. M. Barr, D. Chang, and G. Senjanovic, Phys. Rev. Lett. **67**, 2765 (1991).

[39] F. Bezrukov, H. Hettmansperger, and M. Lindner, Phys. Rev. D **81**, 085032 (2010), arXiv:0912.4415 [hep-ph] .

[40] M. Nemevsek, G. Senjanovic, and Y. Zhang, JCAP **07**, 006 (2012), arXiv:1205.0844 [hep-ph] .

[41] G. Beall, M. Bander, and A. Soni, Phys. Rev. Lett. **48**, 848 (1982).

[42] G. Ecker and W. Grimus, Nucl. Phys. B **258**, 328 (1985).

[43] P. Langacker and S. U. Sankar, Phys. Rev. D **40**, 1569 (1989).

[44] A. Abada *et al.* (FCC), Eur. Phys. J. C **79**, 474 (2019).

[45] A. Abada *et al.* (FCC), Eur. Phys. J. ST **228**, 261 (2019).

[46] A. Abada *et al.* (FCC), Eur. Phys. J. ST **228**, 755 (2019).

[47] P. Agostini *et al.* (LHeC, FCC-he Study Group), J. Phys. G **48**, 110501 (2021), arXiv:2007.14491 [hep-ex] .

[48] T. C. S. Group, (2018), arXiv:1809.00285 [physics.acc-ph] .

[49] M. Dong *et al.* (CEPC Study Group), (2018), arXiv:1811.10545 [hep-ex] .

[50] G. Aarons *et al.* (ILC), *ILC Reference Design Report Volume 1 - Executive Summary*, Tech. Rep. (2007) arXiv:0712.1950 [physics.acc-ph] .

[51] G. Aarons *et al.* (ILC), *International Linear Collider Reference Design Report Volume 2: Physics at the ILC*, Tech. Rep. (2007) arXiv:0709.1893 [hep-ph] .

[52] G. Aarons *et al.*, (2007), arXiv:0712.2361 [physics.acc-ph] .

[53] G. Aarons *et al.* (ILC), (2007), arXiv:0712.2356 [physics.ins-det] .

[54] E. Accomando *et al.* (CLIC Physics Working Group), in *11th International Conference on Hadron Spectroscopy*, CERN Yellow Reports: Monographs (2004) arXiv:hep-ph/0412251 .

[55] M. Aicheler, P. Burrows, M. Draper, T. Garvey, P. Lebrun, K. Peach, N. Phinney, H. Schmickler, D. Schulte, and N. Toge, *A Multi-TeV Linear Collider Based on CLIC Technology: CLIC Conceptual Design Report*, Tech. Rep. (2012).

[56] CERN (CLIC accelerator), *The Compact Linear Collider (CLIC) - Project Implementation Plan*, Tech. Rep. (CERN, 2018) arXiv:1903.08655 [physics.acc-ph] .

[57] J. P. Delahaye, M. Diemoz, K. Long, B. Mansoulié, N. Pastrone, L. Rivkin, D. Schulte, A. Skrinsky, and A. Wulzer, (2019), arXiv:1901.06150 [physics.acc-ph] .

[58] S. Gourlay *et al.*, (2022), arXiv:2209.14136 [physics.acc-ph] .

[59] C. Aime *et al.*, (2022), arXiv:2203.07256 [hep-ph] .

[60] K. M. Black *et al.*, (2022), arXiv:2209.01318 [hep-ex] .

[61] C. Accettura *et al.*, (2023), arXiv:2303.08533 [physics.acc-ph] .

[62] P. S. B. Dev, R. N. Mohapatra, and Y. Zhang, Nucl. Phys. B **923**, 179 (2017), arXiv:1703.02471 [hep-ph] .

[63] P. S. B. Dev, R. N. Mohapatra, and Y. Zhang, Phys. Rev. Lett. **120**, 221804 (2018), arXiv:1711.08430 [hep-ph] .

[64] P. S. B. Dev, M. J. Ramsey-Musolf, and Y. Zhang, Phys. Rev. D **98**, 055013 (2018), arXiv:1806.08499 [hep-ph] .

[65] P. S. Bhupal Dev and Y. Zhang, JHEP **10**, 199 (2018), arXiv:1808.00943 [hep-ph] .

[66] P. S. Bhupal Dev, R. N. Mohapatra, and Y. Zhang, Phys. Rev. D **98**, 075028 (2018), arXiv:1803.11167 [hep-ph] .

[67] S. S. Biswal and P. S. B. Dev, Phys. Rev. D **95**, 115031 (2017), arXiv:1701.08751 [hep-ph] .

[68] T.-P. .-.-.-. Cheng and L.-F. .-.-.-. Li, *Gauge Theory of Elementary Particle Physics* (Oxford University Press, Oxford, UK, 1984).

[69] Y. Ne'eman, Nucl. Phys. **26**, 222 (1961).

[70] M. Gell-Mann, (1961), 10.2172/4008239.

[71] M. Gell-Mann, Phys. Rev. **125**, 1067 (1962).

[72] G. Zweig, *An SU(3) model for strong interaction symmetry and its breaking. Version 1*, Tech. Rep. (CERN, 1964).

[73] M. Gell-Mann, Phys. Lett. **8**, 214 (1964).

[74] H. Fritzsch, M. Gell-Mann, and H. Leutwyler, Phys. Lett. B **47**, 365 (1973).

[75] D. G. Boulware, Annals Phys. **56**, 140 (1970).

[76] G. Aad *et al.* (ATLAS), Phys. Lett. B **716**, 1 (2012), arXiv:1207.7214 [hep-ex] .

[77] S. Chatrchyan *et al.* (CMS), Phys. Lett. B **716**, 30 (2012), arXiv:1207.7235 [hep-ex] .

[78] The ATLAS Collaboration, Nature **607**, 52 (2022), [Erratum: Nature 612, E24 (2022)], arXiv:2207.00092 [hep-ex] .

[79] H. Georgi and S. Weinberg, Phys. Rev. D **17**, 275 (1978).

[80] M. Gell-Mann and A. Pais, Phys. Rev. **97**, 1387 (1955).

[81] B. Pontecorvo, Camb. Monogr. Part. Phys. Nucl. Phys. Cosmol. **1**, 25 (1991).

[82] B. Pontecorvo, Zh. Eksp. Teor. Fiz. **37**, 1751 (1959).

[83] B. Pontecorvo, Sov. Phys. JETP **6**, 429 (1957).

[84] B. Pontecorvo, Zh. Eksp. Teor. Fiz. **34**, 247 (1957).

[85] Q. R. Ahmad *et al.* (SNO), Phys. Rev. Lett. **89**, 011301 (2002), arXiv:nucl-ex/0204008 .

[86] K. Eguchi *et al.* (KamLAND), Phys. Rev. Lett. **90**, 021802 (2003), arXiv:hep-ex/0212021 .

[87] S. P. Mikheyev and A. Y. Smirnov, Sov. J. Nucl. Phys. **42**, 913 (1985).

[88] L. Wolfenstein, Phys. Rev. D **17**, 2369 (1978).

[89] B. D. Fields, K. A. Olive, T.-H. Yeh, and C. Young, JCAP **03**, 010 (2020), [Erratum: JCAP 11, E02 (2020)], arXiv:1912.01132 [astro-ph.CO] .

[90] V. A. Rubakov and D. S. Gorbunov, *Introduction to the Theory of the Early Universe: Hot big bang theory* (World Scientific, Singapore, 2017).

[91] V. A. Kuzmin, V. A. Rubakov, and M. E. Shaposhnikov, Phys. Lett. B **155**, 36 (1985).

[92] C. Jarlskog, Phys. Rev. Lett. **55**, 1039 (1985).

[93] M. E. Shaposhnikov, JETP Lett. **44**, 465 (1986).

[94] K. Kajantie, M. Laine, K. Rummukainen, and M. E. Shaposhnikov, Phys. Rev. Lett. **77**, 2887 (1996), arXiv:hep-ph/9605288 .

[95] T. S. van Albada, J. N. Bahcall, K. Begeman, and R. Sancisi, Astrophys. J. **295**, 305 (1985).

[96] D. Clowe, M. Bradac, A. H. Gonzalez, M. Markevitch, S. W. Randall, C. Jones, and D. Zaritsky, Astrophys. J. Lett. **648**, L109 (2006), arXiv:astro-ph/0608407 .

[97] M. Srednicki, *Quantum field theory* (Cambridge University Press, 2007).

[98] A. A. Belavin, A. M. Polyakov, A. S. Schwartz, and Y. S. Tyupkin, Phys. Lett. B **59**, 85 (1975).

[99] C. Abel *et al.*, Phys. Rev. Lett. **124**, 081803 (2020), arXiv:2001.11966 [hep-ex] .

[100] G. Senjanovic and V. Tello, (2020), arXiv:2004.04036 [hep-ph] .

[101] G. 't Hooft and M. J. G. Veltman, Ann. Inst. H. Poincare Phys. Theor. A **20**, 69 (1974).

[102] P. Minkowski, Phys. Lett. B **67**, 421 (1977).

[103] J. A. Casas and A. Ibarra, Nucl. Phys. B **618**, 171 (2001), arXiv:hep-ph/0103065 .

[104] P. D. Bolton, F. F. Deppisch, and P. S. Bhupal Dev, JHEP **03**, 170 (2020), arXiv:1912.03058 [hep-ph] .

[105] A. Boyarsky, O. Ruchayskiy, and M. Shaposhnikov, Ann. Rev. Nucl. Part. Sci. **59**, 191 (2009), arXiv:0901.0011 [hep-ph] .

[106] O. Ruchayskiy and A. Ivashko, JCAP **10**, 014 (2012), arXiv:1202.2841 [hep-ph] .

[107] K. A. U. Calderón, I. Timiryasov, and O. Ruchayskiy, (2022), arXiv:2206.04540 [hep-ph] .

[108] E. K. Akhmedov, V. A. Rubakov, and A. Y. Smirnov, Phys. Rev. Lett. **81**, 1359 (1998), arXiv:hep-ph/9803255 .

[109] A. Pilaftsis and T. E. J. Underwood, Nucl. Phys. B **692**, 303 (2004), arXiv:hep-ph/0309342 .

[110] S. Antusch, O. Fischer, A. Hammad, and C. Scherb, JHEP **02**, 157 (2019), arXiv:1811.03476 [hep-ph] .

[111] R. Foot, H. Lew, X. G. He, and G. C. Joshi, Z. Phys. C **44**, 441 (1989).

[112] R. N. Mohapatra and J. W. F. Valle, Phys. Rev. D **34**, 1642 (1986).

[113] E. K. Akhmedov, M. Lindner, E. Schnapka, and J. W. F. Valle, Phys. Lett. B **368**, 270 (1996), arXiv:hep-ph/9507275 .

[114] E. Ma, Phys. Rev. Lett. **81**, 1171 (1998), arXiv:hep-ph/9805219 .

[115] E. Ma, (2009), arXiv:0905.0221 [hep-ph] .

[116] S. Weinberg, Phys. Rev. Lett. **43**, 1566 (1979).

[117] S. Centelles Chuliá, R. Srivastava, and J. W. F. Valle, Phys. Lett. B **781**, 122 (2018), arXiv:1802.05722 [hep-ph] .

[118] M. Berbig, (2023), arXiv:2307.14121 [hep-ph] .

[119] N. G. Deshpande, J. F. Gunion, B. Kayser, and F. I. Olness, Phys. Rev. D **44**, 837 (1991).

[120] G. Barenboim, M. Gorbahn, U. Nierste, and M. Raidal, Phys. Rev. D **65**, 095003 (2002), arXiv:hep-ph/0107121 .

[121] K. Kiers, M. Assis, and A. A. Petrov, Phys. Rev. D **71**, 115015 (2005), arXiv:hep-ph/0503115 .

[122] W. Dekens and D. Boer, Nucl. Phys. B **889**, 727 (2014), arXiv:1409.4052 [hep-ph] .

[123] P. S. B. Dev, R. N. Mohapatra, and Y. Zhang, JHEP **05**, 174 (2016), arXiv:1602.05947 [hep-ph] .

[124] A. Maiezza, G. Senjanović, and J. C. Vasquez, Phys. Rev. D **95**, 095004 (2017), arXiv:1612.09146 [hep-ph] .

[125] P. S. Bhupal Dev, R. N. Mohapatra, W. Rodejohann, and X.-J. Xu, JHEP **02**, 154 (2019), arXiv:1811.06869 [hep-ph] .

[126] S. Bertolini, A. Maiezza, and F. Nesti, Phys. Rev. D **89**, 095028 (2014), arXiv:1403.7112 [hep-ph] .

[127] A. Maiezza, (2020), arXiv:2012.01960 [hep-ph] .

[128] G. Senjanović and V. Tello, Phys. Rev. Lett. **114**, 071801 (2015), arXiv:1408.3835 [hep-ph] .

[129] G. Senjanović and V. Tello, Phys. Rev. Lett. **119**, 201803 (2017), arXiv:1612.05503 [hep-ph] .

[130] G. Senjanovic and V. Tello, Phys. Rev. D **100**, 115031 (2019), arXiv:1812.03790 [hep-ph] .

[131] G. Senjanovic and V. Tello, Int. J. Mod. Phys. A **35**, 2050053 (2020), arXiv:1912.13060 [hep-ph] .

[132] W.-Y. Keung and G. Senjanovic, Phys. Rev. Lett. **50**, 1427 (1983).

[133] R. Ruiz, Phys. Rev. D **103**, 015022 (2021), arXiv:2008.01092 [hep-ph] .

[134] G. Aad *et al.* (ATLAS), (2023), arXiv:2304.09553 [hep-ex] .

[135] A. Tumasyan *et al.* (CMS), JHEP **04**, 047 (2022), arXiv:2112.03949 [hep-ex] .

[136] G. Aad *et al.* (ATLAS), JHEP **03**, 145 (2020), arXiv:1910.08447 [hep-ex] .

[137] A. M. Sirunyan *et al.* (CMS), JHEP **05**, 033 (2020), arXiv:1911.03947 [hep-ex] .

[138] A. M. Sirunyan *et al.* (CMS), JHEP **06**, 128 (2018), arXiv:1803.11133 [hep-ex] .

[139] G. Aad *et al.* (ATLAS), Phys. Rev. D **100**, 052013 (2019), arXiv:1906.05609 [hep-ex] .

[140] M. Nemevšek, F. Nesti, and G. Popara, Phys. Rev. D **97**, 115018 (2018), arXiv:1801.05813 [hep-ph] .

[141] G. Cottin, J. C. Helo, M. Hirsch, and D. Silva, Phys. Rev. D **99**, 115013 (2019), arXiv:1902.05673 [hep-ph] .

[142] S. Alekhin *et al.*, Rept. Prog. Phys. **79**, 124201 (2016), arXiv:1504.04855 [hep-ph] .

[143] O. Castillo-Felisola, C. O. Dib, J. C. Helo, S. G. Kovalenko, and S. E. Ortiz, Phys. Rev. D **92**, 013001 (2015), arXiv:1504.02489 [hep-ph] .

[144] S. Mandal, M. Mitra, and N. Sinha, Phys. Rev. D **96**, 035023 (2017), arXiv:1705.01932 [hep-ph] .

[145] D. Curtin *et al.*, Rept. Prog. Phys. **82**, 116201 (2019), arXiv:1806.07396 [hep-ph] .

[146] G. Aad *et al.* (ATLAS), JHEP **07**, 162 (2015), arXiv:1506.06020 [hep-ex] .

[147] M. Aaboud *et al.* (ATLAS), JHEP **01**, 016 (2019), arXiv:1809.11105 [hep-ex] .

[148] M. Aaboud *et al.* (ATLAS), Phys. Lett. B **798**, 134942 (2019), arXiv:1904.12679 [hep-ex] .

[149] S. Chatrchyan *et al.* (CMS), Phys. Rev. Lett. **109**, 261802 (2012), arXiv:1210.2402 [hep-ex] .

[150] V. Khachatryan *et al.* (CMS), JHEP **03**, 077 (2017), arXiv:1612.01190 [hep-ex] .

[151] A. M. Sirunyan *et al.* (CMS), JHEP **07**, 121 (2017), arXiv:1703.03995 [hep-ex] .

[152] A. M. Sirunyan *et al.* (CMS), JHEP **03**, 170 (2019), arXiv:1811.00806 [hep-ex] .

[153] A. M. Sirunyan *et al.* (CMS), JHEP **05**, 148 (2018), arXiv:1803.11116 [hep-ex] .

[154] V. Tello, M. Nemevsek, F. Nesti, G. Senjanovic, and F. Vissani, Phys. Rev. Lett. **106**, 151801 (2011), arXiv:1011.3522 [hep-ph] .

[155] P. S. Bhupal Dev, S. Goswami, M. Mitra, and W. Rodejohann, Phys. Rev. D **88**, 091301 (2013), arXiv:1305.0056 [hep-ph] .

[156] J. de Vries, G. Li, M. J. Ramsey-Musolf, and J. C. Vasquez, JHEP **11**, 056 (2022), arXiv:2209.03031 [hep-ph] .

[157] G. Dvali, A. Maiezza, G. Senjanovic, and V. Tello, (2023), arXiv:2303.17261 [hep-ph] .

[158] H. Georgi, Hadronic J. **1**, 155 (1978).

[159] M. A. B. Beg and H. S. Tsao, Phys. Rev. Lett. **41**, 278 (1978).

[160] K. S. Babu and R. N. Mohapatra, Phys. Rev. Lett. **62**, 1079 (1989).

[161] A. Maiezza and M. Nemevšek, Phys. Rev. D **90**, 095002 (2014), arXiv:1407.3678 [hep-ph] .

[162] S. Bertolini, A. Maiezza, and F. Nesti, Phys. Rev. D **101**, 035036 (2020), arXiv:1911.09472 [hep-ph] .

[163] W. Dekens, L. Andreoli, J. de Vries, E. Mereghetti, and F. Oosterhof, JHEP **11**, 127 (2021), arXiv:2107.10852 [hep-ph] .

[164] C. Hati, S. Patra, P. Pritimita, and U. Sarkar, Front. in Phys. **6**, 19 (2018).

[165] A. Hook, PoS **TASI2018**, 004 (2019), arXiv:1812.02669 [hep-ph] .

[166] J.-M. Frere, T. Hambye, and G. Vertongen, JHEP **01**, 051 (2009), arXiv:0806.0841 [hep-ph] .

[167] H. Cheng *et al.* (CEPC Physics Study Group), in *Snowmass 2021* (2022) arXiv:2205.08553 [hep-ph] .

[168] T. Barklow, J. Brau, K. Fujii, J. Gao, J. List, N. Walker, and K. Yokoya, *ILC Operating Scenarios*, Tech. Rep. (ILC, 2015) arXiv:1506.07830 [hep-ex] .

[169] P. Bambade *et al.*, *The International Linear Collider: A Global Project*, Tech. Rep. (ILC, 2019) arXiv:1903.01629 [hep-ex] .

[170] LHC, "Longer term LHC schedule," (2022), accessed: 2023-07-17.

[171] J. Tang *et al.*, (2015), arXiv:1507.03224 [physics.acc-ph] .

[172] R. K. Ellis *et al.*, (2019), arXiv:1910.11775 [hep-ex] .

[173] R. B. Palmer, Rev. Accel. Sci. Tech. **7**, 137 (2014).

[174] F. Zimmermann and M. Benedikt, JACoW **eeFACT2022**, 7 (2023).

[175] J. Gao (CEPC Accelerator Study Group), (2022), arXiv:2203.09451 [physics.acc-ph] .

[176] U. Bassler, CERN Council Meeting (2019).

[177] M. Banks (Physics World), "Disappointment as Japan fails to commit to hosting the International Linear Collider," (2019).

[178] M. Banks (Physics World), "Panel calls on physicists to shelve notion of Japan hosting the International Linear Collider," (2022).

[179] T. G. Rizzo, Phys. Rev. D **25**, 1355 (1982), [Addendum: Phys.Rev.D 27, 657–659 (1983)].

[180] M. Lusignoli and S. Petrarca, Phys. Lett. B **226**, 397 (1989).

[181] T. G. Rizzo, Phys. Rev. D **45**, 42 (1992).

[182] J. Maalampi, K. Mursula, and R. Vuopionpera, Nucl. Phys. B **372**, 23 (1992).

[183] J. Maalampi, A. Pietila, and J. Vuori, Nucl. Phys. B **381**, 544 (1992).

[184] N. Lepore, B. Thorndyke, H. Nadeau, and D. London, Phys. Rev. D **50**, 2031 (1994), arXiv:hep-ph/9403237 .

[185] K. Huitu, J. Maalampi, A. Pietila, M. Raidal, and R. Vuopionpera, (1997), arXiv:hep-ph/9701386 .

[186] J. Barry, L. Dorame, and W. Rodejohann, Eur. Phys. J. C **72**, 2023 (2012), arXiv:1203.3365 [hep-ph] .

[187] R. Mertig, M. Bohm, and A. Denner, Comput. Phys. Commun. **64**, 345 (1991).

[188] T. Hahn, Comput. Phys. Commun. **140**, 418 (2001), arXiv:hep-ph/0012260 .

[189] A. Roitgrund, G. Eilam, and S. Bar-Shalom, Comput. Phys. Commun. **203**, 18 (2016), arXiv:1401.3345 [hep-ph] .

[190] A. Alloul, N. D. Christensen, C. Degrande, C. Duhr, and B. Fuks, Comput. Phys. Commun. **185**, 2250 (2014), arXiv:1310.1921 [hep-ph] .

[191] R. E. Shrock, eConf **C8206282**, 261 (1982).

[192] H. E. Logan, (2022), arXiv:2207.01064 [hep-ph] .

[193] D. A. Dicus and H.-J. He, Phys. Rev. D **71**, 093009 (2005), arXiv:hep-ph/0409131 .

[194] D. A. Dicus and H.-J. He, Phys. Rev. Lett. **94**, 221802 (2005), arXiv:hep-ph/0502178 .

[195] C. H. Llewellyn Smith, Phys. Lett. B **46**, 233 (1973).

[196] J. M. Cornwall, D. N. Levin, and G. Tiktopoulos, Phys. Rev. Lett. **30**, 1268 (1973), [Erratum: Phys.Rev.Lett. 31, 572 (1973)].

[197] J. M. Cornwall, D. N. Levin, and G. Tiktopoulos, Phys. Rev. D **10**, 1145 (1974), [Erratum: Phys.Rev.D 11, 972 (1975)].

[198] A. Maiezza, M. Nemevšek, and F. Nesti, Phys. Rev. Lett. **115**, 081802 (2015), arXiv:1503.06834 [hep-ph] .

[199] R. K. Ellis, W. J. Stirling, and B. R. Webber, *QCD and collider physics*, Vol. 8 (Cambridge University Press, 2011).

[200] E. Byckling and K. Kajantie, *Particle Kinematics: (Chapters I-VI, X)* (University of Jyvaskyla, Jyvaskyla, Finland, 1971).

[201] J. Alwall, M. Herquet, F. Maltoni, O. Mattelaer, and T. Stelzer, JHEP **06**, 128 (2011), arXiv:1106.0522 [hep-ph] .

[202] W. Kilian, T. Ohl, and J. Reuter, Eur. Phys. J. C **71**, 1742 (2011), arXiv:0708.4233 [hep-ph] .

[203] K. Bondarenko, A. Boyarsky, D. Gorbunov, and O. Ruchayskiy, JHEP **11**, 032 (2018), arXiv:1805.08567 [hep-ph] .

[204] J. Alimena *et al.*, J. Phys. G **47**, 090501 (2020), arXiv:1903.04497 [hep-ex] .

[205] S. Knapen and S. Lowette, (2022), arXiv:2212.03883 [hep-ph] .

[206] G. Aad *et al.* (ATLAS), JHEP **03**, 041 (2015), arXiv:1412.0237 [hep-ex] .

[207] G. Moortgat-Pick *et al.*, Phys. Rept. **460**, 131 (2008), arXiv:hep-ph/0507011 .

[208] M. D. Schwartz, *Quantum Field Theory and the Standard Model* (Cambridge University Press, 2014).

[209] S. Alipour-Fard *et al.* (CLIC, CLICdp), (2018), arXiv:1812.07986 [hep-ex] .

[210] M. Antonello (RD-FA), Nuovo Cim. C **43**, 27 (2020).

[211] H. Aihara *et al.*, (2009), arXiv:0911.0006 [physics.ins-det] .

[212] A. Blondel, E. Graverini, N. Serra, and M. Shaposhnikov (FCC-ee study Team), Nucl. Part. Phys. Proc. **273-275**, 1883 (2016), arXiv:1411.5230 [hep-ex] .

[213] S. Antusch, E. Cazzato, and O. Fischer, Int. J. Mod. Phys. A **32**, 1750078 (2017), arXiv:1612.02728 [hep-ph] .

[214] S. Antusch, E. Cazzato, and O. Fischer, JHEP **12**, 007 (2016), arXiv:1604.02420 [hep-ph] .

[215] M. Aaboud *et al.* (ATLAS), Eur. Phys. J. C **79**, 481 (2019), arXiv:1902.03094 [hep-ex] .

[216] M. Chrząszcz, M. Drewes, and J. Hajer, Eur. Phys. J. C **81**, 546 (2021), arXiv:2011.01005 [hep-ph] .

[217] B. Kayser, F. Gibrat-Debu, and F. Perrier, *The Physics of massive neutrinos*, Vol. 25 (1989).

[218] M. Zralek, Acta Phys. Polon. B **28**, 2225 (1997), arXiv:hep-ph/9711506 .

[219] C. Giunti and C. W. Kim, *Fundamentals of Neutrino Physics and Astrophysics* (2007).

[220] E. Majorana, Nuovo Cim. **14**, 171 (1937).

[221] J. Heeck and W. Rodejohann, EPL **103**, 32001 (2013), arXiv:1306.0580 [hep-ph] .

[222] L. F. Li and F. Wilczek, Phys. Rev. D **25**, 143 (1982).

[223] B. Kayser and R. E. Shrock, Phys. Lett. B **112**, 137 (1982).

[224] B. Kayser, Phys. Rev. D **26**, 1662 (1982).

[225] C. S. Kim, (2023), arXiv:2307.05654 [hep-ph] .

[226] P. Vilain *et al.* (CHARM-II), Phys. Lett. B **281**, 159 (1992).

[227] P. Vilain *et al.* (CHARM-II), Phys. Lett. B **320**, 203 (1994).

[228] P. Vilain *et al.* (CHARM-II), Phys. Lett. B **335**, 246 (1994).

[229] J.-L. Tastet and I. Timiryasov, JHEP **04**, 005 (2020), arXiv:1912.05520 [hep-ph] .

[230] W. Dekens, in *50th Rencontres de Moriond on EW Interactions and Unified Theories* (2015) pp. 515–518, arXiv:1505.06599 [hep-ph] .

[231] E. Fuchs, S. Thewes, and G. Weiglein, Eur. Phys. J. C **75**, 254 (2015), arXiv:1411.4652 [hep-ph] .

[232] C. F. Uhlemann and N. Kauer, Nucl. Phys. B **814**, 195 (2009), arXiv:0807.4112 [hep-ph] .

[233] R. L. Workman *et al.* (Particle Data Group), PTEP **2022**, 083C01 (2022).

[234] B. Colquhoun, C. T. H. Davies, R. J. Dowdall, J. Kettle, J. Koponen, G. P. Lepage, and A. T. Lytle (HPQCD), Phys. Rev. D **91**, 114509 (2015), arXiv:1503.05762 [hep-lat] .

[235] A. Bharucha, D. M. Straub, and R. Zwicky, JHEP **08**, 098 (2016), arXiv:1503.05534 [hep-ph] .

[236] V. Lubicz, A. Melis, and S. Simula (ETM), Phys. Rev. D **96**, 034524 (2017), arXiv:1707.04529 [hep-lat] .

[237] R. J. Dowdall, C. T. H. Davies, T. C. Hammant, and R. R. Horgan, Phys. Rev. D **86**, 094510 (2012), arXiv:1207.5149 [hep-lat] .